European Commission

technical steel research

Steelmaking processes

Effects of operational factors on the formation of toxic organic micropollutants in EAF steelmaking

R. Fisher, A. M. W. Briggs, S. S. Baker
Corus UK Ltd
Swinden Technology Centre, Moorgate, Rotherham S60 3AR, United Kingdom

M. I. Pistelli
CSM
Via di Castel Romano, 100, I-00128 Rome

G. Harp
BFI
Sohnstraße 65 — Postfach 105145, D-40237 Düsseldorf

J. Pereira Gomes
ISQ
Apartado 119, P-2781-951 Oeiras

Contract No 7210-PR/200
1 July 2000 to 31 December 2003

Final report

Directorate-General for Research

2005 EUR 21432 EN

Europe Direct is a service to help you find answers to your questions about the European Union

Freephone number (*)**:**
00 800 6 7 8 9 10 11

(*) Certain mobile telephone operators do not allow access to 00 800 numbers or these calls may be billed.

A great deal of additional information on the European Union is available on the Internet.
It can be accessed through the Europa server (http://europa.eu.int).

Cataloguing data can be found at the end of this publication.

Luxembourg: Office for Official Publications of the European Communities, 2005

ISBN 92-79-00083-7

Printed in Luxembourg

PRINTED ON WHITE CHLORINE-FREE PAPER

Abstract

Electric arc furnace (EAF) steelmaking is an important route for the production of steel and approximately 38% of the total steel output in the EU is produced in this way. Furthermore, it is envisaged that the proportion of steel produced by the EAF process will be maintained, or perhaps increased in the next twenty years or so. The EAF route is particularly important because of its role in the recycling of steel scrap and its importance in this respect seems likely to increase as a result of the European Directive 94/612/EC on Packaging and Packaging Waste and other Directives on End of Life Vehicles and Waste from Electrical and Electronic Equipment. However, EAF plants are significant sources of organic pollutants such as polycyclic aromatic hydrocarbons (PAHs), polychlorinated biphenyls (PCBs), polychlorinated dibenzo-p-dioxins (PCDDs) and polychlorinated dibenzofurans (PCDFs) and volatile organic compounds (VOC). Emission limits for some of these species are already applied in some European countries and it is expected that these will become tighter and more uniformly applied across the whole of the EU in the near future. Clearly, a better understanding of the fundamental factors that influence the formation of PAHs, PCBs and PCDD/Fs would be of considerable benefit in preventing, or minimising the formation of these substances in EAFs and in scrap pre-heating systems on EAFs. However, it must also be recognised that secondary abatement measures may still be required to meet stricter emission limits that are likely to be applied in the future.

These issues were addressed in the integrated research project which is the subject of this report. The main objectives of the work were to:

(i) develop a fundamental understanding of the operational factors that influence the formation of PAHs, PCBs and PCDD/Fs in EAF steelmaking;

(ii) identify conditions that promote and/or prevent the formation of toxic organic micropollutants in the EAF via the de novo synthesis mechanism;

(iii) investigate the formation of organic micropollutants in a pre-heating shaft;

(iv) develop measures for preventing the emission of organic micropollutants from shaft pre-heaters by use of internal post-combustion;

(v) identify optimum design for pre-heating systems on EAFs to meet environmental and economic demands; and,

(vi) investigate the reversible adsorption of organic micropollutants on technical plastics as a cost-effective means of removing such substances from EAF waste gases.

The studies were performed by a fully co-ordinated programme of work involving Corus UK Limited, BFI, CSM and ISQ. The main focus of work for each partner was as follows:

(i) Corus UK Limited studied the influence of process conditions on the formation of PCDD/Fs, PCBs and PAHs in EAF shops with single- and two-furnace operation without scrap pre-heating, and the use of plastics as adsorbents for the collection of organic compounds.

(ii) BFI investigated the formation of organic micropollutants during scrap pre-heating in a gas-fired experimental heating shaft and measures to prevent the formation of such compounds by internal post-combustion.

(iii) CSM carried out studies on a pilot scale system to investigate the de novo synthesis of PCDD/Fs.

(iv) ISQ carried out studies on a production plant to study the effects of scrap quality on the formation of PCDD/Fs, PAHs and PCBs.

On the basis of plant-based measurements on EAF plants it was established that PCDD/Fs and PCBs were mainly formed in sections of the waste gas system where the temperature exceeded 500°C. There was little evidence of de novo synthesis of PCDD/Fs or PCBs in sections of the extraction system where lower temperatures were found.

There was a strong correlation between the concentrations of PCDD/Fs and WHO-12 PCBs, with the I-TEQ of PCDD/Fs being approximately 16.5 times higher than that of WHO-12 PCBs. This suggests that the formation mechanisms of PCBs and PCDD/Fs are linked.

The PCDD/F congener profiles in samples from the direct and secondary extraction ducts at the EAF plants at Corus UK Limited were similar. In each instance the profile was dominated by PCDFs, which contributed typically 80 to 87% to the overall I-TEQ concentration. Invariably it was found that 2,3,4,7,8-PeCDF contributed more than half of the I-TEQ concentration. However, this contribution increased to between 60 and 70% of the I-TEQ in the emission from the bag filter plant, which was presumed to be due to the increased partitioning of less volatile higher chlorinated compounds to the dust. Emissions from the bag filter plants at Corus UK Limited and SN's Long Products Plant in Portugal exhibited similar congener profiles, which suggests a common formation mechanism for PCDD/Fs in these EAF plants.

The PCB congener profiles were very consistent and the main congeners present were PCBs 77, 105 and 118. However, the main contributor to the WHO-12 I-TEQ was PCB 126.

Trials at SN's Long Products plant showed that scrap quality had a significant influence on the emission of PCDD/Fs. Higher emission concentrations of PCDD/Fs were obtained with scrap containing PVC and cutting oils.

From studies on the adsorption and desorption behaviour of PCDD/Fs on EAF dust and plastics it was found that the volatilisation of PCDD/Fs from EAF dust exhibited an approximate seventh-power dependency on temperature. The work also showed that under appropriate conditions it is possible to predict the PCDD/F concentration in the waste gas from the temperature profile of the emission. This finding indicates that the temperature profile, i.e. the time – temperature history is more important than the mean temperature in determining the PCDD/F concentration in the waste gas. Relatively short-term peaks can, therefore, have a strong influence on overall mean PCDD/F concentrations. It was also shown that historical data on EAF emissions from Corus UK Limited were consistent with the temperature effects reported in the literature.

The efficiency of the bag filter for the abatement of PCDD/Fs, PAHs and PCBs is critically dependent on the waste gas temperature. In the current work, at a mean bag filter temperature of 67 to 76°C, it was observed that more than 90% of the PCDD/Fs reported to the dust, whereas only 60-70% of WHO-12 PCBs and 20-30% of PAHs reported to the dust. These findings are ascribed to the fact that PCBs and PAHs are generally more volatile than PCDD/Fs. Indeed the relatively low efficiency of the bag filter with respect to the abatement of PAHs is easily explained since the PAH profile is dominated by the more volatile 2- or 3-ring PAHs such as naphthalene, acenaphthene, anthracene and phenanthrene.

Polypropylene powder was shown to have better PCDD/F absorption capacity than polypropylene granules (5 mm spheres). The optimum temperature for PCDD/F absorption on polypropylene powder was 90°C. At lower temperatures, only trace amounts of PCDD/F were detected downstream of the absorption unit. At 120°C, breakthrough occurred consisting of the lower-chlorinated PCDD/F.

From laboratory studies on the mechanisms of formation of PCDD/Fs in the EAF and scrap pre-heating it was concluded that PCDD/F were formed from oily substances introduced in the charge. Other carbon sources were not involved in the PCDD/F formation mechanisms. The main formation mechanism identified under the EAF conditions considered, is based on precursor formation at high temperature (>500-600°C). Catalytic action (considered in de novo synthesis), that permits precursor formation at temperature <500°C, gives a low contribution (less than 10%) to the total PCDD/F formation.

Kinetic expressions were developed that permitted the potential for PCDD/F formation in an EAF system equipped with a tunnel scrap pre-heater to be assessed.

From pilot scale studies on the emission of VOCs from a shaft-type scrap pre-heating system it was shown that at the commencement of scrap pre-heating the VOC concentration increased sharply and reached a peak value after 3 min. Thereafter, the VOC concentration decreased and fell to zero after 2 h. The corresponding mean scrap temperature at the maximum VOC emission concentration was about 400°C with a temperature gradient of 600 and 250°C between the hot and cold ends of the scrap charge.

More than 95% of the total VOC emission occurred within the first 30 minutes of the trial duration and the relative amount of VOC produced was independent of the oil concentration on scrap. At oil concentrations of up to 2.5% by weight less than 15% by weight of the carbon in the oil was released as VOCs under oxygen-free conditions. This observation shows clearly that most of the carbon content of the oil must be pyrolysed to non-volatile elementary carbon remaining on the scrap surface, because combustion of the oil is impossible under oxygen free conditions.

The relative amount of VOC produced in the presence of 10% by volume of oxygen is slightly higher than that produced under oxygen-free conditions and typically around 15% by weight. This leads to the conclusion that oxidative destruction of VOC is impossible via oxygen enrichment of the pre-heating gas, since the VOCs are generated at moderate temperatures below 600°C which are too low for oxidative destruction to occur.

Simulation experiments on the post-combustion of VOCs from scrap pre-heating showed that the VOCs were completely oxidised when the oxygen content in the off-gas was at least 4 vol.-%, the gas temperature was above 700°C, and the mean residence time greater than 0.3 s. These conditions must be fulfilled for any industrial use of in-shaft post-combustion. Post-combustion of VOCs in typical scrap pre-heating installations takes place in a separate downstream combustion chamber. A more economical approach is an operating mode in

which the generated emissions are combusted directly at the top of the shaft through the mixing of hot VOC-free furnace off-gases and VOC-containing off-gases from the scrap charge. Therefore the off-gas stream must be split such that part of the pre-heating gas stream passes through the scrap layer while the other part bypasses the shaft. Both streams are recombined in the upper part of the shaft beneath the off-gas hood of the shaft. The split ratio is controlled by a temperature adjustment. The mean temperature must be at least 700°C, thereby ensuring that conditions are maintained for the combustion of VOCs at the top of the shaft.

CONTENTS

List of Tables

List of Figures

42. The partitioning of the sum of all targeted PCDD/F to the ESP dust, plastic container, PUF and plastic absorber of the experimental apparatus using 5 and 10 mm spheres

(a) 5 mm polypropylene spheres
(b) Commercial powder

43. The effect of polypropylene temperature on PCDD/F absorption

(a) ng/kg
(b) ng I-TEQ/kg

44. The effect of polypropylene temperature on PCDD/F absorption

(a) ng/kg
(b) ng I-TEQ/kg

45. PCDD/F distribution in desorption experiments

46. Homologue proportion of vapour PCDD/F, I-TEQ/kg in desorption experiment conducted at 120°C

47. Estimated PCDD/F homologue loading profile in polypropylene

(a) ng/kg
(b) ng I-TEQ/kg

48. The effect of polypropylene temperature on PCDD/F homologue distribution in ng/kg

(a) Dust
(b) PUF
(c) Container

49. The effect of polypropylene temperature on PCDD/F homologue distribution in ng I-TEQ/kg

(a) Dust
(b) PUF
(c) Container

50. The effect of polypropylene temperature on PCDD/F congener distribution in ng/kg

(a) Dust
(b) PUF
(c) Container
(d) Plastic

51. The effect of polypropylene temperature on PCDD/F congener distribution in ng I-TEQ/kg

(a) Dust
(b) PUF
(c) Container
(d) Plastic

52. Scrap temperature profile in the scrap pre-heating chamber for a selected scrap pre-heating trial

53. VOC-concentration (CnHm) at the exit of the scrap pre-heating chamber for a selected pre-heating trial with oil contaminated scrap

54. Relative VOC amount on scrap pre-heating with oxygen-free pre-heating gas with varying oil concentration on scrap

55. Relative VOC amount with varying oil concentration on scrap (10% O_2 in pre-heating gas)

56. Conversion of hydrocarbon v temperature (hydrocarbon amount: 2500 ppm)

57. Scheme of post-combustion in a shaft

1. Introduction

Electric arc furnace (EAF) steelmaking is an important route for the production of steel and approximately 38% of the total steel output in the EU is produced in this way. Furthermore, it is envisaged that the proportion of steel produced by the EAF process will be maintained, or perhaps increased in the next twenty years or so. The EAF route is particularly important because of its role in the recycling of steel scrap and its importance in this respect seems likely to increase as a result of the European Directive 94/612/EC on Packaging and Packaging Waste and other Directives on End of Life Vehicles and Waste from Electrical and Electronic Equipment. However, EAF plants are significant sources of organic pollutants such as polycyclic aromatic hydrocarbons (PAHs), polychlorinated biphenyls (PCBs) and polychlorinated dibenzo-p-dioxins (PCDDs) and polychlorinated dibenzofurans (PCDFs), which are important because of their toxicity and persistence in the environment and their tendency to bio-accumulate. Emission standards for PCDD/Fs and PAHs are already applied in some European countries and it is expected that these will become tighter and more uniformly applied across the whole of the EU in the near future. Indeed, an emission standard of 0.1 ng I-TEQ/Nm^3 is already applied to emissions of PCDD/Fs from municipal waste incinerators in the EU. Concentrations of PCDD/Fs found in emissions from European EAF plants lie mainly in the range 0.01-1.07 ng I-TEQ/Nm^3 [1-4] and, although there is as yet no uniform emission standard for PCDD/Fs in EAF plants across the EU, it is likely that there will be pressure for such plants to meet the standard of 0.1 ng I-TEQ/Nm^3 currently applied to municipal waste incinerators.

In considering techniques available for reducing organic emissions from EAF plants the distinction needs to be drawn between primary and secondary measures. With primary measures, which are also referred to as process-integrated techniques, the main objective is to prevent or minimise the formation or release of pollutants at source. Secondary measures, however, are used to capture or destroy pollutants present in the waste gas stream leaving the process and hence are commonly referred to as end-of-pipe techniques. Where possible, primary techniques should be applied since these methods actually prevent or control the formation of pollutants in the process. However, in order to develop suitable primary measures for controlling organic emissions it is necessary to have a fundamental understanding of the formation mechanisms and the influence of process operational factors.

Two earlier ECSC research projects [1,5] were concerned with the formation and abatement of PCDD/Fs in the EAF process. In the first of these projects, which was carried out under agreement number 7210.CB/901, it was not possible to establish a clear mechanism for the formation of these compounds, nor which parts of the cycle might be critical to their formation. In the second project, which was carried out under agreement number 7210.CB/902, secondary control measures based on catalytic destruction, incineration and adsorption on lignite coke were evaluated for the removal of PCDD/Fs from EAF process gases. It was concluded that catalytic destruction was technically feasible only after removal of the dust particles from the gas stream, but the need to reheat the gas to the operating

temperature of the catalyst (350°C) renders the process uneconomical. Trapping of PCDD/Fs by adsorption on lignite coke particles in entrained flow process, with subsequent collection of the adsorbent particles in a bag filter, was shown to be more than 99% efficient. However, the main disadvantages of this process are the risk of ignition of the coke particles and the need to dispose of PCDD/F-contaminated adsorbent either by landfilling or by incineration in a hazardous waste facility.

Most of the mechanistic studies on PCDD/F formation have been concerned with municipal solid waste incinerators and hazardous waste incinerators [6-8], where the most important mechanism for PCDD/F formation, the so-called de novo synthesis, was first elucidated by Vogg and Stieglitz [9]. The de novo synthesis involves the formation of PCDD/Fs from carbon and inorganic chloride on the surface of fly ash particles produced in the incineration process. Within this process, copper has also been identified as a powerful catalyst for PCDD/F formation. Scholz et al [10] later demonstrated that PCBs could also be formed by the de novo synthesis. Moreover, it was shown that PCBs formed by the de novo synthesis could also act as direct precursors for the formation of PCDFs but not for PCDDs. The implication here is that any steps taken to prevent the formation of PCDD/Fs may also prevent, or minimise the formation of PCBs.

The optimum temperature range for formation of PCDD/Fs is 250-450°C and in municipal waste incineration processes PCDD/F formation largely occurs in the waste gas extraction system downstream of the incineration process. A similar situation may occur in the EAF steelmaking process since it is likely that any PCDD/Fs formed during the initial scrap melting will be destroyed under the conditions pertaining in the combustion leg of the waste gas system. However, EAF plants differ widely in their design and it is necessary to take account of these differences. In this respect it is necessary to consider the possibilities for formation of organic pollutants in EAF plants with and without scrap pre-heating facilities. Scrap pre-heaters of different design [11-14] have been developed and these afford significant advantages in terms of energy conservation and productivity. However, concerns have been raised with regard to the potential for increased organic emissions from such systems and it is therefore important that the formation of organic micropollutants in scrap pre-heating should be considered in more detail.

There are numerous process variables that may influence the formation of PCDD/Fs in combustion processes, but the temperature profile of the waste gas system, the physicochemical characteristics of particulates in the waste gas system, and kinetic and thermodynamic factors controlling PCDD/F formation are probably of greatest importance. Various workers [15-17] have shown that the formation of PCDD/Fs in municipal waste incinerator systems may be reduced by up to 80-90% by injection of chemical inhibitors such as ammonia, ethanolamines and ethylenediaminetetra-acetic acid (EDTA) into the waste gas stream. In principle this approach could be applied in the EAF since it seems possible that there will be some de novo synthesis of PCDD/Fs on particulates in the waste gas system.

Clearly, a better understanding of the fundamental factors that influence the formation of PAHs, PCBs and PCDD/Fs would be of considerable benefit in preventing, or minimising the formation of these substances in EAFs and in EAF scrap pre-heating systems. However, it must be recognised that secondary abatement measures may still be required to meet stricter emission limits that are likely to be applied in the future. As already discussed, the secondary measures that have been evaluated to date all have reasonable PCDD/F removal efficiencies but they are either costly to operate or carry a safety risk. There is therefore an opportunity for the development of cost-effective means of collecting PCDD/Fs in waste gas streams. Kreisz et al [18] examined the adsorption and desorption properties of technical plastics such as polyethylene, polypropylene, polyvinyl difluoride and polyterafluoroethylene and showed that

polyethylene and polypropylene were excellent adsorbers for PCDD/Fs in the temperature range 60-100°C. Moreover, the PCDD/Fs could be desorbed at 130°C thus offering a potentially attractive means of removing PCDD/Fs from EAF waste gases.

This report presents the findings of a multi-partner multinational research project the main objectives of which were:

(i) To develop a fundamental understanding of the operational factors that influence the formation of PAHs, PCBs and PCDD/Fs in EAF steelmaking.

(ii) To identify conditions that promote and/or prevent the formation of organic micropollutants in the EAF via the de novo synthesis mechanism.

(iii) To investigate the formation of organic micropollutants in a pre-heating shaft.

(iv) To develop measures for preventing the emission of organic micropollutants from shaft pre-heaters by use of internal post-combustion.

(v) To identify optimum design for pre-heating systems on EAFs to meet environmental and economic demands.

(vi) To investigate the reversible adsorption of organic micropollutants on technical plastics as a cost-effective means of removing such substances from EAF waste gases.

2. Organisation of the work

The work was carried out by a fully co-ordinated programme of studies involving Corus UK Limited, BFI, ISQ and CSM. The main focus of work for each partner was as follows:

(i) Corus UK Limited studied the influence of process conditions on the formation of PCDD/Fs, PCBs and PAHs in EAF shops with single- and two-furnace operation without scrap pre-heating, and the use of plastics as adsorbents for the collection of organic compounds.

(ii) BFI investigated the formation of organic micropollutants during scrap pre-heating, in a gas-fired experimental heating shaft, and measures to prevent the formation of such compounds by internal post-combustion.

(iii) CSM carried out studies on a pilot scale system to investigate the de novo synthesis of PCDD/Fs.

(iv) ISQ carried out studies on a production plant to study the effects of scrap quality on the formation of PCDD/Fs, PAHs and PCBs.

3. Background and terminology

PCDD/Fs, PAHs and PCBs represent three large classes of toxic organic compounds that are of environmental concern owing to their toxicities and environmental persistence. General information on the nomenclature, terminology, chemical structures and important sub-groups of these compounds is given in Appendix 1. For the purpose of the work reported here the following terms shall apply:

(i) The term PCDD/Fs refers to the concentration of the 17 targeted 2,3,7,8-chloro substituted PCDDs and PCDFs, expressed in terms of I-TEQ units.

(ii) The term PAHs refers to the mass concentration of the 16 US EPA priority pollutant PAHs.

(iii) The term EC7-PCBs refers to the mass concentration of the 7 so-called EC-7 indicator PCBs.

(iv) The term WHO-12 PCBs refers to the concentration of the 12 so-called WHO-12 'dioxin-like' PCBs, expressed in I-TEQ units.

4. Characterisation of EAF plants with respect to PCDD/F formation

PCDD/Fs and other toxic compounds may be formed as a result of incomplete combustion of organic material. This happens mainly when the temperature is too low, especially between 200 and 600°C. In the EAF, if there is enough air and the combustion temperature is above 950°C and the residence time is long enough, all PCDD/F and other organic material should effectively be destroyed. However, dusts can still contain traces of carbon, chlorine (in form of salts) and trace metals so that as the off-gases cool down, PCDD/Fs and related compounds may be formed by the de novo synthesis on the surface of the dust particles. The amounts of PCDD/Fs formed are dependent on:

(i) The cooling speed of the off-gases, especially the time around 300°C.

(ii) The amount of dust.

(iii) The presence of trace metals, especially copper, which is a very good catalyst for the formation of PCDD/Fs

(iv) The carbon and chloride content of the dust.

(v) The presence of oxygen.

PCDD/F emissions vary from plant-to-plant dependent upon the configuration of the waste gas cleaning system and the temperature profile across it. As part of this project, therefore, it was considered necessary to try to develop a better understanding of the influence of waste gas temperature on PCDD/F formation. Such a study would be easier to conduct if the EAF steelmaking were a continuous process with essentially constant waste gas temperature. However, as is well known the process operates in batch mode and there is often considerable batch-to-batch variation in the operating conditions. As a result the waste gas temperature varies considerably within a given cycle, as shown in Fig. 1, and the peak temperatures and their duration vary from one heat to another. In considering the effects of temperature, therefore there are two factors that need to be investigated:

(i) The de novo synthesis of PCDD/Fs within the waste gas system; and,

(ii) the partitioning of PCDD/Fs between the gas and particulate.

The formation of PCDD/Fs via the de novo synthesis involves the generation of PCDD/Fs by reaction of inorganic chlorides with carbon present in the iron oxide fume in the waste gas system. This mechanism is well established as a means of formation of PCDD/Fs in iron ore sintering and waste incineration processes. The optimum temperature range for this reaction is

250 to 400°C and, in order to minimise formation of PCDD/Fs by this mechanism, it is necessary to ensure that heating or cooling through this range occurs as rapidly as possible. Clearly, in the production of steel by the EAF process the waste gas temperature will pass through the cited temperature range in each batch. The extent of PCDD/F formation will, therefore, depend on the time taken for the temperature change and high levels of PCDD/F formation can be expected to occur if there are sections of the waste gas system where temperatures in the range 250-400°C persist for significant time periods.

The efficiency of bag filters for the collection of PCDD/Fs is critically dependent on the gas/solid partitioning of PCDD/Fs. At low temperatures the volatility of PCDD/Fs is reduced and they tend to partition to the dust particles that are subsequently collected in the bag filter. This effect has been well demonstrated by Werner [19] and it has been noted in the European BAT reference notes [20]. It is important, therefore, to maintain the bag filter temperature below 75°C to ensure that emissions remain below 1 ng I-TEQ/Nm^3 and below 60°C to achieve a PCDD/F concentration below 0.1 ng I-TEQ/Nm^3. The temperature in the bag filter will depend on upstream temperatures, which can vary substantially within and between heats, and the ability of the waste gas cooling system to cope adequately with these variations.

4.1 Measurements on Corus UK Limited EAF plants

All of the trials were performed at the Aldwarke Melting Shop in Rotherham, which is a two-furnace EAF plant, but for part of the time it was operated as a single-furnace shop. This permitted some investigations to be made as to the effects of operating with one and two furnaces for production. The plant layout is shown in Fig. 2 together with some of the sampling locations used in the trials. Essentially, each furnace waste gas system is identical and in each instance the furnace gases pass through a combustion zone where combustion air is supplied via a slice gap in an elbow in the extraction system. The combustion products then pass through a water-cooled section of ductwork into a non-cooled section of ductwork, and finally into a mixing chamber, where canopy air from the secondary extraction system is added to cool the gas prior to cleaning in a bag filter. The waste gases from each furnace are combined and cleaned in a common bag filter plant. Previous unpublished work on a non-Corus EAF plant had indicated that de novo synthesis of PCDD/Fs was possible in the direct extraction system prior to final gas cooling and it was considered important to investigate this possibility as part of the project. Three different sets of trials were performed as follows:

(i) Simultaneous sampling for trace organic compounds was performed at two different points along the direct extraction systems of both furnaces to establish whether de novo synthesis was occurring in the waste extraction system. The sampling points were located as close as possible to the water-cooled duct at one end and to the mixing tower at the other end.

(ii) Measurements were made of PCDD/Fs in the canopy air collected above each furnace in order to ascertain the contribution of secondary air to the PCDD/F concentration at the inlet to the bag filter plant.

(iii) Simultaneous measurements were made of PCDD/F concentrations at the inlet and outlet from the bag filter used for gas cleaning in order to assess the efficiency of the bag filter for the collection of PCDD/Fs.

4.2 Measurements on SN's Long Products Plant at Maia

Measurements were made of PCDD/Fs, PAHs and EC7-PCBs before and after the de-dusting units connected to the EAF. The sampling operations for samples before the de-dusting unit were performed in the main duct of exhaust gases. However, it should be noted that this duct also takes the waste gas from the ladle furnace. This matter was discussed with the plant operators but it was not possible to install a sample probe in any other location that would enable the two gas streams to be distinguished without disturbing production activities.

In addition to gaseous samples, the sampling campaign also included samples of dust collected from the bottom of the horizontal main duct before the de-dusting unit, on one hand; and samples of dust collected in the de-dusting unit on the other hand.

On all samples, the presence of micropollutants, such as PCDDs, PCDFs, PAHs and PCBs were investigated.

5. Effect of scrap composition on formation of PCDD/Fs, PCBs and PAHs

The quality and hence the price of scrap used in the EAF may vary considerably. Some scrap types have a greater organic content than others and it is generally considered that such materials have a greater potential for formation of trace organic compounds. Thus, oily scrap, painted steel, organic-coated steel, steel scrap containing waste plastics from shredding of motor cars and tyre wire may lead to the introduction of significant amounts of organic material into the EAF. Recycling of used tyres is a topic of major current interest. The wire within such tyres is estimated to amount to over 60 kt/a in the UK alone and is one of the few steel scraps not routinely recycled in significant quantities. Changes in legislation banning the use of landfilling for the disposal of tyres, and other legislative drivers such as the end of life vehicle directive will increase pressure to recycle this material. Recovered tyre wire may contain 4 to 7% by weight of residual rubber and pyrolysis of the residual rubber in the EAF may lead to the formation and emission of organic micropollutants. Preliminary trials were therefore carried out during the project to investigate the effects of recycling tyre wire on the emissions of organic micropollutants from the EAF.

5.1 Studies at SN's Long Products Plant at Maia

A specific role of ISQ was to study the influence of scrap composition on the formation of PCDD/Fs in EAF systems. An initial review of scrap usage in SN revealed that the scrap used in the EAF comprised on average about 71% of scrap bought in the national market, 26% of scrap produced internally and 3% of imported scrap.

As outlined above SN receives several different types of scrap, the composition of which may vary according to their origin. For this particular campaign several types of scrap were tested, which did not necessarily represent the type of scrap used routinely for steel production, but were used for the purpose of the investigation. However, in order not to disturb actual steel production, limitations to the test had to be taken into account, and this included controlling the variability of scrap composition within reasonable limits, so that scrap composition could lead to a liquid steel bath that could effectively be regulated by additions.

The initial measurements, made for system tuning, after the de-dusting systems are presented in Table 1, and lead to the conclusion that tighter scrap composition control was needed as no definite trends were observed at all. In this series of tests no PCBs and PAHs

determinations were reported owing to the variability of results. Also, during sampling difficulties were experienced owing to the very high content of dust in flue gases, which caused filter blockage. Particular care therefore had to be taken during this operation, which included the interruption of sampling for filter changing, which could be the source of the variation observed emission values. This, together with the clean-up of samples, prior to laboratory analysis led to highly variable and probably erroneous PAH and PCB emission values which were subsequently disregarded. In some measurements for PAHs, results for benzo(a)pyrene and benzo(ghi)perylene were found with associated coefficients of variation between samples of up to 75%. With regard to EC7 PCBs, these compounds were also found ranging from 40 to 60% of Cl, but the amounts were below the method detection limit. Both these observations for PAHs and PCBs indicate problems related to loss of compounds during the sample clean-up step. As explained before, scrap composition was not controlled during this series of tests, which can also be linked to these erroneous results, which were disregarded.

In fact, the cited process limitations only allowed variability in about 40% (in weight) of the scrap feed to EAF. Nevertheless it was possible to conduct these tests for 4 different types of scrap:

(i) Scrap containing cutting oils.

(ii) Scrap containing PVC (from the automobile industry).

(iii) Scrap without chlorine compounds but with additions of $CaCl_2$.

(iv) Scrap 'without chlorine'.

5.2 Recycling of tyre wire scrap at Corus UK Limited

A trial was conducted during a period of single furnace operation at Corus EAF Melting Shop, and it was arranged that tyre wire additions would be made only in the first basket charge of each melt. Emission sampling was therefore undertaken specifically over the melting of the first basket as well as over the whole steel production cycle. Composite samples were collected over 3 heats with tyre wire addition at the rate of 5 tonnes per heat on one day, and over 5 heats on the second day without the addition of tyre wire. It was possible to monitor only 3 heats with tyre wire addition owing to plant operating difficulties. Details are given in Table 2.

The bag filter plant at the melting shop is equipped with an extractive duct to facilitate the representative sampling of emissions from the process. The extractive duct consists of two separate parts that enable emissions to be sampled from the north and south sides of the ridge vent, respectively, as illustrated in Fig. 3. From the north end duct, waste gas sampling was undertaken during the whole period of the melting cycle for several heats, while from the south end sampling was undertaken during first basket melting only.

6. Laboratory experiments on PCDD/F formation and emission

6.1 Study of the mechanism of formation of PCDD/Fs

Micropollutants, such as PCDD/Fs, are produced through three different chemical mechanisms as reported by international literature [21-31] based on incineration of urban refuse and metallurgical processes. These mechanisms are:

(i) direct synthesis;

(ii) trace-of-the-fire mechanism; and,

(iii) de novo synthesis.

As described in the direct synthesis, micropollutants are formed by direct synthesis from specific reagents (chlorobenzenes or PCBs) present in the loaded materials.

In the trace-of-the-fire mechanism, precursors are formed during the heating at high temperature (600-850°C), via thermal degradation/transformation of organic matter in aromatic compounds with 2 rings.

The above-mentioned mechanisms envisage a reaction of precursors (formed by molecular condensation or re-arrangement) in the gaseous phase (homogeneous reaction) at lower temperature (200-500°C).

The de novo synthesis involves:

- Partial gasification of organic compounds at high temperature. In particular, it is supposed that coal or fly ashes containing carbon, subjected to oxidation up to maximum temperatures of 850°C, give rise to compounds (turbostratic carbon Fig. 4) able to form complex structures involving carbon and oxygen. These structures participate in the subsequent degradation of carbon that produces CO and CO_2 and organic precursors of PCDD/Fs. In this phase, to give rise to precursor formation, the concentration of oxygen must be <6% at high temperature (in the 700-850°C range) and >3% at low temperature (200-700°C).

- The organic products subsequently react at low temperature (200-500°C) with solid inorganic salts containing chloride.

- Precursors and PCDD/Fs are generated when the cooling rate is less than 300°C/s.

- This reaction needs a solid catalyst (heterogeneous mechanism).

Therefore, the process involves the interaction between oxygen and carbon, initially, followed by the production of PCDD/F precursors (temperature range 700-850°C) and, finally the synthesis of PCDDs and PCDFs (temperature range 200-500°C).

A flowchart, describing the conditions necessary for PCDD/PCDF formation, is shown in Fig. 5.

6.1.1 Experimental system for studying PCDD/F formation mechanisms

An experimental system was designed comprising two reactors capable of operating independently at different temperatures. The first reactor operated between 500-1000°C whilst the second reactor was heated in the range 300-450°C. The latter temperature range affords, according to literature data (regarding municipal waste incinerators), the maximum rate of PCDD/F formation starting from precursors.

The first reactor was loaded with 3-5 kg of the synthetic dust (similar in composition to dust produced in the EAF process). Precursor molecules were produced in the first reactor, by the reaction of the oxygen and carbon (or other complex organic particles) present on the dust surface. The experimental system was designed for operating at pilot scale, with a gaseous flow rate of about 2 m^3/h. The gas in the first reactor was a mixture of N_2, O_2, CO and CO_2 similar in composition to the off-gas from an EAF with or without scrap pre-heating.

In the second reactor, according to the theory in the literature, precursors react at 300-450°C producing PCDD/Fs. The PCDD/Fs formed were quantified after different fixed times thus enabling the formation kinetics to be studied. Kinetic experiments were carried out under different oxygen concentrations and reaction temperatures.

6.1.2 Design and construction of the experimental system

The experimental equipment is shown schematically in Fig. 6 and the technical design is shown in Fig. 7. The equipment is named HEART (Heater Apparatus Relating Toxic-compounds). Photographs of the equipment are shown in Appendix 2.

The first reactor of the HEART system operated in the temperature range 350-900°C and was used to generate PCDD/F precursors under different thermal conditions. This heater is a rotary kiln equipped with internal mixing blades. The reactor was rotated at constant speed during the different experiments in order to ensure reproducible solid-gas interaction.

The HEART second reactor was operated at constant temperature: 350 ± 10°C, which is considered, according to the literature, the optimum temperature range to transform the precursors into PCDD/Fs. A system for trapping PCDD/Fs in the gas flow from the two heaters, permitted the total amount of PCDD/Fs produced to be determined as a function of both time and temperature.

Initial setting up and testing of the HEART equipment was carried out to verify that the required temperatures could be achieved and maintained throughout a run. Industrial EAF dust was used for testing and optimising the apparatus. After the first preliminary tests, some modifications to the apparatus were made to ensure that the individual reaction steps were well separated (i.e., gaseous precursor formation in the first heater and PCDD/F formation in the second heater). The geometry of the first reactor was modified and a refractory filter was installed between the reactors to prevent dust carry over from the first reactor to the second one (see Fig. 8).

6.1.3 Experimental design

The experimental design was based on:

(i) the definition of a kinetic model; and,

(ii) preliminary plant data collection.

The first was used to plan the experiments and the second to establish the HEART temperature and oxygen range.

(a) Kinetic model definition

Different mathematical kinetic models were formulated in this phase of the research, on the basis of the more recent literature analysis [21,26]. All the hypothetical mechanisms, to define the kinetic model, were based on the following reactions:

$$n(½\,O_2 + Cs) \xrightarrow{k_1} [C(O)] \xrightarrow{k_2} P_D \qquad \ldots (1)$$

in which C_S are the active sites of the carbon substrate and n is the number of units (½ O_2+ C_S) involved in precursor formation.

The supposed PCDD/F production mechanism could follow two different paths:

$$P_D \rightarrow D \qquad \ldots (2a)$$

or

$$2P_D \rightarrow D \qquad \ldots (2b)$$

The first path supposes a change of configuration while the second path involves a reaction between molecules of precursor.

The kinetic equations for precursors and PCDD/F formation are:

$$\frac{dC_p}{d\tau} = k_a\, C_{O_2}^{0.5}\left(C_O - k_{ps}\tau\right) - k_2\, C_P^{\,2} \qquad \ldots (3)$$

$$\frac{dC_D}{d\tau} = k_2\, C_P^2 \qquad \ldots (4)$$

Where C_p, C_D, and CO_2 are, respectively, the precursor, PCDD/F and oxygen concentrations at time τ, and k_a, k_{ps}, k_2 are kinetic constants where, respectively, $k_{a=}$ (k_1*n_s), i.e. the product between kinetic constant and active sites number, k_{ps} = precursor formation kinetic constant and k_2 = precursor disappearance (to form PCDD/Fs).

This system of differential equations arises from more chemical reactions in series (details of which are give in Appendix 3).

The solution of this system of differential equations was effected through numerical methods (Runge Kutta and trapezium methods) and equations of PCDD/F production with time of reaction were obtained.

These methods determine values of the kinetic constants (k_1 and k_2) values that minimise the summation of the quadratic differences between the experimental value of the PCDD/F concentration and the corresponding value obtained from the mathematical model. Inputs to the model are the experimental conditions: initial powder load, total gas flow, oxygen concentration.

The curve that fits the experimental points describes the reaction evolution with time and the slope gives an indication of the kinetic constants.

(b) Preliminary industrial data collection

An EAF equipped with a scrap pre-heater system was analysed and the data were utilised to set the HEART temperature range and oxygen concentration range in the experiments.

Principal characteristics of the plant were as follows:

- Furnace AC type/EBT
- Cooled panels and roof
- Interchangeable shell
- Shell diameter 5.40 m
- Tapping capacity 75 t
- Liquid heel 40 t
- Total capacity 115 t
- Operating power supply 35 MW
- Minimum tap-to-tap time 52 min
- Coal consumption 15-30 kg/t
- Conveyor total length 48.5 m
- Pre-heating tunnel length 24.25 m

The furnace is equipped with one oxygen and one coal injection lance.

Other collected data were:

- Air injectors position in the pre-heater tunnel (post-combustion running)
- Injection air flow in the tunnel
- Gas flow rate, compositions and temperature in the tunnel
- Layer thickness of the scrap in the pre-heater
- Scrap rate in the tunnel
- Carbon and pure oxygen amount introduced into the EAF

A model, developed at CSM, was used to predict relationship between operating parameters and parameters that were not directly measured. This model is based on a mass-energy balance of the furnace/tunnel system. The outputs are gas flow rate, compositions and temperature in the furnace, the energy losses in the furnace and in the tunnel.

The main operating characteristics and some relevant process parameters obtained in the two different operating practices are shown in Table 3 together with the corresponding values calculated by using the model.

(c) Collection and analysis of EAF dusts

Dusts necessary for setting up the experimental trials were collected from two Italian EAF plants in order to compare their composition. The first was from an EAF with a pre-heater, while the second one was from an EAF without pre-heater.

In the EAF equipped with the pre-heater, the dusts were collected immediately after the charging tunnel, in the settling chamber (see Fig. 9).

In the EAF without a pre-heater, the dust was sampled from the fume treatment bag filter.

Chemical and physical characterisation of the dusts were carried out and the results are given in Tables 4 and 5.

6.1.4 Experiments with the HEART apparatus

It was not feasible to use the process dusts as substrates in the HEART experiments since it was not possible to perform controlled experiments to investigate the effects of variables such as type of carbon and type of chloride salt. Therefore, in order to simplify matters synthetic dusts were prepared that were typical of the two situations considered.

The experiments were organised into five different sets, each of which was designed from the results of the preceding experimental set. These were as follows:

(i) A first set of trials with graphite added to the synthetic dust as carbon source;

(ii) A second set of trials with an 'activated' form of graphite;

(iii) A third set of trials with carbon normally injected into the EAF as carbon source;

(iv) A fourth set of trials with carbon produced by the decomposition of organic compounds in the synthetic dust; and,

(v) A fifth set of trials with 'organic carbon' under different conditions of temperature and oxygen content.

In each set of experiments analyses were performed for PCDD/Fs in the following samples:

- fume evolved during pre-heating in inert atmosphere to identify the presence of potential PCDD/F precursors evolved during this phase,
- fume collected during the treatments at the selected temperatures,
- solvent from cleaning the second reactor after each trial.

(a) Experiments with graphite as carbon source

This first set of experiments was performed in order to compare the PCDD/F formation mechanisms of the dusts coming from EAFs with and without pre-heating systems.

Two types of synthetic dusts were prepared:

- Type 1 was similar in composition to dust collected in the off-gas treatment plant of an EAF without a scrap pre-heater.
- Type 2 was similar in composition to the average quality of a dust collected in the pre-heater of an EAF with scrap pre-heating.

In the preparation of these dusts, the following conditions were applied:

- the carbon added was a graphite type as normally used in the EAF
- the chloride salts were 50% $CuCl_2$ and 50% $FeCl_3$
- the other metals were present as oxides.

The composition of these two types of dusts is reported in Tables 6 and 7.

Five trials were performed using the HEART system with the operating conditions reported in Table 8: two trials (A, B,) were performed with the type 1 dust and three (C, D, E) with the type 2 dust

(b) Experiments with 'activated' graphite as carbon source

This second set of experiments was performed to determine whether an 'activated carbon' could give PCDD/F formation.

The graphite was 'activated' through a thermal treatment. The fly ash (containing carbon) generated by this thermal treatment was collected, analysed and used for preparing the dust with a composition equivalent to the elementary 'PE EAF' (Pre-heater-equipped EAF) (type 2 dust).

According to the conditions of maximum micropollutants formation, as reported in the literature [21,22], two trials (G, F, see Table 8) were carried out under the specified conditions.

(c) Experiments with carbon normally injected into EAF as carbon source

PE EAF electrode residues and other carbon residues that were present in the EAF at temperatures higher than 2000°C were used as carbon source in the third set of trials.

In this case, the following analyses were performed on this source of carbon:

- PCDD/F content; the results showed that the material did not contain these compounds (below the detectable analytical limit),
- X-ray diffraction analysis was performed to ensure that a large proportion of the carbon was present in amorphous form. The results are presented in Fig. 10(a) and 10(b). The X-ray diffraction pattern of pure graphite is shown in Fig. 11, and comparison with Fig. 10(a) and 10(b) confirms the presence of amorphous carbon in the latter. Dusts were prepared containing this material as carbon source and a trial (H, as shown in Table 8) was carried out.

(d) Experiments with carbon produced by decomposition of organic compounds as carbon source

The fourth set of experiments was carried out to assess the capability of organic species present on the particulates in the off-gas from a pre-heater (derived from decomposition of organic compounds in scrap at the inlet to the pre-heater) to produce PCDD/Fs.

The following tests were performed:

(i) Sampling of the normal PE EAF raw materials (scrap not degreased). These raw materials were treated with carbon tetrachloride to extract the organic compounds, which were chemically analysed.

(ii) The more important organic compounds identified by chemical analysis were treated in the HEART system at 700°C with a low oxygen atmosphere (3%) for 30 minutes. Fly ashes collected in the second part of reactor, were analysed.

(iii) Samples of the dusts, after the pre-heater, were collected and qualitatively analysed for identification of organic compounds.

(iv) Comparison was made between the organic compounds present in the fly ashes collected within the reactor [point (ii)] and the organic compound present in the dust [point (iii)].

(v) A new type of synthetic dust was prepared. In this mixture, the carbon substrate was obtained from incompletely burned organic compounds present at the scrap inlet on the PE EAF, with the addition of a very small amount of benzo(a)anthracene, benzo(b+j)fluoranthene benzo(k)fluoranthene and metal oxides (in the same proportion as given by the pre-heater outlet dust analysis). This dust was called Type 2bis.

Appendix 4 shows the identification of organic compounds present on the scrap at the entrance of the PE EAF (Tables A4.1 and A4.2, and in Fig. A4.1). The compounds found were principally long chain fatty acids (LCFA), typically found in lubricants used in hot rolling mill operation.

Appendix 4 also shows the results (Tables A4.3 and A4.4) from the analysis by gas chromatography - mass spectrometry of fly ash extracts and dust collected after the pre-heater, and in Table A4.5 the composition of organic matter of the synthetic dust type 2 is presented.

In order to distinguish between PCDD/Fs formed by the de novo synthesis and PCDD/Fs formed by other mechanisms, two types of experiment were carried out:

(a) Trials with dust type 2bis without inorganic chloride salts

(b) Trials with dust type 2bis with $CuCl_2$ and $Fe\ Cl_3$

In the first HEART reactor, where precursors could be produced, the temperature was fixed at 550°C, which is, according to the literature, the temperature of the maximum rate of precursor production.

Samples were collected at different times (30, 45, 60, 90, 120 minutes) in each trial.
The related experimental conditions are summarised in Table 8 (trials L to O).

(e) Experiments with 'organic carbon' as carbon source

Type 2bis dust (see previous section) was used to obtain the kinetic curve.

Two sets of experiments were carried out with and without inorganic chloride salts, to distinguish between the PCDD/Fs formed by the de novo synthesis and those formed by the other formation mechanisms.

In the first HEART reactor temperature was fixed again at 550°C (that is, according to the literature, the temperature of maximum rate of production of precursor).

Samples were collected at different times between 30 and 120 minutes and subsequently analysed for PCDD/Fs. In cases where significant amounts of micropollutants were produced further trials were carried out in order to define more clearly the influence of oxygen and temperature.

In the experiments the material charge and the gas flow rate were fixed (initial powder load 5 kg; total gas flow 26.5 l/h), whilst the oxygen concentration had three initial values of (5%) 10% and 20%.

Conditions of the whole set of these experiments are summarised in Tables 9 and 10.

6.2 Study of the adsorption and desorption characteristics of PCDD/Fs on EAF dust and plastic

Bag filters are commonly used for gas cleaning on EAF plants because of their high efficiency for the capture of fine particulate. However, their efficiency for the removal of PCDD/Fs from EAF off-gas is dependent on the extent to which the PCDD/Fs partition to the solid phase, which is in turn dependent on the waste gas temperature as demonstrated by Werner [2,19]. Work was therefore carried out to try to develop a better understanding of the effect of temperature on the partitioning of PCDD/Fs towards the solid phase.

Plastics, for example polypropylene and polyethylene, are commonly used in the construction of wet scrubbers due to their corrosion resistance properties and low cost of material. Several reports [31,32] indicate that plastics are capable of PCDD/F adsorption under MWSI (multiple waste solids incinerator) conditions and therefore can be applied as PCDD/F abatement technology in flue gases of thermo-processes. The capacity for PCDD/F adsorption is governed by the equilibrium load on the plastics. The equilibrium load is a function of temperature and PCDD/F concentration [33]. An increase in the temperature or decrease in gas concentration will lead to PCDD/F desorption to the gas phase.

6.2.1 Construction of a laboratory system for studying the adsorption and desorption characteristics of PCDD/Fs on EAF dust and plastics

A laboratory system was designed and constructed to enable experiments to be carried out to study the volatility of PCDD/Fs present in EAF dust in order evaluate the effect of waste gas temperature on the efficiency of the bag filter for PCDD/F removal. For studies on EAF dust, the system, which is illustrated in Fig. 12, comprised three main parts: a regulated supply of nitrogen carrier gas, a sample holder contained within a temperature-controlled oven and a polyurethane foam (PUF) plug for trapping PCDD/Fs entrained in the carrier gas.

For studies on the adsorption and desorption behaviour of PCDD/Fs on plastics, the system was modified as shown in Fig. 13 by the addition of a second temperature-controlled oven so that the temperature of the plastic absorption cell could be varied. The temperatures employed were 60°C, 75°C, 90°C and 110°C. The mass of plastic used was kept constant at 18 g. All connecting parts were glass or PTFE. Two other parts of the experimental rig were analysed for PCDD/F in addition to the ESP dust and the PUF: (1) the glass adsorption cell and (2) the

plastic adsorber. Attempts to extract PCDD/F from plastic using a Soxhlet apparatus were unsuccessful owing to the high temperature employed and also due to the solubility of the plastics in toluene, which was used as solvent for extraction of PCDD/Fs.

7. Pilot plant trials on the formation and destruction of PCDD/Fs in scrap pre-heaters

The exhaust gas of an EAF contains a large amount of energy as heat and chemical energy from incompletely burned components. In order to recover at least a part of this energy, different technologies for scrap pre-heating have been developed and applied in industrial or pilot plant operations.

The EAF off-gas contains a large number of organic compounds, which originate from combustion and pyrolysis of organic materials associated with the scrap charge. The EAF is not an incinerator, but some of the organic material charged with the scrap is burnt in the vessel. The contamination of scrap by organic compounds arises from the fact that scrap originates from end-of-life goods, which are broken down to reclaim the various component materials [34-44]. The EAF and its exhaust system thus behave as a very complex reactor that carries out pyrolysis, combustion and synthesis reactions. Some organic molecules are produced and destroyed within its confines, but others are released outside of the system. Organic molecules that can be produced in this way form a very long list and they are generally referred to in a global way as volatile organic compounds (VOCs) or total hydrocarbon compounds (THC).

The specific contribution of BFI was concerned with the investigation of the formation of organic micropollutants during scrap pre-heating in a shaft pre-heater system and with the development of measures to prevent the formation of such compounds by internal post-combustion. The studies were carried out on a gas-fired experimental plant which was specially modified for the project.

7.1 Design of the pilot scale shaft scrap pre-heater

The pilot scale shaft pre-heater system (see Fig. 14) was designed on the basis of available data from an industrial scale EAF-shaft (Table 11). For industrial scale EAF-shaft pre-heaters, the off-gas flow varies between 10-12 m^3/s and the off-gas temperature ranges from 30°C in the loaded shaft to 1400°C when the shaft is empty. At a scrap flow rate of 100 t/h the specific energy input in the shaft is estimated at 350 kJ/kg scrap, assuming that the energy input and the losses of the shaft are constant during the empty and loaded states. One design criterion for the laboratory shaft was to keep the specific energy input into the scrap and also the specific energy input for the thermal decomposition of organic contamination of the scrap constant. A second design criterion was the composition of the EAF off-gas. The EAF off-gas contains during the entire heating period up to 25% CO and 12% H_2 in the unoxidised area of the off-gas duct. For safety reasons such a high content of combustible gases could not be used in the laboratory so the aim was to generate an oxygen-free hot gas from a gas-fired oven.

The experimental plant, which is shown schematically in Fig. 15, consists of a gas-fired furnace connected to the refractory lined scrap pre-heating chamber, a gas cooling unit and a suction fan. The hot pre-heating gas was generated by combustion of natural gas. The oxygen content of the pre-heating gas was controlled by adjusting the gas/combustion air ratio in the combustion chamber, while the pre-heating gas temperature was adjusted by varying the combustion gas volumetric flow. The hot pre-heating gas was conducted through the scrap-filled pre-heating chamber and a gas cooler by a suction fan. At the entrance of the scrap pre-

heating chamber and at the exit of the gas cooler the gas temperature and composition (O_2, CO, CO_2) was measured by thermocouples and gas analysers. The total volumetric flow of gas through the pre-heating chamber was measured by a Pitot tube located behind the gas cooler. The VOC content of the gas was measured by flame ionisation detector at the entrance to and exit from the scrap pre-heating chamber.

A schematic diagram of the cylindrical scrap pre-heating chamber is shown in Fig. 16. It consists of a steel tube with a length of 500 mm and a diameter of 200 mm. The inner surface is refractory lined to a thickness of 25 mm to reduce the thermal load on the steel shell. To reduce energy losses through the tube wall, the scrap pre-heating chamber was equipped with external heat insulation of mineral fibre and aluminium foil. The inner diameter of the scrap pre-heating chamber is 150 mm corresponding to a scrap volume of nearly 10 l. Using double shredded scrap (see Fig. 17) with a spherical shape as raw material, charge weights of about 18 kg could be achieved compared with charge weights of around 10 kg for low density tin scrap (see Fig. 18). A series of 5 thermocouples was installed within the bulk at one side of the pre-heating chamber to enable the scrap temperature to be measured at different heights in the shaft. The distance between each thermocouple was 100 mm. The first thermocouple was located 50 mm away from the pre-heating gas entry of the scrap pre-heating chamber. The temperature and gas composition, viz., total VOC, CO, CO_2 and O_2, were measured at the shaft inlet and outlet.

7.2 Operation of the scrap pre-heater

Trials were started after heating up the combustion chamber to the required gas temperature with an open connection to the scrap pre-heating chamber. The shut-off valve at the suction fan was closed. To prevent the penetration of hot combustion gas through the open line between combustion and scrap pre-heating chamber, a small amount of nitrogen was forced to flow into the line at the hot entry of the scrap pre-heating chamber. When the required gas temperature in the combustion chamber was reached, the fan was started, the nitrogen flow was isolated, the shut-off valve was opened and adjusted to the preset gas volumetric flow through the scrap pre-heating chamber. Standard material for the trials was double shredded scrap, which has shown no organic contamination.

8. Results

8.1 Characterisation of EAF plants with respect to PCDD/F formation

8.1.1 Studies at Corus UK Limited

(a) Measurements in the direct extraction system

The optimum temperature range for de novo synthesis of PCDD/Fs and PCBs lies in the range 250 to 350°C. Preliminary measurements made at sampling point D (see Fig. 2) in the direct extraction system of N furnace indicated that temperatures within this range were likely to occur (as shown in Fig. 1) in the section of unlined ductwork between the end of a water-cooled duct and the mixing tower, where the canopy air is added to provide final gas cooling. The transit times along the unlined sections of ductwork are of the order 3 to 5 s, which affords the possibility for de novo synthesis of PCDD/Fs and PCBs to occur. Simultaneous sampling was therefore carried out at the extreme ends of the section of unlined ductwork on both N and T furnaces. For measurements on N furnace sampling points A and B, as indicated in Fig. 2, were used, while corresponding sampling points were used in the extraction system on T furnace.

A total of 12 measurement campaigns covering different stages of operation was carried out with simultaneous sampling. To this end the process was divided into 3 sampling periods of roughly equal duration as follows:

(i) First basket melting.

(ii) Second basket melting and 5 MWh into the third basket melting period.

(iii) From 5 MWh into third basket melting to tap.

In each instance composite samples were obtained by sampling over the appropriate periods of several successive melts. The results of these measurements are presented in Tables 12 and 13.

In early work on N furnace it was found that there was little evidence of PCDD/F formation along the section of unlined ducting between the sampling ports A and B during most of the furnace cycle. There was some indication of an increase in PCDD/F concentrations between the two sampling positions during the first basket melting period. However, later results over the first basket melting period, on both N and T furnace, did not confirm this and further investigations suggested that for some of the sampling time the sample collected at position A may not have been representative of the total flow stream. This is because an air bleed damper, close to this measurement position, opened automatically to limit the waste gas temperature during certain parts of the furnace cycle. The system is designed to protect the unlined steel duct that carries the waste gas across the scrap bay roof before it is cooled in the mixing tower where it mixes with the cooler air from the roof extraction hoods. The air bleed system attempts to restrict the gas temperature to around 480°C in the unlined duct and was found to operate for some time during 7 out of the 12 sampling periods. It can be seen by reference to Tables 12 and 13 that throughout all the samples during which the air bleed remained closed, the PCDD/F levels were very similar at sampling positions A and B. This indicates that, under the conditions pertaining during these tests, little de novo synthesis occurred in this section of the extraction system.

In the light of these findings it is apparent that the tentative relationship between moisture content and increase in PCDD/F between sampling points A and B suggested in the earlier work [45] is not valid. Indeed, under the conditions pertaining at the time of the tests it is not surprising that no relationship could be found between increase in PCDD/F and sampling time spent in the de novo synthesis range ~200 - 350°C. However, the concentrations measured at position B, (where the gases should be fully mixed) are quite variable being in the range 1.5 to 14.5 ng I-TEQ/Nm^3 on N furnace and 3.6 to 39.4 ng I-TEQ/Nm^3 on T furnace for the different parts of the steelmaking process.

PCDD/F concentrations during first basket melting, discounting results that might have been affected by the air bleed damper opening, were in the range 2.9 to 14.5 ng I-TEQ/Nm^3 for N furnace and 3.6 to 6.4 ng I-TEQ/Nm^3 for T furnace. During the second basket to tap periods concentrations were generally lower on N furnace, being in the range 1.5 to 5.3 ng I-TEQ/Nm^3, and higher on T furnace being in the range 4.5 to 39.4 ng ITEQ/Nm^3. It is perhaps not surprising that concentrations are different in the two EAF systems because PCDD/F formation will depend on the necessary precursors being available (which originate from the scrap charge) and on the waste gas temperature history and composition. However, no correlation could be established between scrap type and PCDD/F concentration. Furthermore, no correlation could be found between the concentrations of residuals (Cu and Sn) at melt out and PCDD/F concentrations measured in the direct extraction ducts.

It is known that some grades of scrap are more likely to contain small amounts of coated material or electrical wiring but it cannot be assumed that every charge that contains this grade also contains coated material or electrical wiring. Consequently, it is not known whether the precursors are always present and further, if they are, that conditions in the extraction system are conducive to the formation of PCDD/Fs.

In the later trials, data were also obtained on the concentrations of WHO-12 PCBs and PAHs in the direct extraction system. Concentrations of PCBs were typically about one-sixteenth of the concentrations of PCDD/Fs and were in the range 0.19 to 2.4 ng I-TEQ/Nm^3. The PCDD/F and PCB data exhibited a strong linear correlation as is evident from Fig. 19. The concentrations of PAHs were mostly in the range 8.3 to 169 µg/Nm^3, although much higher concentrations were observed (570 to 607 µg/Nm^3) on a heat on N furnace that was subject to a production delay. These higher concentrations are regarded as being atypical of normal practice. Further analysis of the data showed that there was no correlation between the concentrations of PAHs and PCDD/Fs.

8.1.2 Measurements in the secondary extraction system

The secondary extraction system is designed to capture fugitive fume released during periods when the direct extraction is not available, e.g., during charging and tapping, or when the extraction is unable to cope with the rate of fume generation. From a consideration of the operation it was anticipated that the potential for release of PCDD/Fs to the secondary extraction system would be highest during basket charging when the furnace roof was removed. Any organic matter present in the charge would be expected to undergo pyrolysis leading to the generation of a complex mixture of organic degradation products. Once the furnace roof has been replaced the direct furnace extraction should ensure that the release of organic degradation products is minimised. Two types of sample were therefore collected from the secondary extraction systems of N and T furnaces. These comprised continuous samples collected over a number of casts, and incremental samples where the sampling was performed only during basket charging or tapping. For N furnace the location of the sampling point is indicated in Fig. 2, whilst an equivalent sampling point was used for sampling from T furnace secondary extraction system. Details of the measurements carried out and the results obtained are summarised in Table 14.

Initial results indicated that PCDD/F concentrations in N canopy duct during continuous sampling were generally less than 0.1 ng I-TEQ/Nm^3 although one continuous sample exhibited a PCDD/F concentration of 0.15 ng I-TEQ/$Nm^{3.}$ It was considered that PCDD/F emissions in the secondary extraction would peak during basket charging and tapping events, as VOC concentrations do, and consequently a sample was collected which incorporated several basket charging and tapping events over three consecutive days. This sample yielded a PCDD/F concentration of 0.12 ng I-TEQ/Nm^3, higher than all the continuous samples apart from one. Later continuous samples from both N and T furnace secondary extraction ducts again afforded PCDD/F concentrations below 0.1 ng I-TEQ/Nm^3. It is worth noting that the three highest results all involved sampling when fragmented scrap or no. 1 basic scrap was used as part of the charge. This material on occasions can contain some electrical wiring or coated material. However, there were occasions when fragmented scrap or no. 1 basic scrap had been used during the sampling period and PCDD/F concentrations were found to be much lower, 0.02 to 0.051 ng I-TEQ/Nm^3. Again no correlation could be found between the concentration of residuals (Cu and Sn) at melt out and PCDD/F concentrations measured in the secondary extraction ducts.

The concentrations of PAHs in the secondary extraction systems were typically in the range 26.4 to 55.7 µg/Nm^3 for continuous samples and 64 µg/Nm^3 for the incremental sample, while PCB concentrations were in the range 0.003 to 0.006 ng I-TEQ/Nm^3 on two continuous samples.

8.1.3 Measurements at the inlet and outlet of the bag filter plant

(a) Measurements at Corus UK Limited

Simultaneous 4 h continuous samples were undertaken at the inlet to the bag filter plant and the extractive ducts at the bag filter outlet vent, and the results are summarised in Tables 15 to 17. The PCDD/F concentration at the inlet to the bag filter was around 1.0 ng I-TEQ/Nm^3. Most of the PCDD/Fs were associated with the dust, with approximately 6% in the vapour phase, see Table 15. The average inlet gas temperatures recorded during sampling were 76°C and 67°C for the two samples undertaken. The corresponding minimum and maximum temperatures during sampling were 46 and 119°C and 42 and 104°C. The lower average temperature during the second sample collected can be attributed to a production delay of 84 min on one of the furnaces. The concentrations of WHO-12 PCBs were between one sixteenth and one twentieth of the PCDD/F concentrations and were in the range 0.047 to 0.063 ng I-TEQ/Nm^3 as shown in Table 16. In this instance between 27 and 36% of the PCBs were in the vapour phase, which is attributed to the fact that PCBs are generally more volatile than PCDD/Fs. However, PAHs were mostly present in the vapour phase, with less than 20% associated with the dust (see Table 17).

At the bag filter outlet PCDD/F emission concentrations were in the range 0.13 to 0.16 ng I-TEQ/Nm^3 and 0.07 to 0.12 ng I-TEQ/Nm^3 for the pairs of samples collected. The lower values on each occasion were obtained from the South end of the extractive duct. These values are higher than the vapour phase concentration at the inlet to the bag plant but this is not surprising as a slight discolouration was observed on the filter papers used at this location showing that a small amount of dust was passing through the filter.

(b) Measurements at SN's Long Products Plant at Maia

The results are summarised in Tables 18 to 23 and Figs. 20 to 32. With regard to the waste gas samples the following observations may be made:

(i) the concentrations of PCDD/Fs, PAHs and EC7-PCBs are substantially reduced in the bag filter,

(ii) the congener profile of PCDD/Fs in gaseous samples collected in the main duct exhibit a consistent profile,

(iii) the relative amounts of micropollutants present in the off-gas decreases in the order PAHs>EC7- PCBs>PCDD/Fs both for samples collected before and after the de-dusting unit,

(iv) the observed profiles for PCDDFs are slightly different from samples collected before and after the de-dusting unit. While, for samples before the de-dusting unit, OCDD and OCDF exhibit high concentration levels, in samples collected after the de-dusting unit, these same compounds were present in much smaller quantities. This is attributed to the fact that these compounds have low volatility and partition to the dust in the bag filter,

(v) the observed profiles for PAHs are similar both from samples collected before and after the de-dusting unit.

With regard to solid samples:

(i) samples of dust collected from the de-dusting unit show large quantities of micropollutants, mainly of PAHs and EC7-PCBs, but also PCDDs/PCDFs,

(ii) samples of dust collected from the bottom of the stack, before the de-dusting unit, are almost free of EC7-PCBs as the detected concentrations for these compounds were close to the detection limits of the analytical methods,

(iii) the fingerprint profile for all micropollutant species (PCDD/Fs, PAHs and EC-7PCBs) is similar for both samples collected before and after the de-dusting unit.

The results show that under the temperature conditions found in the bag filter all three families of micropollutants are reduced to varying degrees depending upon their relative volatilities.

8.2 Effect of scrap type on formation of PCDD/Fs, PCBs and PAHs

8.2.1 Results obtained at SN's Long Products Plant at Maia

The chemical composition of EAF dusts associated with the PVC-containing scrap (ii) is presented in Table 24. As may be seen the dust collected in the de-dusting system contains levels of chlorine, ranging from 21.2% to 33.8%, in charges 54668, 54671, 54673, 54682, 54694 and 54696.

The gases were sampled before and after the de-dusting units. Sampling operations on the dirty gas were particularly difficult owing to the very high dust content, which ranged from 8100 to 9600 mg/m^3, with an average value of 9363 mg/m^3. In these instances the sampling had to be interrupted for some minutes to allow filters to be changed in the sampling system.

A second series of tests was made, with sampling before and after the de-dusting system, and the results are summarised in Table 25. The sampling tests were made over 6 h, using the procedure described above, and no significant changes in temperature, pressure and flow were observed during the different sampling operations. In general the ranges of the main parameters were, waste gas temperature 89-95°C; pressure 1008-1018 hPa; moisture content 2.0-2.2%; O_2 content 19.0-19.5%, gas velocity 11.5-13.5 m/s. The sampling volume was around 10 Nm^3. As expected, higher emissions of PCDDs/PCDFs were obtained with scrap containing PVC, the second highest emissions were observed for scrap with cutting oils, then scrap with $CaCl_2$ and the lowest for scrap 'without chlorine'. These emission levels seem consistent with the findings at other existing steelworks.

8.2.2 Results of tyre wire recycling trials at Corus UK Limited

The emission concentrations for PCDD/Fs and PAHs are shown in Table 26 and for SO_2, NO_x and VOC (as total carbon) in Table 27.

For the sampling period that included full heats, PCDD/F and PAH emissions did not increase with the addition of tyre wire at 5 tonnes per heat. The PCDD/F results were 0.074 and 0.033 ng I-TEQ/Nm^3 for baseline and with addition, respectively, and are both substantially below the limit of 0.5 ng I-TEQ/Nm^3 set by the UK Environment Agency for EAF emissions. They are also below the limit of 0.1 ng I-TEQ/Nm^3 set by the European Waste Incineration Directive.

The mean emissions of NO_x and VOCs were also not affected, although there was a small increase in the mean SO_2 emission from 5.1 to 10.8 mg/Nm^3. These results indicate that this practice of tyre wire addition at 5 tonnes per heat does not significantly affect emissions of PCDD/Fs, PAHs, SO_2, NO_x and VOCs.

For first basket melting periods, PCDD/F emissions increased from 0.087 ng I-TEQ/Nm^3 for normal operation to 0.13 ng I-TEQ/Nm^3 with tyre wire addition, and PAH emissions from 2.3 to 3.7 ug/Nm^3. It should be noted, however, that the PCDD/F concentration of 0.13 ng I-TEQ is still substantially below the limit of 0.5 ng I-TEQ/Nm^3 set by the UK Environment Agency for EAF emissions.

These increases could be due to the tyre wire addition or to an atypical production delay that occurred during the first heat with tyre wire addition. After the first basket charge with the tyre wire, the furnace was off-power for about one hour owing to the need to effect a roof delta change. This may have caused the rubber on the wire to be heated for a relatively long period of time within the temperature range of 250 - 350°C that is associated with the formation of PCDD/Fs. During normal production this is unlikely to occur as there is usually very rapid heating and any dioxins formed are likely to be destroyed within the post-combustion chamber. Emissions of NO_x and VOC were similar for both normal operation and tyre wire addition but SO_2 emissions increased from 0.5 to 9.7 mg/Nm^3 during first basket melting.

8.3 Laboratory experiments on mechanism of PCDD/F formation and emission

8.3.1 Experiments with graphite as carbon source

In this first set of experiments, as seen in Table 8, PCDD/Fs were not present in either the fumes or solvent coming from the cleaning of the second reactor after the trial. On the basis of the results obtained and, also, on the basis of the organic analysis of the two different industrial dusts, where no significant differences were noticed, only dust type 2 was used in later experiments.

8.3.2 Experiments with 'activated' graphite as carbon source

Complete absence of PCDD/Fs was found, hence it was decided to use another form of carbon for addition to synthetic dust.

8.3.3 Experiments with carbon normally injected into EAF as carbon source

No PCDD/Fs were detected in these experiments. Owing to the absence of formation of micropollutants in the previous steps, additional trials were conducted to establish the source of the 'non- extractable carbon' [21-23] in the fly ashes, that gives rise the normal level (50-5000 pg/g) [23] of micro pollutants in the EAF.

8.3.4 Experiments with carbon produced by decomposition of organic compounds as carbon source

The experiments carried out with synthetic dust containing organic carbon, are shown in Table 8. These results show a maximum micropollutants production of 170 pg/g. This value resulted from a combination of all the micropollutant formation mechanisms.

8.3.5 Experiments with 'organic carbon' as carbon source

The results of the first, second and third sets of experiments clearly demonstrated that there was no formation, or at least no detectable formation of PCDD/Fs. No difference was noticed between Type 1 dust (similar to dust of an EAF without scrap pre-heater) and Type 2 dust (similar to the PE EAF). This absence of micropollutants was probably due to the materials used for the carbon in the dust (graphite and 'graphite similar') and to the conditions of high energy necessary for the degeneration of microcrystalline graphite layers, a condition not reached in any of the aforementioned trials. In the third set trials, in which scrap carbon electrode material was used, the absence of PCDD/F production was also observed. As a consequence the energy did not reach a sufficient level to activate the carbon injected in PE EAF.

In the trials carried out with 'organic carbon' a maximum micropollutants production of 250 pg/g was observed involving a combination of all PCDD/F formation mechanisms. This value suggests that the de novo synthesis contributes to the total PCDD/F production to a lower degree than the other formation mechanisms.

Although the maximum indicated value (175 pg/g) is lower, with respect to those normally detected in the off-gas from EAFs as reported in the literature, minimisation of PCDD/F emissions could be achieved, on the basis of the following evidence derived from these experiments:

(i) carbon fly ashes derived from 'graphite similar' carbon injected into the EAF, are not a potential source of PCDD/Fs,

(ii) the source of carbon for all PCDD/F formation mechanisms is produced by partial combustion of organic compounds.

From these considerations, it follows that a direct correlation of potential formation of micropollutants with carbon amount in the fly ashes (that is typical of the kinetic studies on de novo synthesis carried out for municipal waste fly ashes [22]), cannot be achieved for EAF fly ashes, in which a part of fly ash carbon matrix comes from 'graphite-like' carbon (or pure graphite).

Attention must then be focused on the minimisation of the organic compounds charged to the EAF. It has been demonstrated that the presence of chloride salts is a negligible factor compared with organochlorine compounds, present in the atmosphere as precursor formed at high temperature.

8.3.5 Definition of a kinetic expression for PCDD/Fs

The HEART trials permitted all the formation mechanisms viz., direct synthesis, trace-of-the-fire mechanism and the de novo synthesis, to be analysed. The last mechanism could be quantified, through the difference in the amounts of PCDD/Fs observed in trials with and without $CuCl_2$ and $FeCl_3$.

The kinetic curve obtained experimentally exhibits qualitatively different trends for the trials with and without inorganic chloride salts, so different approaches were followed for the evaluation of the results.

8.3.6 Kinetic expression for direct synthesis and trace-of-the-fire mechanism

Important boundary conditions and simplifications were introduced, following the analysis obtained by experimental trials without chloride salts. These simplifications were performed to improve fitting of the experimental points and to produce a more realistic representation of the PCDD/F production with time.

Exact and immediate solution of the differential equations is possible taking into account the considerations described in the following:

(i) No detectable oxygen flow variation was observed between the inlet and outlet gas flows in the reactor during the trials.

(ii) The production of micropollutants was 5 orders of magnitude lower than the amount of organic carbon introduced. So active site concentration, and the amount of active carbon could be supposed to be constant with time.

(iii) In these two mechanisms, in which there is an absence of a catalyst, precursor formation is negligible, according to the literature, so at T<500°C, with reference to reaction (1) (see below), $k_2 >> k_1$.

(iv) It is assumed that the precursors have a structure very similar to the final ones and that the PCDD/F formation is achieved through a rearrangement of the precursor. This means that the second formation mechanism (trace-of-the-fire) is more important than direct synthesis. This observation is confirmed by the industrial dust analyses that do not contain primary precursors (organochlorine compounds with one aromatic ring).

(v) According to the considerations in Section 6.1.3 (a) on the definition of the kinetic model the reaction of PCDD/F formation (2) becomes:

$$P_D \rightarrow D \qquad \ldots (5)$$

And the Equation (3), for the considerations 1, 2 and 3, becomes:

$$\frac{dC_p}{d\tau} = -k_2 C_p \qquad \ldots (6)$$

Therefore,

$$\frac{dC_p}{C_p} = -k_2 \, d\tau \qquad \ldots (7)$$

Integration with respect to time gives:

$$\ln C_p = -k_2 \tau \quad \ldots (8)$$

$$C_P = C_p^0 e^{-k_2 \tau} \quad \ldots (9)$$

where C_p^0 is the precursor concentration that could potentially give PCDD/F. This value, to a first approximation, is proportional to the initial amount of introduced organic compounds.

Inserting Equation (9) in Equation (6)

$$\frac{dC_D}{d\tau} = k_2 C_P^0 * e^{-k_2 \tau} \quad \ldots (12)$$

Also in this case it is possible to solve exactly the differential equation:

$$C_D = k_2 C_P^0 \int e^{-k_2 \tau} d\tau \quad \ldots (13)$$

$$C_D = C_P^0 \left[1 - e^{-k_2 \tau}\right] \quad \ldots (14)$$

Trials permit quantification of C_p^0 and k_2 for the different T.

In Appendix 3 the analysis of the results of the experimental trials is reported.

This analysis gives as a result that the values of C_p^0 are temperature and oxygen independent, confirming the fact that the precursors are already present, being formed in the treatment at T>700°C.

So the average value is:

$$C_p^0 = 164.71 \pm 8 \text{ (pg/g)} \quad \ldots (15)$$

The following relation gives the trend of C_D with temperature:

$$C_D = (164.71 \pm 8)\left[1 - e^{(0.0024x^3 - 0.0835x^2 + 0.9074x - 1.5667)\tau}\right] \quad \ldots (16)$$

($x = O_2\%$)

the equation that gives the best fit to the experimental data point k_2 v $O_2\%$ (see Appendix 3) is:

$$k_2 = 0.0024 O_2^3 - 0.0835 O_2^2 + 0.9074 O_2 - 1.5667 \quad \ldots (17)$$

(a) Kinetic expression for de novo synthesis

The difference between PCDD/F formation, obtained operating with and without inorganic chloride salts, represents the contribution of de novo synthesis.

The following considerations, through analysis elaborations, were possible:

(i) For each set of trials (with fixed initial O_2) the oxygen concentration in the reaction atmosphere could be considered constant, in space and time.

(ii) The PCDD/F formation is clearly influenced by the initial amount of oxygen and the reaction temperature.

(iii) Produced micropollutants are, in this case, six orders of magnitude less than the organic carbon introduced. So concentration of active sites, and the amount of carbon active (C_g) could be considered constant with time.

(iv) According to the literature, the precursor formation, thanks to the catalytic action, is possible at T<500°C.

(v) It is assumed (according to Huang and Buekens [21]) that one or two molecules of precursors are involved for PCDD/F formation.

(vi) The mathematical models described in Appendix 3 were used.

The precursor concentrations vary with time as follows:

$$\left(\frac{dC_p}{d\tau}\right) = k_a C_{O_2}^{0.5}\left(C_0 - k_{ps}\tau\right) - k_2 C_p \qquad \ldots (18)$$

in the case where one precursor molecule forms one PCDD/F molecule.

The PCDD/F production is described by:

$$\frac{dC_D}{d\tau} = k_2 C_P \qquad \ldots (19)$$

In the case where two precursor molecules form one PCDD/F molecule, the kinetic equations are:

$$\left(\frac{dC_p}{d\tau}\right) = k_a C_{O_2}^{0.5}\left(C_0 - k_{ps}\tau\right) - k_2 C_p^{\,2} \qquad \ldots (20)$$

and

$$\frac{dC_D}{d\tau} = k_2 C_P^2 \qquad \ldots (21)$$

It follows that the unknown parameters of the system are k_1 and k_2.

The integration of the system was performed by numerical methods such as the Runge Kutta and trapezium methods.

The resolution gives a cubic curve.

This curve, theoretically, could be explained with the following considerations: if precursor concentration depends only on formation, the term $-k_2C_p$ in Equation (18) could be ignored. So:

$$C_p = C_p^0 + a\,t - b\,t^2 \quad \ldots (22)$$

where

$$a = k_a C_{O_2}^{0.5} C_0 \text{ and } b = \tfrac{1}{2} * k_a\, k_{ps}\, C_{O_2}^{0.5} \quad \ldots (23)$$

and the expression of PCDD/F concentration with time becomes a cubic polynomial.

$$C_D = C_{D0} + m\,t + nt^2 + ot^3 \quad \ldots (24)$$

where

$$m = k_2 C_p^0,\ n = 1/2 * k_a\, k_2 C_{O_2}^{0.5} C_0 \text{ and } o = -\,1/6 * k_a\, k_2\, k_{ps}\, C_{O_2}^{0.5} \quad \ldots (25)$$

In Table 28 the values of the coefficients, were obtained by trial result calculations. The coefficient m depends on temperature, while coefficients n and o, depend on the oxygen concentration (%), (see also Appendix 6, Fig. A6.1- A6.3, Table A6.2), according to the following expressions:

$$m = 4.5 * 10^{-3}\, T^2 - 3.257\, T + 586.09 \quad (T = \text{temperature } ^\circ C) \quad \ldots (26)$$

$$n = -3.333\, O_2^3 + 29.64 O_2^2 - 77.02\, O_2 + 66 \quad \ldots (27)$$

$$o = -0.2781\, O_2^2 + 3.664\, O_2 - 12.027 \quad \ldots (28)$$

From the evaluation of the data, it is possible to develop a simplified expression that gives the PCDD/F hourly production, due to de novo synthesis, taking into account that:

(i) the PCDD/F hourly formation is clearly influenced by oxygen (Tables A6.1- A6.3) and,

(ii) the PCDD/F hourly production (see Table A6.4) is approximately constant with the temperature variation (the variation is similar to the measurement error.

So, as reported in Appendix 6, being in conservative state, the PCDD/F hourly production could be quantified as follows:

$$\text{PCDD/F (pg/g h)} = 0.271 * e^{\,0.278 * O_2} \quad \ldots (29)$$

(b) Kinetic equation discussion

Identification of the kinetic expression owing to the different mechanisms of PCDD/F formation in EAF (with pre-heater) was carried out by consideration of experimental trial results.

A generalisation of this expression could be made considering that:

(i) The de novo gives an order of magnitude less than the 'direct synthesis' and 'trace-of-the-fire' mechanisms;

(ii) In the 'direct synthesis' and ' trace-of-the-fire ' mechanisms, the C_P^0 value could be considered, in first approximation, proportional to the initial concentration of the organic matter present in the scrap:

$$C_P^0 = aC_P^0 \quad \ldots (30)$$

where C_P^0 is the organic carbon initially present expressed in ng/g.

From the kinetic expression (15) the value of a is given by:

$$a=0.164/1700 = 9.65.10^{-5} \quad \ldots (31)$$

So the PCDD/Fs with time could be well represented (with an error of 10%) by the expression:

$$CD = \left(9.65.10^{-5} C^{\circ}C\right)\left[1 - e^{\left(0.0024x^3 - 0.0835x^2 + 0.9074x - 1.5667\right)\tau}\right] \quad \ldots (32)$$

This expression permits the rate of production of PCDD/Fs to be evaluated, for different oxygen concentrations present in the reaction atmosphere (x=O2%).

(c) Optimum design for pre-heating systems to meet environmental and economic demands

In the EAF conditions for micropollutants formation could, typically, be reached in different process phases and plant areas, in particular during the transient conditions and in some fume treatment zones.

In this context, the EAFs equipped with pre-heaters are not subject to some degree to such drawbacks, thanks to the continuous scrap loading and to the whole plant being structured to maintain steady state.

The EAF considered in this activity has been equipped with a system for cleaning the off-gases produced in the different sections of the plant. This system is equipped with on line temperature and oxygen sensors, which permit the necessary countermeasures against micropollutant emissions to be effected. In addition, on the basis of the analysis carried out in the present work, the identification and quantification of the conditions necessary for the micropollutants minimisation are obtained.

With the aim of highlighting potential micropollutant formation zones and the possible operational countermeasures, the following were performed:

(i) Examination of the existing industrial situation,

(ii) definition of the principal parameters (oxygen, temperature and fume residence time) for each section of the plant.

- Data for theoretical qualitative forecast of micropollutant formation

The data used to define temperature, oxygen concentration and residence time in the different plant sections were derived by direct measures or by a custom-built mass and energy balance model (MB).

The data refer to stationary and continuous scrap loading.

A theoretical study was carried out using a scheme for an Italian EAF equipped with a pre-heater, which may be divided into four sections as follows:

(i) EAF.

(ii) Pre-heater.

(iii) Connection tunnel between furnace off-gas and pre-heater.

(iv) Gas cleaning plant and stack (cooler, bag filter, stack).

EAF

The temperature of the gases in the EAF, measured inside the furnace is higher than 1400°C (1500°C ± 100°C).

MB calculations, supported from direct measurements, were carried out for the determination of oxygen and CO.

The model hypothesizes different flows of excess air that partially reacts with the carbon, being the total quantity of excess air entering the EAF dependent on the plant configuration (type of used lance, degree of opening of the slagging door and type of connection between pre-heater and furnace).

Owing to incomplete combustion, the gas leaving the EAF contains non-equilibrium concentrations of CO, CO_2 and O_2.

In Appendix 6 diagrams and figures for the theoretical qualitative forecast of micropollutant formation are presented. Table 31 presents an example of the course and composition evaluated with the MB model (RAF: Reactive excess air); NRAF: non-reactive false air).

The residence time is estimated from the following data:

- Average waste gas flow rate: 7500 Nm^3/h, equal to 6.25 m^3/s),
- waste gas temperature 1500°C,
- EAF gas volume of 22 m^3.

Therefore, the gas residence time in the furnace is of the order 3-4 s.

Pre-heater

The temperature profile in the pre-heater was determined using recorded temperatures in fixed sections of the pre-heater at 2, 15, 20 m from the EAF.

The resulting temperatures were in the range 800°C-1200°C; the actual temperatures close to the EAF and near the scrap loading section being 1050°C ± 100°C and 900°C ± 100°C, respectively.

The oxygen concentrations in the pre-heater were obtained by direct measurement at the beginning and at the end of the pre-heater tunnel. These values were in the range of 3-7% (near EAF) and 8-10% (near the scrap loading section).

The value of gas pre-heater flow, calculated from the carbon mass balance, was in the range 15,000-20,000 Nm^3/h.

The linear velocity and residence time of the gas in the pre-heater were about 5 m/s and 5 s, respectively. These values were calculated assuming a duct cross-sectional area of 4 m^2 and an average gas flow of 19,000 Nm^3/h, equivalent to 57,000 m^3/h at the average gas temperature of 1000°C.

Gas connection tunnel

Gas temperature and oxygen concentration were measured about 20 m from the exit of the pre-heating tunnel.

The average temperature was 710 ± 100°C and the oxygen concentration was in the range 13-14%.

The gas residence time was about 4-5 s.

Gas cleaning plant

Because direct measurements were not available for this section, extrapolation of the accessible information was carried out.

The following assumptions were made:

- a gas temperature change of about 300°C in the cooler
- a temperature change of about 60°C before the bag house
- an average temperature in the bag filter of 100°C
- a temperature at the stack in the range 80-120°C.

The oxygen concentration was taken to be in the range 13-21%, to a first approximation, a linear variation.

Based on a fume flow rate 50-60 Nm^3/s, cooler volume of about 70 m^3, a duct volume of 600 m^3, and a bag filter volume of about 240 m^3, the residence times are:

- 1s in cooler
- 10 s in duct
- 4 s in the bag filter.

(d) Qualitative prediction of micropollutant formation in the EAF

The plant is shown schematically in Fig. 33. Thermal profile, oxygen and gas residence times in the different section of the plant are reported.

The plant situation could be summarised as follows:

EAF

High temperatures (>1250°C). Possibility of PCDD/F formation: nil.

In this area there is, therefore, low risk of PCDD/F production and no countermeasures are required.

Pre-heater

- Gas temperature above the scrap surface is in the range 950-1150°C,
- oxygen content is 3-6%,
- gas residence time with O_2 concentration >6%: 5 s.

From these data, the possibility for micropollutant formation in the pre-heater atmosphere is very low. Table 29 presents the value obtained using expression (32), considering that the PCDD/F content in the fumes is due to the particulates in the fume (conservative condition:150 mg/Nm^3), with the temperature of the fume about 100°C. (PCDD/F present at solid phase).

$C_D = 0.164\text{-}0.164 * e^{-k_2 t} = 0.160795532$ (ng/kg in 1 h)

If the dust concentration is the waste gas in

0.00015 kg dust/Nm^3:

then the resulting PCDD/F emission is

0.02411933 ng/Nm^3

Precursor formation could occur if the temperature of the gas above the scrap was notably different from the temperature of the air trapped in the existing interstices (between the pieces of scrap).

Nevertheless, in this case, there is the possibility of adopting a rapid and efficient countermeasure having identified the zone concerned, through appropriate controls (temperature under the scrap and presence of oxygen).

Such controls could be affected both by regime and transient conditions.

Figure 34 represents, as an example, the location of the zone (ABCD area) to be optimised. In this zone the process must guarantee a temperature over 700°C, in presence of oxygen >6% for a time (>2 s) necessary to completely destroy all the organic matter.

Gas connection tunnel

The conditions existing in the fume connection tunnel are as follows:

- Temperatures from 700° at the entrance up to 600°C at the exit (with a variation of 100°C),
- oxygen content 6-20%,
- residence time of gas about 6 s.

In this section the recorded gas temperature is >600°C, which does not permit PCDD/F formation, although precursor formation is possible. Nevertheless in the cooler the temperature falls rapidly and if the cooling is always under control the possibility for micropollutant generation is slight.

Gas cleaning plant

In this section the temperature is always <250°C. There is, therefore, no possibility for PCDD/F formation. This area is characterised by a low risk of micropollutant production and no countermeasures are required.

8.4 Studies on the adsorption and desorption characteristics of PCDD/Fs on EAF dust and plastics

8.4.1 Desorption of PCDD/Fs from EAF dusts

A series of experiments was carried out to evaluate the performance of the laboratory system wherein samples of EAF dust were heated for 20 h at 80, 110 and 150°C. At the end of the heating period the EAF dust and the PUF were analysed for PCDD/Fs in order to determine the extent to which PCDD/Fs had been mobilised from the dust to the gas stream. The results are presented in Table 30, from which it may be seen that the release of PCDD/Fs increases with temperature. Interestingly, however, the total I-TEQ of PCDD/Fs found on the PUF and EAF dust after heating was significantly greater (~20-32%) than that present initially in the dust. The total concentration of tetra-to-octa PCDD/Fs (i.e., the sum of targeted 2,3,7,8-congeners and other non-2,3,7,8-congeners) also increased on heating by ~13-24%. Such large discrepancies are not easily accounted for in terms of analytical uncertainties in the determination of PCDD/Fs, and these data suggest the possibility of PCDD/F formation at temperatures in the range 80-150°C, with increasing rate of mobilisation of the PCDD/Fs as the temperature is increased. The average concentration of PCDD/Fs in the exit gas is plotted as a function of temperature (t) in Fig. 35 and the equation of this curve indicates that the PCDD/F concentration is proportional to the 6.5th power of the temperature. The increased amount of PCDD/Fs (as either I-TEQ or total tetra-to-octaCDD/Fs) found after heating in inert atmosphere was surprising but a possible explanation is that lower chlorinated congeners (mono-, di- and triCDD/Fs) are converted to higher chlorinated species by reaction with inorganic chloride present in the dust. It should be emphasised, however, that these were preliminary experiments and will need further investigation to confirm their validity. Nevertheless, these experiments illustrate the importance of temperature on the gas/solid partitioning of PCDD/Fs and hence on their retention in bag filters.

8.4.2 Re-examination of earlier information on PCDD/F emissions from the EAF

The results of the laboratory studies reported in Section 8.4.1 prompted a re-examination of data, predating this project, that was collected at Aldwarke Melting Shop, which it was thought would be relevant to the work in this project. This earlier work was aimed at investigating the effect of scrap type on emissions. In the event, it proved difficult to arrange for sufficient control of scrap input to allow proper evaluation of this aspect, but a considerable number of samples were taken, analysis of which has proved interesting.

At the time this work was undertaken the extractive ducts had not been installed on the bag filter outlet at Aldwarke Melting Shop and, therefore, samples were collected by sampling along the ridge vent of the bag filter. In this work, short-term samples were taken from the ridge vent of the bag filter using a non-standard technique. Normally, sampling for PCDD/F involves continuous extraction of a dust and gas sample for 4 - 6 h, giving very limited time resolution. However, it was calculated that a sufficient mass of material for analysis could be collected by using a modified high volume sampling system (as used for environmental sampling of ambient air) in about half an hour, so that resolution could be improved. The high volume samplers were fitted with polyurethane foam filters (PUFs) to act as PCDD/F sorbent traps instead of the more usual XAD resin. This had previously been shown to give equivalent results. Typical volumes sampled were 3 to 8 m^3.

The measurements taken were made on a single filter compartment each time, to give a manageable number of samples for analysis, and on any day comprised several short-term samples, with a longer term high volume sample encompassing the totality of short-term samples for check purposes.

A plot of the PCDD/F concentration versus mean bag filter temperature for the short-term samples (see Fig. 36) appears to confirm bag filter temperature as the major influence on emission level. Scrap type did not seem to have a large effect since, for any particular temperature range, all the PCDD/F concentrations appear to form part of the same population. It should be remembered, however, that scrap type influences off gas and hence bag filter temperature, particularly during the early stages of melting each basket of scrap.

Figure 37 shows the results plotted on a logarithmic concentration scale for comparison with the data reported by Werner [2]. Also included are some longer-term samples from the same filter from these and earlier tests, and some results from other plants, including data from DDS reported in an earlier ECSC study. All appear to follow the temperature trend shown by Werner, although the spread is quite wide. The DDS measurements and those from another non-Corus UK plant were made in the stacks after the filters, and stack temperatures have been used for the plot: the corresponding bag filter temperatures would be expected to be several degrees higher, which would move the points nearer to the Aldwarke data.

For some of the samples, the PCDD/F in the gas phase and that associated with the dust particles were analysed separately. Less than 10% of the PCDD/F was associated with the particulate material, suggesting that volatilisation or some form of desorption was a major mechanism in determining emissions. It is also likely that, for these samples, PCDD/F emissions are hardly related to dust emissions.

In an attempt to quantify the temperature effect, results for the total set of short-term samples for the 3 days were plotted as a single series and a regression line fitted. This is shown in Fig. 38 where a dependence on temperature to the power 5.6 is given, i.e., a similar order of magnitude to that observed in the laboratory data. Although the relationship is reasonably clear (R^2 = 0.88) there is still a spread of about a factor of 2 in concentration for a given

temperature. The process operating data pertaining to each sample period were examined in an endeavour to explain this. No consistent factors were evident, but it was noticed that for some of the samples the variation of bag filter temperature over the period was quite small. These points, shown as circles in Fig. 37, appeared to lie on a smooth curve similar to the regression line, suggesting that instantaneous temperature might be the chief controlling factor.

To test whether the relationship holds at higher temperatures, plots of bag filter temperature for samples in which higher temperatures were encountered were taken, and a series of constant temperatures applied to approximate the real time curve (see Fig. 39). Concentrations in the range covered by the curve in Fig. 38 were ascribed to these levels, except for the highest temperature. The concentration corresponding to this temperature was then evaluated by equating the sum of the time weighted known concentrations plus the unknown value for the highest temperature to the measured mean concentration for the sample. The square points in Fig. 38 were determined by this method, and again seem to fit the relationship well.

Since these new points pertained to consistent temperature levels, they were plotted, with those originally seen to have a small temperature variation, in Fig. 40. To extend the range to lower temperatures some data from a stainless steel producing plant, with very low emissions were included. The relationship derived, i.e. concentration (ng I-TEQ/Nm^3) = 2.9×10^{-14} x temperature$^{6.98}$ appeared to give a remarkably precise fit, with an R^2 value in excess of 0.99.

Ostensibly, therefore, PCDD/F emissions for Aldwarke at this time could be predicted, taking the curve in Fig. 40 to represent the instantaneous emission level at any particular temperature. It is also possible that at least some of the spread of concentration for a given mean temperature in Figs. 36, 37 and 38 might be explained by the possibility of generating a particular mean temperature from a variety of temperature histories. A mean temperature derived from a profile incorporating large variations above and below the mean would be expected (because of the dependency of emissions on the 7th power of temperature) to correspond to a higher mean emission than that of a flatter profile. It is reasonable, therefore, that the curve in Fig. 40 lies towards the bottom of the spread in Fig. 38.

As a check on the consistency and validity of this relationship, PCDD/F emissions for all the sample periods in the 3 trial days were predicted. The relationship was applied to the bag filter temperature in each time increment (1 min 44 s) of the logged data, the mass emission calculated using the predicted concentration and logged instantaneous flow, and the summed mass emissions divided by the total volume passed through the filter during the sample period.

These predicted mean emissions are compared with the measured values in Fig. 41. The linear regression line of unit slope, small zero error, and high correlation, gives confidence that emissions could be predicted to acceptable accuracy.

At the time of these short-term sampling tests, typical PCDD/F concentrations in the dust collected by the filter were 1000 - 2000 ng-ITEQ/kg. In the more recent work forming part of this project, concentrations on the dust were much lower (see Table 32) lying in the range 97 to 1190 ng I-TEQ/kg but mostly within the range 97 to 642 ng I-TEQ/kg, and the measured emissions were lower. Moreover, the measured values were lower by an order of magnitude than the levels that could be predicted from filter temperature records using the relationship derived from the earlier short-term samples. It would appear, therefore, that the temperature relationship holds only where there is sufficient PCDD/F in the dust adhering to the filter bags to act as a more or less inexhaustible source for volatilisation.

8.4.3 Adsorption and desorption characteristics of PCDD/Fs on plastics

In order to investigate the possibility of using technical plastics for removal of PCDD/Fs a range of experiments with varying parameters was conducted. These experiments are listed in Table 32. The initial experiments were conducted using PTFE tubing to connect some parts of the system, which resulted in adsorption of PCDD/F onto surfaces of the plastic. The amounts of PCDD/F lost in this way could not be quantified since the recovery of PCDD/F from the analysis of the tubing could not be achieved through the standard rinsing procedure used in US EPA Methods 23 and 1613, and this resulted in errors in the overall PCDD/F mass balances in experiments 1, 2, 3 and 4 where PTFE tubing was employed.

The partitioning of the total targeted PCDD/Fs to different parts of the experimental apparatus using (i) 5 mm polypropylene spheres, and (ii) commercial polypropylene powder was investigated. As seen in Fig. 42, the 5 mm polypropylene spheres were not efficient at adsorbing PCDD/Fs. It is possible that as these uniform spheres were produced from molten polypropylene, which has been extruded, there is a lack of the necessary surface texture for PCDD/F capture i.e. pore surface is small. Polypropylene powder, on the other hand, was able to adsorb 2622.6 ng/kg or approximately 12% of total PCDD/F. Table 33 shows PCDD/F concentration for each targeted congener in the different parts of the experiment of system when polypropylene spheres (5 mm) were used as adsorber and Table 34 shows PCDD/F concentration for each targeted congener in the different parts of the experimental apparatus when polypropylene powder was used as adsorber.

Experiments 5-10 (see Table 32) were conducted using glass tubing. Similar to blank experiment 1, blank experiment 5 was used as a comparison to estimate PCDD/F adsorption on to connecting tubing. Glass tubing gave better recoveries than PTFE. This is evident from a comparison of the recoveries of ^{37}Cl and ^{13}C labelled PCDD/F isotopes used as sampling standards in blank experiments 1 and 5 (Table 35), where an approximate 30% difference was observed between the recoveries with the two different types of tubing used. This finding suggests that PTFE also has the capacity for PCDD/F absorption. Table 36 presents the mass balances of PCDD/Fs in the experimental apparatus using PTFE tubing. This table also shows the PCDD/F loss owing to adsorption on PTFE and the remaining unaccounted loss of PCDD/Fs. The percentage loss of PCDD/F to PTFE (PTFE loss, L) is obtained by subtracting the percentage of vapour phase PCDD/F congeners in blank experiment 5 from the percentage of vapour phase PCDD/F congeners in blank experiment 1. The initial concentrations of dust phase PCDD/F congeners were the same in each experiment. As expected the lower chlorinated congeners exhibited a higher loss to PTFE than the less volatile chlorinated congener. The unaccounted loss of PCDD/Fs from the system is hard to explain but was approximately 20-30% for all congeners. As seen in Fig. 43, there was a slight increase in observed PCDD/F adsorption onto polypropylene with an increase in temperature from 60°C to 90°C. At these temperatures PCDD/Fs were not detected in the PUF.

Figure 44 is a more accurate representation of PCDD/F distribution, which is a percentage based on vapour phase PCDD/F. Polypropylene heated from 60°C to 75°C resulted in a small increase in PCDD/F absorption of 2%. However, with a further increase in temperature by 15°C to 90°C, a further 15% PCDD/F adsorption onto polypropylene was observed. Based on percentage of I-TEQ the total PCDD/F absorption on polypropylene at 90°C was approximately 65%. This temperature range was higher than the typical temperature range for PCDD/F absorption of 60°C - 70°C reported by Andersson et al [33] in a wet scrubbing system. At 90°C, the total PCDD/F load was 1 ng/g of polypropylene used. This value is lower when compared to 6 µg/g load reported by Kreisz et al [46]. Since the container is also part of the PCDD/F removal system a near total capture of PCDD/F is achieved up to 90°C. At 110°C,

the effect of PCDD/F desorption was observed indicating that the polypropylene has achieved its optimum temperature dependent load at 90°C.

Kreisz et al [46] reported a higher rate of PCDD/F desorption (ten-fold increase) with similar increase in temperature during sampling of PCDD/F polypropylene construction material of a wet scrubber in a MSWI operated at 65°C, 80°C and 95°C. The same authors also reported desorption of PCDD/F from polypropylene at a lower temperature (80°C). This higher rate of PCDD/F absorption and desorption in the latter work may be attributed to the presence of particle phase PCDD/Fs in the waste gas, which is not present in gas stream of this experiment i.e. the adsorption and desorption rate reported was a combination of pure PCDD/F and particle bound PCDD/F. The difference in the amount and the shape of polypropylene used can also effect the rate of desorption. In this experiment polypropylene powder was packed in a glass tube as compared to the thin coating layer employed in a wet scrubber.

Experiment 10 was conducted to study PCDD/F desorption. Polypropylene containing PCDD/F was obtained from experiment 6 (plastic heated at 75°C for 8 h). At 120°C, 5% or 2.1 ng/Nm^3 of PCDD/F captured on polypropylene was desorbed and released into the vapour phase (Fig. 45). This amount was smaller than the vapour phase PCDD/F in experiment 9. This observation can be attributed to the fact that some of the PCDD/F in experiment 9 was not captured by polypropylene and is released directly into the vapour phase at this temperature. This also indicates that PCDD/F once absorbed onto polypropylene is not easily released. Figure 46 shows the homologue proportion of vapour phase PCDD/F in the desorption experiment conducted at 120°C. The bulk of vapour phase PCDD/F consists mainly of tetra- and penta-PCDD/F. Desorption of dioxins from polypropylene will continue with increasing temperatures up to 130°C (Kreisz et al [18,31]), which is the softening point of the polymer. Kreisz et al [31] reported a complete desorption of PCDD/F from polypropylene spheres (100 µm diameter) at 130°C after 24 h.

In Fig. 47 the PCDD/F adsorption on polypropylene powder is presented. The polypropylene PCDD/F profile contains higher concentrations of tetra- and penta-substituted congeners when compared to those of the dust samples after heating at temperature between 60°C-90°C. This profile was similar to that of vapour phase PCDD/Fs when the polypropylene filter was not attached to the experimental equipment. All congeners increased at a steady rate with increase in temperature in the range 60°C-90°C. At 110°C there were more octa- and hepta-substituted congeners owing to desorption of lighter congeners. This finding provides further evidence that separation of PCDD/F on to polypropylene occurred through absorption rather than adsorption. This is because the absorption process is affected by the vapour pressure of the substance to be absorbed at a given temperature whereas in the adsorption process is not. Kreisz et al [46] reported relatively small amounts of tetra- and penta-substituted PCDD/F on polypropylene material in a wet scrubber of a MSWI at 60°C. The polypropylene loading profile reported was more similar to those of profiles observed at 110°C. This was reasonable since the MSWI gas cleaning system has been reported to be operational for a long period time.

Figures 48 and 49 show the effect of temperature on PCDD/F homologue distribution within other components of the experimental apparatus in ng/kg and I-TEQ/kg respectively. All profiles from the different parts of the apparatus were typical of steelworks dust and did not change substantially with temperature except the container and the PUF contained a higher concentration of lower chlorinated PCDD/F. This was expected since lower chlorinated congeners have higher vapour pressures. The vapour pressures of PCDD/Fs decrease by approximately one order of magnitude per extra chlorine atom (Rordorf [47]). In addition, the diffusivities of lower chlorinated PCDD/F in polypropylene are higher compared higher

chlorinated species (Kreisz et al [32]. The most significant change was within the PUF at 90°C-110°C. At this temperature, the concentration of PCDD/F homologues and also the 2,3,7,8-congeners increased owing to desorption of PCDD/Fs from the glass container and also to an extent from the plastics (Table 37). It is interesting to note that desorption of penta- and tetra-PCDD/F originated from the dust or the plastics and is not adsorbed onto the container or the glass tubing leading from the dust holder to the plastics.

Figures 50 and 51 show the effect of temperature on 2,3,7,8-PCDD/F congener distributions within the experimental rig in ng/kg and I-TEQ/kg respectively. The PCDD/F concentration of the dust was not constant throughout experimentation despite similar conditions used. Although observed in total PCDD/F concentration and homologue figures, this phenomenon is more evident when the 17 2,3,7,8-congeners are considered.

The studies performed in the work suggest that polypropylene powder is a better absorber of PCDD/Fs than polypropylene granules (5 mm diameter of spheres).

The optimum temperature for PCDD/F absorption on polypropylene powder was 90°C but at 120°C, breakthrough occurred consisting of the lower-chlorinated and more toxic PCDD/F.

8.5 Formation and destruction of VOCs in scrap pre-heaters

8.5.1 Studies on the generation of VOCs in the pilot-scale scrap pre-heater

Trials were run in three stages:

(i) Study of scrap pre-heating behaviour.

(ii) Study of VOC emissions with known organic contamination at the scrap surface without oxygen in the pre-heating gas.

(iii) Study of VOC emissions with known organic contamination at the scrap surface with oxygen in the pre-heating gas.

All trials of stages (i) and (ii) were carried out at a pre-heating gas temperature of 900°C and a gas flow of 50 m^3/h. As base material double shredded scrap was used, because this material exhibited no VOC emissions in preliminary scrap pre-heating tests. To ensure a clean scrap charge the material was thermally treated at 800°C before the addition of defined amounts of oil for the pre-heating trials.

Figure 52 shows the heating properties (T_1 to T_5) at different scrap levels in the shaft as a function of time during a selected pre-heating trial. At the beginning of the trial the scrap temperature at the hot entry rose steeply and reached a temperature of more than 600°C after 3 min. Subsequently the rate of temperature rise decreased owing to decreasing temperature difference between pre-heating gas and scrap as driving force for the heat transfer. With increasing distance from the hot entry the temperature increase was reduced. The charge was totally heated up after about 2 h, at which time the temperature difference between entry and exit of the scrap pre-heating chamber was about 50°C owing to the thermal losses through the wall of the pre-heating chamber.

Figure 53 shows the measured VOC concentration in the off gas versus time during a selected scrap pre-heating trial. At the start of scrap pre-heating the VOC concentration increased sharply and reached maximum concentration in excess of 1200 ppm after 3 min. Then the VOC concentration decreased and was almost zero after 2 h. The corresponding mean scrap temperature at the peak VOC concentration was about 400°C with a temperature gradient of 600 to 250°C between the hot and cold ends of the scrap charge. After about 0.5 h the mean scrap temperature reached about 650°C, when the corresponding VOC concentration had decreased to 25 ppm. It was observed that more than 95% of the total VOC emission occurred within the first 30 min of the commencement of heating.

From a mass balance the relative amount of VOC, which is defined as the ratio of the total VOC mass in the off-gas of the scrap pre-heater to the total carbon mass of the oil contamination, was calculated. The total mass of VOCs in the scrap pre-heater off-gas was obtained by numerical integration of the time-dependent VOC concentration. Figure 54 shows the relative amount of VOCs produced during scrap pre-heating with oxygen-free pre-heating gas, as a function of the oil concentration on scrap. The symbols correspond to measured values from selected pre-heating trials. An additional trial with an unusually high oil concentration on the scrap of 2.5% yielded a value of 15% relative VOC amount. These findings lead to the conclusion that the relative amount of VOCs amount is independent of the oil concentration on scrap. The rather low values of the relative VOC amount show clearly that most of the carbon content of the oil must be pyrolysed to non-volatile elementary carbon remaining on the scrap surface, because combustion of the oil is impossible under oxygen-free conditions. It appears that there are two processes that occur simultaneously during pre-heating of oil contaminated scrap under oxygen-free conditions:

(i) evaporation of light molecular weight organic compounds from scrap surface,

(ii) pyrolytic polymerisation of organic compounds to non volatile solid carbon at the scrap surface.

To determine the effect of free oxygen on VOC generation during scrap pre-heating, trials were carried out with an oxygen content of about 10% in the pre-heating gas at the same gas temperature. Figure 55 shows the relative VOC amount versus oil concentration on scrap. Surprisingly, the values of the relative VOC amount were slightly higher in this situation but were in the same range as those found under oxygen-free conditions. This leads to the conclusion that the oxidative destruction of VOC is impossible via oxygen enrichment of the pre-heating gas since the VOCs are generated at moderate temperatures below 600°C which are too low for oxidative degradation.

8.5.2 In-shaft VOC post-combustion trials

The experimental simulation of in-shaft VOC post-combustion involved selectively injecting a hydrocarbon mixture via a dosing nozzle into the stream of hot gas. The oxygen supply was adjusted between 0 and 7 vol.-% during the trials. It was to be examined in the trials to what extent the hydrocarbon mixture in the hot, cleaned scrap charge could be degraded. The concentration of the hydrocarbon mixture in the furnace off-gas as it entered the charge was geared to the levels of hydrocarbons contained in contaminated scrap. Total in-shaft combustion of the organic constituents makes the utilisation of any additional combustion chamber superfluous. The energy gained through post-combustion is negligible. The advantages of in-shaft post combustion are threefold. Firstly, reduction in cost for pre-heating the off-gases upstream; secondly, there is no need for a separate combustion chamber; and, thirdly, there is a smaller space requirement.

The trials that were conducted involved the use of propane/butane mixture and toluene as typical representatives of hydrocarbons. The parameters for the trials, namely oxygen concentration, amount of hydrocarbons, off-gas volume flow and off-gas temperature, were varied and are shown in Table 38.

The maximum concentration of hydrocarbons attained in the off-gas stream amounted to 3500 ppm. This maximum concentration was consistent with the levels that emerged during the heating of contaminated scrap in the preceding trials. The concentration fluctuations arose from the operationally required changes in the off-gas oxygen contents. The VOC concentrations upstream and downstream of the scrap charge were subjected to a comparative analysis in order to determine the influence of the charge on hydrocarbon degradation. It is clearly evident that there were no differences in the measured VOC concentrations, meaning that the scrap charge had no influence on hydrocarbon degradation. The reduction of hydrocarbons in an oxygen-rich off-gas atmosphere consequently took place within the volume of the injection plane and scrap layer entrance. The residence time of the gas in that volume was about 0.3 s. Figure 56 shows the measured hydrocarbon conversion versus temperature. For 4% oxygen in the pre-heating gas the extent of hydrocarbon combustion increased linearly in the range of 40-100% at temperature of 600 to about 690°C and above 700°C the total combustion occurred. At 2% oxygen concentration the extent of combustion was significantly lower, and at 690°C it reached about 40% only. To achieve complete hydrocarbon conversion it is necessary to have a temperature of about 700°C, a mean residence time of 0.3 s and an oxygen concentration in the pre-heating gas of more or equal 4%. All these conditions must be met at industrial installations to be sure of achieving post-combustion of the organic constituents.

8.5.3 Concept for in-shaft post-combustion of organic constituents

At present, post-combustion in the most common type of scrap pre-heating installation, i.e. shaft systems, takes place in a separate downstream combustion chamber, for which energy is additionally needed to heat the gases. A more economical approach is an operating mode in which the generated emissions are combusted directly at the top of the shaft through the mixing of hot furnace off-gases and VOC-laden off-gases from the scrap charge. With the organic emissions being generated entirely during tapping, during the opening of the fingers and during the charging of the scrap into the shaft, the post-combustion can be conducted selectively, for which purpose it is necessary to split the flow of furnace off-gas. As Fig. 57 shows, part of the furnace off-gas is conducted through the cold scrap, as usual. The remainder of the gas flow is passed around the scrap and reunited with the main stream in the upper part underneath the off-gas hood of the shaft. The splitting into two streams of gas takes place after temperature adjustment. When the two streams of gas are reunited, the mean temperature must be at least 700°C, thereby assuring to combustion of the VOCs at the top of the shaft. This by-pass approach represents a simple technical solution for a post-combustion system. Based on an off-gas temperature of 1300°C at the top of the EAF and 400°C at the top of the scrap layer in the shaft simple energy calculations shows that it is necessary to split the off-gas stream in a ratio of 1:2 in order to attain the required combustion temperature of 700°C at the top of the shaft, meaning that only around 30% of the EAF waste gas energy is available for heating the scrap charge. This makes it crucial to control the timing when conducting the off-gas stream through the scrap because VOC emission occurs during short times only. In that way it is possible to minimise energy losses through reduced heating of the scrap during gas splitting. Compared with EAF units where a shaft is used without off-gas stream splitting, the energy requirement increases by roughly 5% for an operation with short time gas splitting during critical VOC emission phases. The main advantage is that there is no need for an additional post combustion chamber operation.

9. Discussion

9.1 Formation of PCDD/Fs, PAHs and PCBs in the EAF

A fundamental part of the research undertaken in this project was to try to understand the mechanisms of formation of trace organic pollutants such as PCDD/Fs, PAHs and PCBs in the EAF steelmaking process. This task is very challenging because of the fact that the EAF operates in batch mode and conditions may vary considerably, even with what is ostensibly the same feedstock, from one heat to another. Furthermore, there are some parts of the process that cannot be investigated directly because of the hostile environment. These problems make it extremely difficult to develop a fundamental understanding of the key factors that influence the formation and emission of such compounds. Notwithstanding these difficulties the work carried out in this project has led to improved knowledge of the PCDD/F and PCB formation mechanisms in the EAF. The laboratory and theoretical studies carried out at CSM concluded that the main formation mechanism was based on precursor formation at temperatures above 500°C and that less than 10% of PCDD/Fs was formed via the de novo synthesis. This conclusion is supported by the plant measurements in the direct extraction system of EAF furnaces operated by Corus UK Limited, in which it was observed that there was no significant formation of PCDD/Fs in parts of the extraction system where the temperature is more conducive to de novo synthesis. The evidence from plant-based measurements suggested that PCDD/Fs and PCBs were largely formed in a section of water-cooled ductwork where the temperature exceeds 500°C, and where presumably the formation does not occur via the de novo system.

An interesting observation that resulted from the work at Corus UK Limited was the fact that there was a strong correlation between the concentrations of PCDD/Fs and WHO-12 PCBs with the PCDD/F concentrations being approximately a factor of 16.5 times higher than those of WHO-12 PCBs. This suggests that the formation mechanisms of PCBs and PCDD/Fs are linked. This is perhaps not so surprising since PCBs have been shown to be precursors of PCDFs, which comprise about 90% of the overall I-TEQ. These findings also show that the contribution of PCBs to the overall I-TEQ (from PCDD/Fs and WHO-12 PCBs) is insignificant.

9.2 Removal of PCDD/Fs, PCBs and PAHs in the bag filter

Previous work by Werner [1,19] has demonstrated the importance of waste gas temperature on the efficiency of the bag filter for the removal of PCDD/Fs. This was confirmed by the work reported here, where it was found that PCDD/F - temperature data from different plants are consistent with the data reported by Werner. In the work carried out by both Corus UK Limited and ISQ it is shown that under appropriate conditions of temperature PCDD/F abatement efficiencies of >90% may be achieved. However, the laboratory studies and analysis of historical data by Corus UK Limited demonstrated the temperature sensitivity of PCDD/F collection in the bag filter. Both laboratory and plant-based studies carried out showed that the volatilisation of PCDD/Fs from EAF dust exhibited an approximate seventh-power dependency on temperature. The work also showed that under appropriate conditions it is possible to predict the PCDD/F concentration in the waste gas from the temperature profile of the emission. This finding indicates that the temperature profile, i.e. the time - temperature variation is more important than the mean temperature in determining the PCDD/F concentration in the waste gas. Relatively short-term peaks can, therefore, have a strong influence on overall mean PCDD/F concentrations. In the current work, at a mean bag filter temperature of 67 to 76°C, it was observed that more than 90% of the PCDD/Fs reported to the dust, whereas only 60-70% of WHO-12 PCBs and 20-30% of PAHs reported to the dust. These findings are ascribed to the fact that PCBs and PAHs are generally more volatile than PCDD/Fs. Indeed the relatively low efficiency of the bag filter with respect to the

abatement of PAHs is easily explained since the PAH profile was dominated by the more volatile 2- or 3-ring PAHs such as naphthalene, acenaphthene, anthracene and phenanthrene.

9.3 Adsorption of PCDD/Fs on technical plastics

Experiments were performed with polypropylene as an adsorbent for PCDD/Fs and these showed that powdered polypropylene was more effective than polypropylene granules. This difference is attributed to the surface characteristics of the two forms of polypropylene. The optimum temperature for adsorption of PCDD/Fs was 90°C while at 120°C desorption of the PCDD/Fs was allowed. Such a small difference in the optimum temperature for trapping of PCDD/Fs and that at which PCDD/Fs are released is a disadvantage since it would mean that a very tight control would need to be extended in order to ensure effective for cleaning. Often adsorbents such as a activated carbon or lignite coke are effective over a wide temperature range.

9.4 Emission and internal post-combustion of VOCs in a shaft pre-heater

Pre-heating trials on the pilot scale shaft pre-heating system at BFI showed that the maximum VOC emission concentration occurred after the start of the pre-heating cycle when the mean scrap temperature had reached around 400°C. After this the VOC concentration fell rapidly and was effectively zero after 2 h. The relative amount of VOC emitted from the pre-heater appeared to be independent of the oil content of the scrap introduced into the shaft and was effectively constant at around 12.5-15%, in both oxygen-free and oxygen-containing gas atmospheres. It may be concluded therefore, that oil introduced with the scrap is partly evaporated from the scrap surface and partly pyrolysed to solid carbon on the scrap. Both these processes occur at relatively low temperatures (<600°C) which are too low for oxidative degradation to occur. The in-shaft post-combustion trials performed demonstrated that with 4% oxygen in the pre-heating gas total oxidation of hydrocarbons from oil, at a concentration of 3500 ppm, could be achieved at a temperature of 700°C and a mean residence time of 0.3 s. The concept was demonstrated of performing in-shaft post-combustion of VOCs by splitting the EAF off-gas flow such that part of the flow by-passes the pre-heater and is reunited with pre-heating gas flow as it leaves the shaft. The key requirement is that the necessary combustion temperature of 700°C is achieved in the re-combined gas stream in order to ensure complete oxidation of the hydrocarbons in the shaft pre-heating gas. It is therefore essential to have accurate control of the gas-switching to coincide with the period when VOC emission occurs. In this way the energy loss through reduced scrap heating during the period when the by-pass is in operation is minimised.

10. Conclusions

On the basis of plant-based measurements on EAF plants the following conclusions may be drawn:

(i) PCDD/Fs and PCBs were mainly formed in sections of the waste gas system where the temperature exceeded 500°C. There was little evidence of de novo synthesis of PCDD/Fs or PCBs in sections of the extraction system where lower temperatures were found.

(ii) There was a strong correlation between the concentrations of PCDD/Fs and WHO-12 PCBs, with the I-TEQ of PCDD/Fs being approximately 16.5 times higher than that of WHO-12 PCBs. This suggests that the formation mechanisms of PCBs and PCDD/Fs are linked.

(iii) The PCDD/F congener profiles in samples from the direct and secondary extraction ducts at the EAF plants at Corus UK Limited were similar. In each instance the profile was dominated by PCDFs, which contributed typically 80 to 87% to the overall I-TEQ concentration. Invariably it was found that 2,3,4,7,8-PeCDF contributed more than half of the I-TEQ concentration. However, this contribution increases to between 60 and 70% of the I-TEQ in the emission from the bag filter plant, which is presumed to be due to the increased partitioning of less volatile higher chlorinated compounds to the dust.

(iv) Emissions from the bag filter plants at Corus UK Limited and SN's Long Products Plant in Portugal exhibited similar congener profiles, which suggests the occurrence of similar formation mechanism for PCDD/Fs in these EAF plants.

(v) The concentrations of WHO-12 PCBs, expressed in terms of I-TEQ values, were typically around one-sixteenth of the PCDD/F I-TEQ concentrations. The congener profiles were very consistent and the main congeners present were PCBs 77, 105 and 118. However, the main contributor to the WHO-12 I-TEQ was PCB 126.

(vi) Trials at SN's Long Products plant showed that scrap quality had a significant influence on the emission of PCDD/Fs. Higher concentrations of PCDD/Fs were obtained with scrap containing PVC and cutting oils.

From studies on the adsorption and desorption behaviour of PCDD/Fs on EAF dust and plastics the following conclusions may be drawn:

(i) The volatilisation of PCDD/Fs from EAF dust exhibited an approximate seventh-power dependency on temperature. The work also showed that under appropriate conditions it is possible to predict the PCDD/F concentration in the waste gas from the temperature profile of the emission. This finding indicates that the temperature profile, i.e. the time - temperature relationship is more important than the mean temperature in determining the PCDD/F concentration in the waste gas. Relatively short-term peaks can, therefore, have a strong influence on overall mean PCDD/F concentrations.

(ii) Historical data from Corus UK Limited were consistent with the temperature effects reported in the literature by Werner [2,19].

(iii) The efficiency of the bag filter for the abatement of PCDD/Fs, PAHs and PCBs is critically dependent on the waste gas temperature. In the current work, at a mean bag filter temperature of 67 to 76°C, it was observed that more than 90% of the PCDD/Fs reported to the dust, whereas only 60-70% of WHO-12 PCBs and 20-30% of PAHs reported to the dust. These findings are ascribed to the fact that PCBs and PAHs are generally more volatile than PCDD/Fs. Indeed the relatively low efficiency of the bag filter with respect to the abatement of PAHs is easily explained since the PAH profile is dominated by the more volatile 2- or 3-ring PAHs such as naphthalene, acenaphthene, anthracene and phenanthrene.

(iv) Preliminary studies suggest that polypropylene powder is a better absorber compared to polyethylene granules based on temperature tolerance. Polypropylene powder is also cheaper and has better PCDD/F absorption load compared polypropylene granules (5 mm spheres).

(v) The optimum temperature for PCDD/F absorption on polypropylene powder is 90°C. At 120°C, breakthrough occurred consisting of the lower-chlorinated PCDD/F.

From laboratory studies on the mechanisms of formation of PCDD/Fs in the EAF and scrap pre-heating the following conclusions may be drawn:

(i) PCDD/Fs are principally formed from oily contaminants introduced in the scrap charge. Other carbon sources are not significantly involved in PCDD/F formation.

(ii) The main formation mechanism, identified under the EAF conditions considered, is based on precursor formation at high temperature (>500-600°C).

(iii) Catalytic action (considered in de novo synthesis), that permits precursor formation at temperature <500°C, makes a small contribution (less than 10%) to the total PCDD/F formation.

(iv) Kinetic expressions were developed that permit the potential for PCDD/F formation in an EAF system equipped with a tunnel scrap pre-heater to be assessed.

From pilot scale studies on the emission of VOCs from a shaft-type scrap pre-heating system the following conclusions may be drawn:

(i) At the commencement of scrap pre-heating the VOC concentration increased sharply and reached a peak value after 3 min. Thereafter, the VOC concentration decreased and fell to zero after 2 h. The corresponding mean scrap temperature at the maximum VOC emission concentration was about 400°C with a temperature gradient of 600 and 250°C between the hot and cold ends of the scrap charge.

(ii) More than 95% of the total VOC emission occurred within the first 30 minutes of the trial duration.

(iii) The relative amount of VOC produced was independent of the oil concentration on scrap at concentrations up to 2.5% by weight. At such oil concentrations, less than 15% by weight of the carbon in the oil was released as VOCs under oxygen-free conditions. This observation shows clearly that most of the carbon content of the oil must be pyrolysed to non-volatile elementary carbon remaining on the scrap surface, because combustion of the oil is impossible under oxygen free conditions.

(iv) The relative amount of VOC produced in the presence of 10% by volume of oxygen was slightly higher than under oxygen-free conditions and typically around 15% by weight. This leads to the conclusion that oxidative destruction of VOC is impossible via oxygen enrichment of the pre-heating gas, since the VOCs are generated at moderate temperatures below 600°C which are too low for oxidative destruction to occur.

(v) Simulation experiments on the post-combustion of VOCs from scrap pre-heating showed that VOCs were completely oxidised when the oxygen content in the off-gas was at least 4 vol.-%, the gas temperature was above 700°C, and the mean residence time greater than 0.3 s. These conditions must be fulfilled for any industrial use of in-shaft post-combustion.

(vi) Post-combustion of VOCs in typical scrap pre-heating installations takes place in a separate downstream combustion chamber. A more economical approach is an operating mode in which the generated emissions are combusted directly at the top of the shaft through the mixing of hot VOC-free furnace off-gases and VOC-containing off-gases from the scrap charge. Therefore the off-gas stream must be split such that part of the pre-heating gas stream passes through the scrap layer while the other part by-passes the shaft. Both streams are recombined in the upper part of the shaft beneath the off-gas hood of the shaft. The split ratio is controlled by a temperature adjustment. The mean temperature must be at least 700°C, thereby ensuring the combustion of the VOCs at the top of the shaft.

11. References

1. J Pederse: 'Optimisation of environment and related energy utilisation in scrap-based steelmaking (Phase I)', Final Report ECSC Research Contract no. 7210-CB/901.

2. C Werner: 'Control of organic micropollutants from the EAF', Proceedings of the ENCOSTEEL Conference on Steel for Sustainable Development, held in Stockholm, Sweden June 16-17 1997.

3. W Theobald: 'Ermittlung und Verminderung der Emissionen von halogenierten Dioxinen und Furanen aus thermischen Prozessen. Untersuchung der Emissionen polychlorierter dibenzodioxine und -furan und von Schwermetallen aus Anlagen der Stahlerzeugung', VDEh Report, November 1995.

4. 'Identification of relevant industrial sources of dioxins and furans in Europe', Materialien no. 43, Report prepared by North Rhine-Westphalia State Environment Agency on behalf of the European Commission DG XI, Contract no. B4-3040/94/884/AO/A3.

5. J T Jensen: 'Optimisation of environment and related energy utilisation in scarp-based steelmaking (Phase II)', Final Report ECSC Research Contract no. 7210-CB/902.

6. J W Lustenhouwer, K Olie and O Hutzinger: 'Chlorinated dibenzo-p-dioxins and related compounds in incinerator effluents: a review of measurements and mechanisms of formation', Chemosphere, 1980, Vol. 9, pp501-522.

7. G G Choudry, K Olie and O Hutzinger: 'Mechanisms in the formation of chlorinated compounds including polychlorinated dibenzo-p-dioxins', Chlorinated dioxins and related compounds, Pergamon Press, New York, 1982, pp275-301.

8. O Hutzinger, M J Blumich, M van der Berg and K Olie: Chemosphere, 1985, Vol. 14, pp581-600.

9. H Vogg and L Stieglitz: 'Thermal behaviour of PCDD and PCDF in fly ash from municipal incinerators', Chemosphere, 1986, Vol. 15, pp1373-1378.

10. M Scholz, L Stieglitz and G Zwick: 'The formation of PCB on fly ash and conversion to PCDD/PCDF', Organohalogen Compounds, 1997, Vol. 31, pp538-541.

11. P Voss-Spilker, J Ehle, and K Rummler: 'Emission prevention and energy saving in electric arc furnaces by the Fuchs Shaft Furnace technology', Paper presented at a conference on Steel and the Environment in the 21st Century', held in London, 2-3 April, 1996.

12. M Haissig: '21st Century electric steelmaking: the integrated meltshop', Iron and Steel Society 25th Advanced Technology Symposium, held in St. Petersburg Beach, Florida, USA, 11-14 May, 1997.

13. T Smith: 'New concept in EAF energy saving commissioned at Sheerness Steel', I&SM, 1992, Vol. 10, pp57-59.

14. G J McManus: 'Scrap pre-heating: a trend gains momentum', Iron and Steel Engineer, 1995, Vol. 8, pp60-61.

15. R Addinck, R H W L Paulus and K Olie: 'Prevention of polychlorinated dibenzo-p-dioxins/dibenzofurans formation on municipal waste incinerator fly ash using nitrogen and sulphur compounds', Environ. Sci. Technol., 1996, Vol. 30, p2350.

16. L Takas and Moilanen G L: 'Simultaneous control of PCDD/F, HCl and NO_X emissions from municipal waste incinerators with ammonia injection', J. Air Manage. Assoc., 1991, Vol. 41, (5), pp716-722.

17. P Ruokojarvi, I A Halonen and K A Tuppurainen: 'Effect of gaseous inhibitors on PCDD/F formation', Env. Sci. Technol., 1998, Vol. 32, pp3099-3103.

18. S Kreisz, H Hunsinger and H Vogg: 'Technical plastics as PCDD/F absorbers', Chemosphere, 1997, Vol. 34, pp1045-1052.

19. C Werner: 'Maitrise des emissions de micropollutants organiques au four electrique', Revue Metallurgie-CIT, April, 1999.

20. Integrated pollution prevention and control, Reference Document on best available techniques in the Iron and Steel industry.

21. H Huang and A Buekens: 'De novo synthesis of polychlorinated dibenzo-p-dioxins and dibenzofurans-Proposal of mechanistic scheme', The Science of the Total Environment 193, 1996, p121.

22. E R Altwicker: 'Relative rates of formation of polychlorinated dioxins and furans from precursor and de novo reactions', Chemosphere, 1996, Vol. 33, p1987.

23. S Harjanto et al: 'Remediation Technologies Ash', ISIJ International, 2000, Vol. 40, (3), p266.

24. F Baldieri and E Repetto: 'The electric oven: the technical options and the safeguard of the environment', The Italian Metallurgy, 2000, Vol. 7-8, p11.

25. K H Klein: 'Low emission, high productivity ARC electric furnace operation', Scandinavian Journal Metallurgy (Supp.) 1997, Vol. 26, pp16-24.

26. E Kaiseet et al: 'Emission control for arc furnace technology', Proceedings METEC United States Congress 99, 6th European Electric Steelmaking Conference, held in Duesseldorf, 13-15 June 1999, p98.

27. A Sanz et al: 'Advanced approaches to electric arc furnace off-gas management', MPT International, 2000, Vol. 4, p72.

28. A Michielan et al: 'The Daniels Danarco furnace ABS', Revue Métallurgie-CIT, June 2000, p745.

29. A Vallomy: 'Retrofitting of the charge pre-heater and continuous feeder at Golds Martin Spa', Steel Times International, March 2000, p24.

30. A Buekens: 'Dioxin from thermal and metallurgical processes', Chemosphere, 2001, Vol. 42, pp729-735.

31. S Kreisz, H Hunsinger and H Seifert: 'Polypropylene as are generable absorber for PCDD/F emissions control', Chemosphere, 2000, Vol. 40, pp1029-1031.

32. S Kreisz, H Hunsinger and H Seifert: 'PCDD/F diffusion velocities in polypropylene', Organohalogen Compounds, 2000, Vol. 45, pp435-437.

33. S Andersson, S Kreisz and H Hunsinger: 'PCDD/F removal from flue gases in wet scrubbers - a novel technique', Organohalogen Compounds, 2002, Vol. 58, pp157-160.

34. J-P Birat: 'Abatement of organic emission in EAF Exhaust Flue Gas', Electric Furnace Conference Proceedings 2000, pp103-116.

35. H Fisher: 'EAF external post-combustion: a new concept to destroy organics and remove recyclable dust', Proceedings 6th European Electric Steelmaking Conference, held in Duesseldorf, 1999, pp103-110.

36. K-H Deppner: 'Verticon - an efficient an environmentally friendly scrap pre-heater', Steel Times International, 1998, Vol. 11, pp20-23.

37. M Haising: 'Electric ARC furnace technology beyond the year 2000', MPT International, 1999, Vol. 1, pp56-63.

38. B Kleimt and S Köhle: 'Schrottvorwärmung und Nachverbrennung bei der Elektrostahlerzeugung', BFI-Bericht no. 2.32.001, (1996).

39. J Ehle, H Knapp and H Mueller: 'Produktion, Kosten und Umwelteinfluesse beim Betrieb eines Fingerschachtofens', Stahl und Eisen, 2001, Vol. 121, (3), pp45-50.

40. D Yanez, M A Pedroza, J Ehle and H Knapp: 'Shaft furnace technology charging DRI and/or hot metal', Proceedings 6th European Electric Steelmaking Conference, held in Düsseldorf, 1999, pp24-28.

41. E L Malamakis, J Lembke and K Schmale: 'Contiarc commissioning of the new contiarc process Halyvourgia Thessalias', Proceedings 6th European Electric Steelmaking Conference, held in Düsseldorf, 1999, pp69-72.

42. E Kaiser, J Lehner, M Bourge and V Knoth: 'Emission control for ARC furnace technology', Proceedings 6th European Electric Steelmaking Conference, held in Düsseldorf, 1999, pp98-101.

43. J Grubbstroem: 'High temperature scrap pre-heating reduction of organic emissions' Electric Furnace Conference Proceedings, 1993, pp283-287.

44. B Lindblad: 'The influence of pre-treatment steel scrap on emissions at the melting process', Electric Furnace Conference Proceedings, 1993, Vol. 295-298.

45. R Fisher, S S Baker and A M W Briggs: 'Effects of operational factors on the formation of toxic organic micropollutants in EAF steelmaking', ECSC project 7210.PA/200, Report no. D6878-5(ST)022, Corus Research, Development & Technology, Swinden Technology Centre, 2003.

46. S Kreisz, H Hunsinger and H Vogg: 'Wet scrubbers a potential PCDD/F source', Chemosphere, 1996, Vol. 32, pp73-78.

47. B Rodorf: 'Prediction of vapour pressures, boiling points and enthalpies of fusion for twenty-nine halogenated dibenzo-p-dioxins and twenty-five dibenzofurans by a vapour correlation method', Chemosphere, 1989, Vol. 18, pp783-788.

Table 1: Preliminary measurements of PCDD/F emissions with no effective segregation of scrap type

Scrap type	Major Cl presence	PCDDFs (ng I-TEQ/m^3)
A	Yes	1.362
B	No	0.232
C	No	0.582
D	Yes	0.437

Table 2: Chronology of heats during tyre wire recycling trials

Baseline day 27/3/03					
Cast no.	N7566	N7567	N7568	N7569	N7570
First basket charge	-	14:12	15:48	17:23	18:51
Power on	12:42	14:15	16:10	17:24	18:53
Second basket charge	13:16	14:32	16:28	17:44	19:10
Tap	14:02	15:16	17:16	18:30	Trial terminated
Tyre wire addition day 28/3/03					
Cast no.	N7584	N7585	N7586	-	-
First basket charge	15:41	18:11	19:27	-	-
Power on	16:40	18:13	19:29	-	-
Second basket charge	17:00	18:30	19:47	-	-
Tap	18:03	19:17	Trial terminated	-	-

Table 3: Process parameters in the industrial trials carried out. The theoretical values are shown in italics.

Heat	Scrap (t/h)	Pig iron (t/h)	Coal (kg/h)	Oxygen (Nm^3/h)	Fluxes (Kg/h)	FeO (%)	CaO (%)	Temp. steel (°C)	Electrical energy consumption (Kw h/t)	Gas temp. tunnel outlet (°C)
Operating practice 1										
Average	76.5	13.5	1000	1445	2240	26	33	*1635*	427	795
Operating practice 2										
Average	72.8	11.9	1600	2000	2244	19	37	*1641*	409	960

The last two columns (electrical energy consumption and temperature of gas at the end of tunnel) are the main outputs of the calculations. The parameters in the remaining columns are inputs for the calculations

Table 4: Chemical composition of EAF dusts

(%)	Sample 1	Sample 2
C	1.7	1.3
H	0.81	0.12
N	< 1	< 1
S	0.69	0.48
O	-	-
Cl	1.03	1.2
Fe	35.5	14.7
Cu	0.25	0.05
Ni	0.5	<0.1
Zn	14.0	39.0
Pb	2.4	1.0
Cd	<0.1	0.1
Ca	3.0	3.0
F	0.3	0.5
Mn	2.1	1.9
Mg	3.4	1.9
Al	0.1	0.2
Cr	2.5	2.7
Si	6.7	5.2
Na/K	1.5	1.3

Table 5: Particle size analysis of EAF dusts

Particle diameter (μm)	Sample 1 (%)	Sample (%)
>250	1	0
250-90	1.5	1.21
90-32	1.98	1.99
32-20	10.22	3.02
<20	85.3	93.78

Table 6: Type 1 synthetic dust composition

Compound	(%)
C	1.70
FeO	45.35
$FeCl_3$	0.86
$CuCl_2$	0.52
ZnO	18.00
PbO	3.76
MgO	6.70
CaO	5.20
MnO	2.00
SiO_2	11.62
S	0.69
Cr_2O_3	3.60
Total	100.00

Table 7: Type 2 synthetic dust composition

Compound	(%)
C	1.30
FeO	18.91
$FeCl_3$	0.06
$CuCl_2$	0.10
ZnO	48.60
PbO	1.15
MgO	3.20
CaO	4.20
MnO	2.40
SiO_2	8.17
S	0.48
Cr_2O_3	3.80
Total	92.37

Table 8: Trials experimental condition and results

Trial	Dust type	C Type	$CuCl_2$* $FeCl_3$ presences	T (°C) I reactor	T (°C) II reactor	O_2 (%)	Oxidation time (h)	PCDD/Fs ITEQ (pg/g)
A	1	Graphite	Yes	450	300	3	2	2.3
B	1	Graphite	Yes	450	300	3	1	<2
C	2	Graphite	Yes	450	300	3	0.5	<2
D	2	Graphite	Yes	450	300	3	2	2.1
E	2	Graphite	Yes	450	300		1	n.e(*)
F	2	Activated graphite	Yes	700	350	10	2	2.3
G	2	Activated graphite	Yes	700	350	20	2	<2
H	2	Graphite electrodes scraps	Yes	700	350	10	2	<2
La	2bis	Organic compounds	No	550	350	10	0.5	70.03
La	2bis	Organic compounds	No	550	350	10	0.75	127.12
Ma	2bis	Organic compounds	No	550	350	10	1	163.09
Na	2bis	Organic compounds	No	550	350	10	1.5	150.17
Ob	2bis	Organic compounds	No	550	350	10	2	170.66
Pa	2bis	Organic compounds	Yes	550	350	10	0.5	68.87
Qb	2bis	Organic compounds	Yes	550	350	10	0.75	124.6
Rb	2bis	Organic compounds	Yes	550	350	10	1	158.09
Sb	2bis	Organic compounds	Yes	550	350	10	1.5	140.57
Tb	2bis	Organic compounds	Yes	550	350	10	2	157.77

(*) not effected

Table 9: Results of trial with dust type 1bis with organic chlorine salt, temperature 700°C, 1.59 Nm^3/h flow rate

Trial	T (°C) II reactor	% O2	Oxydation time (h)	PCDD/Fs ITEQ (pg/g)	PCDD/Fs ITEQ (ng/Nm^3)
	350	5	0,0	0	0
1a	350	5	2,0	146	918
2a	350	5	1,5	127	599
3a	350	5	1,0	110	346
4a	350	5	0,5	68	107
	300	10	0,0	0	0
5a	300	10	2,0	169	1063
6a	300	10	1,5	146	689
7a	300	10	1,0	124	390
	300	20	0,0	0	0
8a	300	20	2,0	213	1340
9a	300	20	1,0	200	629
	350	20	0,0	0	0
10a	350	20	2	255	1604
11a	350	20	1	203	638
12a	350	20	0,5	152	239
	400	5	0	0	0
13a	400	5	1,5	140	660
14a	400	5	1,0	131	412
15a	400	5	0,5	72	113
	400	10	0,0	0	0
16a	400	10	2,0	165	1038
18a	400	10	1,0	129	406
	400	20	0,0	0	0
18a	400	20	2,0	168	1057
19a	400	20	1,0	147	462
	350	10	0,0	0	0
Ia	350	10	0,5	70	110
La	350	10	0,8	128	302
Ma	350	10	1,0	163	513
Na	350	10	1,5	151	712
Oa	350	10	2,0	171	1075

Table 10: Results of experiments with dust type 2bis without organic carbon

Trial	T (°C) II reactor	% O2	Oxydation time (h)	PCDD/Fs ITEQ (pg/g)	PCDD/Fs ITEQ (ng/Nm^3)	PCDD/Fs ITEQ (ng/Nm^3) De Novo	PCDD/Fs ITEQ (pg/g) De Novo
	350	5	0,0	0	0	0	0
1b	350	5	2,0	143	899	19	3
2b	350	5	1,5	124	585	14	3
3a	350	5	1,0	109	343	3	1
4b	350	5	0,5	67	105	2	1
	300	10	0,0	0	0	0	0
5b	300	10	2,0	155	975	88	14
6b	300	10	1,5	140	660	28	6
7a	300	10	1,0	121	381	9	3
	300	20	0,0	0	0	0	0
8b	300	20	2,0	160	1006	333	53
9b	300	20	1,0	157	494	135	43
	350	20	0,0	0	0	0	0
10b	350	20	2	175	1101	503	80
11b	350	20	1	135	425	214	68
12b	350	20	0,5	130	204	35	22
	400	5	0	0	0	0	0
13b	400	5	1,5	135	637	24	5
14b	400	5	1,0	127	399	13	4
15b	400	5	0,5	70	110	3	2
	400	10	0,0	0	0	0	0
16b	400	10	2,0	155	975	63	10
18b	400	10	1,0	125	393	13	4
	400	20	0,0	0	0	0	0
18b	400	20	2,0	160	1006	50	8
19b	400	20	1,0	143	450	13	4
	350	10	0,0	0	0	0	0
Ib	350	10	0,5	69	108	2	1
Lb	350	10	0,8	125	295	7	3
Mb	350	10	1,0	158	497	16	5
Nb	350	10	1,5	141	665	47	10
Ob	350	10	2,0	158	994	82	13

Table 11: Design data for EAF shaft (100 t/h)

Height of shaft	m	4.0	
Volume of shaft	m^3	55.0	
Cross-sectional area	m^2	13.8	
Diameter	m	4.2	
At the outlet		Shaft with load	Shaft empty
Volume flow	m^3/s	12.5	10.2
Volume flow	m^3/h	45 000	36 720
Gas temperature	°C	30	1 400

Table 12: Initial N furnace direct duct measurements

Sampling details	Sampling position A			Sampling position B			Air bleed (open/closed)
	PCDD/Fs (ng I-TEQ/Nm^3)	PAH (of US EPA 16) (µg/Nm^3)	PCBs (ng I-TEQ/Nm^3)	PCDD/Fs (ng I-TEQ/Nm^3)	PAH (of US EPA 16) (µg/Nm^3)	PCBs (ng I-TEQ/Nm^3)	
First basket melting	6.7	13.5	-	14.5	15.2	-	Open
	5.3	19.3	-	8.9	12.5	-	Open
Second basket melting + 5 MW h into third basket	1.8	39.2	-	2.7	48.5	-	Open
Third basket to tap	5.3	19.1	-	4.9	16.2	-	CLOSED
	1.0	3.6	-	1.5	5.8	-	Open
Sampling blank	0.014	11.3	-	0.0064	11.5	-	-

Table 13: N and T furnace direct duct measurements

Sampling details	Furnace	Sampling position A			Sampling position B			Air bleed (open/closed)
		PCDD/Fs (ng I-TEQ/Nm^3)	PAH (of US EPA 16) (µg/Nm^3)	PCBs (ng I-TEQ/Nm^3)	PCDD/Fs (ng I-TEQ/Nm^3)	PAH (of US EPA 16) (µg/Nm^3)	PCBs (ng I-TEQ/Nm^3)	
First basket melting	T	6.4	78.9	0.346	5.8	169.0	0.359	Closed
	T	5.3	75.9	0.300	3.6	53.4	0.190	Closed
Second basket melting to tap	T	4.7	54.8	0.227	4.5	16.8	0.193	Closed
	T	15.7	30.7	0.549	17.6	21.7	0.579	Open
	T	26.7	59.1	1.480	39.4	45.1	2.400	Open
First basket melting	N	14.8	14.2	0.970	12.2	8.3	0.720	Open
	N	4.1	570.0	0.387	2.9	607.0	0.329	Closed
Sampling blank	-	0.025	10.5	0.0023	0.024	13.1	0.0025	-

Table 14: Secondary extraction (canopy) results

Sample ID	Description	Duration (min)	Events	PCDD/F (ng ITEQ/Nm^3)	PAH (of US EPA 16) (µg/Nm^3)	PCBs (ng ITEQ/Nm^3)
OS/02/184 OS/02/185	N Furnace Continuous	157	Sample collected over two full casts and incorporated melting periods, 6 basket charging events, 2 tapping events and 1 turn round.	0.04	33.5	-
OS/02/186 OS/02/187	N Furnace Continuous	224	Sample collected over three casts and incorporated melting periods, 6 basket charging events, 3 tapping events and 2 turn rounds.	0.02	26.4	-
OS/02/199 OS/02/200	N Furnace Continuous	240	Sample collected over three casts and incorporated melting periods, 7 basket charging events, 3 tapping events and 3 turn rounds.	0.15	31.1	-
OS/02/201 OS/02/202	N Furnace Continuous	240	Sample collected over three casts and incorporated melting periods, 9 basket charging events, 2 tapping events and 3 turn rounds.	0.05	32.8	-
OS/02/218	Sampling Blank	-	-	<0.001	6.0	
OS/02/197 OS/02/198	N Furnace Incremental	114	Sample collected over three days and incorporates 18 basket charging events and 6 tapping events.	0.12	64.0	-
OS/03/083 OS/03/084	T Furnace Continuous	145	Sample collected over two casts and incorporated melting periods, 3 basket charging events, 1 tapping event and 1 turn round.	0.07	55.7	0.006
OS/03/085 OS/03/086	N Furnace Continuous	114	Sample collected over two casts and incorporated melting periods, 2 basket charging events, 2 tapping events and 2 turn rounds.	0.02	52.8	0.003
OS/03/092	Sampling Blank	-	-	<0.001	4.4	0.00046

Table 15: Bag filter plant PCDD/Fs - two furnace operation

Sample ID	Description	Events		Inlet PCDD/F (ng ITEQ/Nm^3)			Extractive duct PCDD/F (ng ITEQ/Nm^3)
		N furnace	T furnace	Dust	Vapour	Total	
L/3/W/023 L/3/W/024	4 h continuous sample	Sample collected over almost 3 full casts incorporating melting periods, 9 bskt charging events, 2 taps and 2 turn rounds.	Sample collected over almost 2 full casts incorporating melting periods, 4 bskt charging events, 1 tap and 1 turn round.	0.952	0.064	1.016	0.13 - 0.16
L/3/W/025 L/3/W/026 L/3/W/027	4 h continuous sample	Sample collected over almost 2 full casts incorporating melting periods, 5 bskt charging events, 1 tap and 1 turn round and delay of 84 min.	Sample collected over almost 3 full casts incorporating melting periods, 5 bskt charging events, 2 taps and 2 turn rounds.	0.870	0.060	0.930	0.07 - 0.12
L/3/W/028	Sampling blank	-	-	-	-	0.0037	0.015

Table 16: Bag filter plant PCBs - two furnace operation

Sample ID	Description	Events		Inlet PCBs (ng ITEQ/Nm^3)			Extractive duct PCBs (ng ITEQ/Nm^3)
		N furnace	T furnace	Dust	Vapour	Total	
L/3/W/023 L/3/W/024	4 h continuous sample	Sample collected over almost 3 full casts incorporating melting periods, 9 bskt charging events, 2 taps and 2 turn rounds.	Sample collected over almost 2 full casts incorporating melting periods, 4 bskt charging events, 1 tap and 1 turn round.	0.046	0.017	0.063	0.025 - 0.031
L/3/W/025 L/3/W/026 L/3/W/027	4 h continuous sample	Sample collected over almost 2 full casts incorporating melting periods, 5 bskt charging events, 1 tap and 1 turn round and delay of 84 min.	Sample collected over almost 3 full casts incorporating melting periods, 5 bskt charging events, 2 taps and 2 turn rounds.	0.030	0.017	0.047	0.014 - 0.022
L/3/W/028	Sampling blank	-	-	-	-	0.0004	0.0002

Table 17: Bag filter plant PAHs - two furnace operation

Sample ID	Description	Events		Inlet PAH (of US EPA 16) (µg/Nm^3)			Extractive duct PAH (of US EPA 16) (µg/Nm^3)
		N Furnace	T Furnace	Dust	Vapour	Total	
L/3/W/023 L/3/W/024	4 h continuous sample	Sample collected over almost 3 full casts incorporating melting periods, 9 bskt charging events, 2 taps and 2 turn rounds.	Sample collected over almost 2 full casts incorporating melting periods, 4 bskt charging events, 1 tap and 1 turn round.	2.44	21.76	24.2	16.1 - 16.3
L/3/W/025 L/3/W/026 L/3/W/027	4 h continuous sample	Sample collected over almost 2 full casts incorporating melting periods, 5 bskt charging events, 1 tap and 1 turn round and delay of 84 min.	Sample collected over almost 3 full casts incorporating melting periods, 5 bskt charging events, 2 taps and 2 turn rounds.	3.80	16.06	19.9	11.5 - 12.3
L/3/W/028	Sampling blank	-	-	-	-	1.4	1.7

Table 18: PCDD/Fs in dust before and after bag filter at SN's Long Products Plant at Maia

Dioxins/Furans	05-06-2003 before filter		06-06-2003 after filter	
	ug/kg (ppb)	I-TEQ	ug/kg (ppb)	I-TEQ
2,3,7,8-TetraCDD	0.1	0.117	0.01	0.014
1,2,3,7,8-PentaCDD	1.1	0.572	0.10	0.050
1,2,3,4,7,8-HexaCDD	3.3	0.331	0.16	0.016
1,2,3,6,7,8-HexaCDD	7.3	0.725	0.49	0.049
1,2,3,7,8,9-HxCDD	4.5	0.449	0.31	0.031
1,2,3,4,6,7,8-HeptaCDD	113.4	1.134	2.84	0.028
OCDD	242.0	0.242	3.67	0.004
2,3,7,8-TetraCDF	0.7	0.068	0.30	0.030
1,2,3,7,8-PentaCDF	1.6	0.080	0.33	0.017
2,3,4,7,8 - PentaCDF	2.5	1.246	0.38	0.191
1,2,3,4,7,8-HexaCDF	6.8	0.677	0.67	0.067
1,2,3,6,7,8-HexaCDF	5.4	0.543	0.55	0.055
1,2,3,7,8,9-HexaCDF	3.1	0.308	0.42	0.042
2,3,4,6,7,8-HexaCDF	9.8	0.976	0.83	0.083
1,2,3,4,6,7,8-HeptaCDF	39.9	0.399	1.97	0.020
1,2,3,4,7,8,9-HeptaCDF	7.0	0.070	0.66	0.007
OCDF	47.2	0.047	3.16	0.003
Total ug/kg (ppb)	495.7	7.984	16.85	0.707

Table 19: PAHs in dust before and after bag filter at SN's Long Products Plant at Maia

PAHs ng/g	05-06-2003 before filter	06-06-2003 after filter
Naphthalene	36.3	183
Acenaphthylene	2	24
Acenaphthene	1	1.8
Fluorene	2	40
Phenanthrene	12	307
Anthracene	2	26
Fluoranthene	8.6	238
Pyrene	1	113
Benzo(a)anthracene	1	30
Chrysene	2.6	119
Benzo(b)fluoranthene	2	75
Benzo(k)fluoranthene	2	56
Benzo(a)pyrene	2	28
Indeno(1,2,3)-cd-pyrene	2	80
Benzo(ghi)perylene	2	78
Dibenz(ah)anthracene	2	9.9
total	80.5	1408.7

Table 20: EC7-PCBs in dust before and after bag filter at SN's Long Products Plant at Maia

PCBs ug/kg (ppb)	05-06-2003 before filter	06-06-2003 after filter
PCB 28	5.0	5.0
PCB 52	1.0	2.0
PCB 101	1.0	3.0
PCB 138	1.0	4.0
PCB 153	1.0	3.0
PCB 180	1.0	1.0
Total PCBs	10.0	18.0

Table 21: Average of measurements of PCDD/Fs in waste gas before and after the bag filter at SN's Long Products Plant at Maia

Dioxins/Furans	Before (main duct)	After (stacks)
2,3,7,8-TetraCDD	178	5
1,2,3,7,8-PentaCDD	1123	24
1,2,3,4,7,8-HexaCDD	1293	22
1,2,3,6,7,8-HexaCDD	1868	58
1,2,3,7,8,9-HxCDD	1358	41
1,2,3,4,6,7,8-HeptaCDD	8965	136
OCDD	9443	62
2,3,7,8-TetraCDF	3063	216
1,2,3,7,8-PentaCDF	3985	120
2,3,4,7,8 - PentaCDF	4390	168
1,2,3,4,7,8-HexaCDF	5983	166
1,2,3,6,7,8-HexaCDF	5080	112
1,2,3,7,8,9-HexaCDF	1981	8
2,3,4,6,7,8-HexaCDF	5018	114
1,2,3,4,6,7,8-HeptaCDF	11313	189
1,2,3,4,7,8,9-HeptaCDF	1745	49
OCDF	14700	99

Table 22: Average of measurements of PAHs in waste gas before and the after bag filter at SN's Long Products Plant at Maia

PAHs	Before (main duct)	After (stacks)
Naphthalene	470400	15944
Acenaphthylene	67200	1034
Acenaphthene	4679	41
Fluorene	19480	309
Phenanthrene	85800	782
Anthracene	12060	11
Fluoranthene	39800	98
Pyrene	27000	47
Benzo(a)anthracene	5460	9
Chrysene	11680	16
Benzo(b)fluoranthene	3920	5
Benzo(k)fluoranthene	4300	4
Benzo(a)pyrene	1855	0
Indeno(1,2,3)-cd-pyrene	3476	0
Benzo(ghi)perylene	3500	0
Dibenz(ah)anthracene	455	0

Table 23: Average of measurements of EC7-PCBs in waste gas before and after bag filter at SN's Long Products Plant at Maia

	Before (main duct)	After (stacks)
PCB 28	1277	29
PCB 52	423	13
PCB 101	598	8
PCB 138	231	4
PCB 153	177	3
PCB 180	71	2

Table 24: Chemical composition of EAF dust in SN's Maia plant

Sample / Subs	54668 (%)	54671 (%)	54673 (%)	54682 (%)	54694 (%)	54696 (%)
Sn	0.045	0.048	0.04	0.04	0.037	0.043
Cd	0.035	0.033	0.03	0.044	0.035	0.032
Fe	16.81	19.17	17.38	18.98	19.60	17.64
Mn	0.92	1.48	1.18	0.96	1.16	1.06
Mo	0.0011	0.0010	0.0006	0.001	0.0011	0.0008
Ni	0.013	0.012	0.011	0.016	0.013	0.011
Pb	3.56	3.63	5.46	4.29	3.89	3.22
V	0.0061	0.003	0.0011	0.0008	0.0009	0.001
Zn	18.84	17.00	21.17	17.07	14.39	13.51
Cr	0.062	0.089	0.06	0.075	0.078	0.06
Cu	0.20	0.17	0.15	0.21	0.23	0.18
Al	0.39	0.50	0.36	0.41	0.48	0.41
Na	1.36	0.93	0.91	1.23	1.55	1.54
Mg	0.70	0.82	0.89	0.72	0.93	0.88
Ca	18.54	20.10	18.08	19.37	21.19	22.17
K	1.27	1.02	1.16	1.15	1.00	1.02
As	0.004	0.010	0.007	0.007	0.005	0.006
Cl^-(mg/kg)	21.2	21.2	27.5	32.6	31.2	33.8
SiO_2	3.99	4.79	2.45	3.61	2.75	3.94

Table 25: Results of second series of tests with controlled scrap, before and after de-dusting system

Type of scrap	PCDD/F concentration before de-dusting (ng I-TEQ/Nm^3)		PCDD/F concentration after de-dusting (ng I-TEQ/Nm^3)	
	Individual results	Mean	Individual results	Mean
Scrap with cutting oils	0.812	0.696	0.466	0.464
	0.580		0.462	
Scrap with PVC	13.508	13.917	8.234	9.277
	14.326		10.320	
Scrap with $CaCl_2$	0.484	0.487	0.323	0.325
	0.490		0.327	
Scrap without Cl	0.146	0.139	0.106	0.093
	0.132		0.080	

Table 26: Dioxin and PAH emission concentrations during tyre wire recycling trials

Sampling period	Operation	No of heats	Emission concentration	
			Dioxin (ng I-TEQ/Nm^3)	PAH (µg/Nm^3)
Full heats	Normal operation	5	0.074	14.2
	Tyre wire addition	3	0.033	12.6
First basket melting	Normal operation	5	0.087	2.3
	Tyre wire addition	3	0.13	3.7

Table 27: Emission concentrations of SO_2 NO_x and VOC (as total carbon) during tyre wire recycling trials

Sampling period	Operation	No of heats	Mean emission concentration (mg/Nm^3)		
			SO_2	NO_x	VOC (as total C)
Full heats	Normal operation	5	5.1	17.3	1.6
	Tyre wire addition	3	10.8	10.9	2.0
First basket melting	Normal operation	5	0.5	5.5	1.8
	Tyre wire addition	3	9.7	3.8	2.9

Table 28: Obtained value of m, n, o parameters

Temperature (°C)	Oxygen (%)	m	n	o
300	15	14	4	0
350	10	-2.62	10.98	3.20
350	5	0.16	2	-0.66
350	20	-5.3	124	-50
400	5	3.33	2	-1.33

Table 29: PCDD/F formation in industrial pre-heater: Theoretical calculation

O2 (%)	t(h)	k_2	k_2t	$* e^{-k_2t}$
10	1.00E+00	4.694	4.69E+00	0.019539442
	ng/g	ng/g in 1h	ng/kg in 1 h	
CD =	$0.164-0.164** e^{-k_2t}$ =	0.160795532	160.7955315	
	kg dust/Nm^3	ng/Nm^3		
	0.00015	0.02411933		

Table 30: Results of heating 4 g samples of EAF dust for 20 h at 80, 110 and 150°C

Sample Details	Targeted PCDD/F I-TEQ (pg)			Total Tetra-to-octa PCDD/Fs (pg)		
	Dust	PUF	Dust+PUF	Dust	PUF	Dust+PUF
Base dust	4276	-	-	152236	-	152236
Base dust 80°C	5427	80	5507	176610	4365	180975
Base dust 110°C	4678	452	5130	147570	25028	172598
Base dust 150°C	835	4804	5639	31526	156940	188466

Table 31: Bag filter plant dust sample results

Date	Furnaces operating	PCDD/F (ng ITEQ/Nm^3)	PAH (Σ of US EPA 16) (µg/Nm^3)	PCBs (ng ITEQ/Nm^3)
08/03/02	N	97	1756	-
14/09/02	N	127	3690	-
23/07/03	N & T	335-631	1694-1747	7.3-12.8
19/08/03	N & T	642	1557	11.8
21/08/03	N	464	2301	8.5
28/10/03	N & T	395	2923	12.9
30/10/03	N & T	1190	6459	56.2
04/11/03	N & T	334	1290	10.2
11/11/03	N & T	1001	1976	32.2
20-11/03	N & T	412	2761	10.7

Table 32: Experiments on PCDD/F adsorption using plastics

No.	Plastics properties	Connecting tube material	Temperature (°C)	
			Oven 1	Oven 2
1	-	PTFE	150	75
2	PE powder	PTFE	150	75
3	PP powder	PTFE	150	75
4	PP granules - 5 mm spheres	PTFE	150	75
5	-	Glass	150	75
6	PP powder	Glass	150	75
7	PP powder	Glass	150	60
8	PP powder	Glass	150	90
9	PP powder	Glass	150	110
10	PP powder	Glass	-	120

Table 33: Partitioning of targeted PCDD/Fs to different parts of the experimental system when polypropylene spheres (5 mm) were used as adsorber

	PCDD/F concentration (ng/kg)			
	Dust	Container	PUF	Plastic *
2,3,7,8-TCDD	25.0	0.66	1.01	23.33
1,2,3,7,8-PeCDD	105.0	5.00	0.90	7.90
1,2,3,4,7,8-HxCDD	148.8	7.50	0.00	12.55
1,2,3,6,7,8-HxCDD	420.0	20.00	0.00	30.00
1,2,3,7,8,9-HxCDD	407.5	8.75	0.00	15.05
1,2,3,4,6,7,8-HpCDD	1557.5	41.25	1.25	36.30
OCDD	1166.3	13.75	0.71	10.59
2,3,7,8-TCDF	165.0	0.88	1.24	92.88
1,2,3,7,8-PeCDF	290.0	20.00	1.60	57.20
2,3,4,7,8-PeCDF	771.3	0.99	1.59	227.47
1,2,3,4,7,8-HxCDF	707.5	56.25	1.25	82.50
1,2,3,6,7,8-HxCDF	775.0	57.50	0.00	88.80
2,3,4,6,7,8-HxCDF	1153.8	70.00	0.45	100.80
1,2,3,7,8,9-HxCDF	320.0	16.25	0.00	25.05
1,2,3,4,6,7,8-HpCDF	2410.0	148.75	1.25	147.50
1,2,3,4,7,8,9-HpCDF	370.0	0.68	0.31	25.31
OCDF	1060.0	22.50	0.88	16.62

* estimated

Table 34: Partitioning of targeted PCDD/F to different locations when polypropylene powder was used as adsorber

	PCDD/F concentration (ng/kg)			
	Dust	Container	PUF	Plastic *
2,3,7,8-TCDD	0.5	0.7	0.9	48.0
1,2,3,7,8-PeCDD	75.0	6.3	0.0	37.6
1,2,3,4,7,8-HxCDD	121.3	16.3	0.0	31.3
1,2,3,6,7,8-HxCDD	332.5	42.5	0.0	95.0
1,2,3,7,8,9-HxCDD	331.3	20.0	1.0	79.1
1,2,3,4,6,7,8-HpCDD	1558.8	66.3	0.6	10.7
OCDD	1321.3	20.0	0.8	Negative
2,3,7,8-TCDF	148.8	0.9	1.0	109.5
1,2,3,7,8-PeCDF	200.0	16.3	0.0	152.6
2,3,4,7,8-PeCDF	506.3	65.0	1.3	428.8
1,2,3,4,7,8-HxCDF	526.3	97.5	1.3	222.5
1,2,3,6,7,8-HxCDF	586.3	101.3	0.7	233.1
2,3,4,6,7,8-HxCDF	972.5	128.8	0.8	222.9
1,2,3,7,8,9-HxCDF	281.3	30.0	0.0	50.1
1,2,3,4,6,7,8-HpCDF	2166.3	241.3	0.3	299.7
1,2,3,4,7,8,9-HpCDF	335.0	18.8	0.0	42.6
OCDF	1152.5	32.5	0.8	Negative

* estimated

Table 35: Percentage PCDD/F distribution in the experimental rig using PTFE tubing

	Glass tubing (experiment 5)				PTFE tubing (experiment 1)			
Sampling standards	Dust	PUF	Container	Sum	Dust	PUF	Container	Sum
^{37}Cl-2,3,7,8-TCDD	17	40	2	59	18	14	NA	31
^{13}C-2,3,4,7,8-PeCDF	25	35	15	75	23	18	NA	41
^{13}C-1,2,3,4,7,8-HxCDF	33	24	23	80	24	20	NA	44
^{13}C-1,2,3,4,7,8,9-HpCDF	36	13	23	72	36	17	NA	53
^{13}C-1,2,3,4,7,8-HxCDF	36	19	24	79	29	19	NA	48

Table 36: PCDD/F mass balance in the experimental apparatus using PTFE tubing

Congener	PCDD/F distribution (%)				
	Dust, D	Vapour, V	PTFE loss, L*	Sum D, L and V	Total lost**
2,3,7,8-TCDD	19.2	19.2	32.7	71.2	28.8
1,2,3,7,8-PeCDD	38.0	5.0	36.2	79.2	20.8
1,2,3,4,7,8-HxCDD	49.2	6.6	17.4	73.2	26.8
1,2,3,6,7,8-HxCDD	52.6	6.3	15.3	74.2	25.8
1,2,3,7,8,9-HxCDD	65.9	3.8	12.5	82.2	17.8
1,2,3,4,6,7,8-HpCDD	74.0	3.7	3.7	81.4	18.6
OCDD	74.0	1.6	1.1	76.7	23.3
2,3,7,8-TCDF	21.7	12.5	45.0	79.3	20.7
1,2,3,7,8-PeCDF	30.5	8.3	45.0	83.8	16.2
2,3,4,7,8-PeCDF	33.1	9.9	39.1	82.0	18.0
1,2,3,4,7,8-HxCDF	46.9	9.3	22.0	78.2	21.8
1,2,3,6,7,8-HxCDF	48.6	9.2	20.1	77.9	22.1
2,3,4,6,7,8-HxCDF	54.1	8.0	15.5	77.6	22.4
1,2,3,7,8,9-HxCDF	46.1	5.9	14.1	66.1	33.9
1,2,3,4,6,7,8-HpCDF	71.3	8.8	6.1	86.2	13.8
1,2,3,4,7,8,9-HpCDF	58.8	4.2	6.0	69.0	31.0
OCDF	59.4	2.2	1.2	62.9	37.1
Sum	49.6	7.0	16.3	72.9	27.1

Table 37: Desorption of PCDD/F form container and polypropylene adsorber at 110°C

	PCDD/F concentration (ng/kg)				
Congeners	Container 90°C	Container 110°C	PUF and Container 110°C	Desorption from container at 110°C	Desorption from plastics at 110°C
TeCDDs	3.8	8.8	33.9	0	30.1
PeCDDs	56.3	45.2	85.3	11.1	29.1
HxCDDs	291.3	158.1	184.3	133.2	0
HpCDDs	153.8	84	103.2	69.7	0
OCDDs	31.3	18.8	18.8	12.4	0
TeCDFs	17.5	31.4	353.7	0	336.2
PeCDFs	651.3	562	1294.5	89.3	643.3
HxCDFs	1323.8	767.7	1155.3	556.1	0
HpCDFs	620	327.4	449.1	292.6	0
OCDFs	45	37.6	45.2	7.4	0.2

Table 38: Experimental variables for post-combustion of hydrocarbons

	Off-gas temperature (°C)	Hydrocarbon (l/h)	Off-gas volume flow (m^3/h)
Rich in oxygen	600, 650, 700, 750, 800	50, 100, 150	50, 25
Poor in oxygen	650, 800	100, 150	50, 25

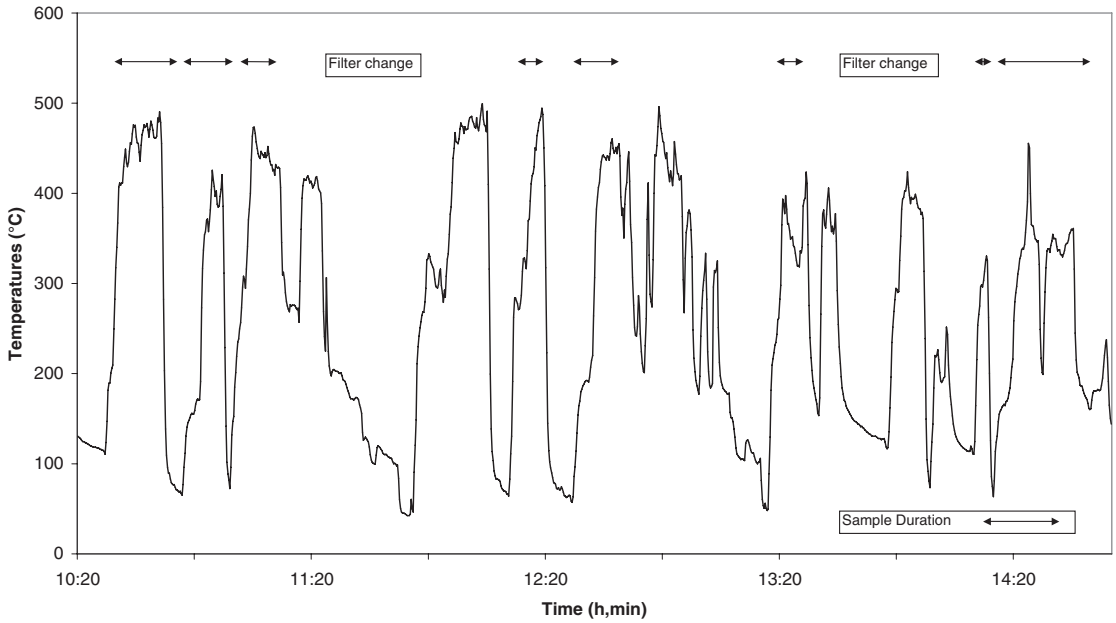

Fig. 1: Waste gas temperature profile during EAF operation

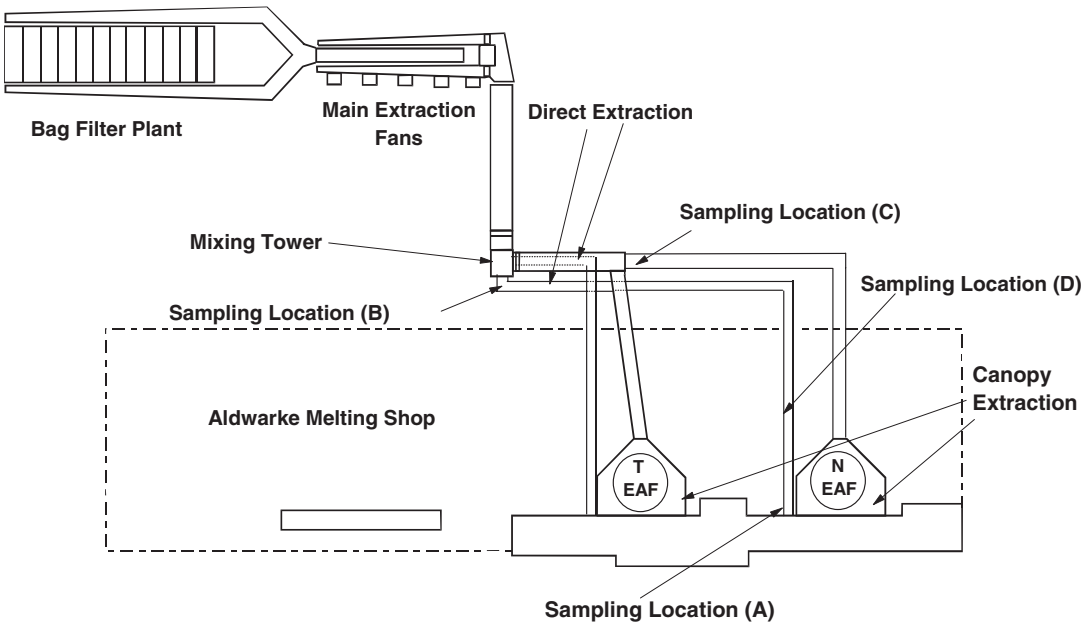

Fig. 2: Plant layout showing sampling locations

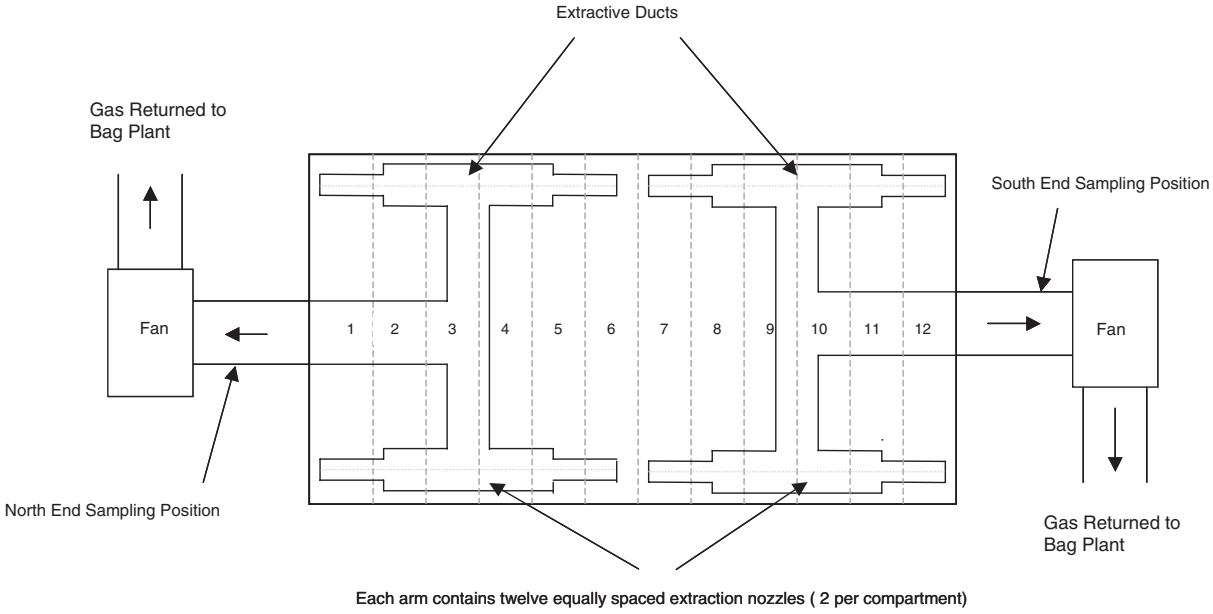

Fig. 3: Schematic arrangement of the extractive sampling ducts in the bag filter vent at Aldwarke Melting Shop

A: Turbostratic carbon

B: Oxygen

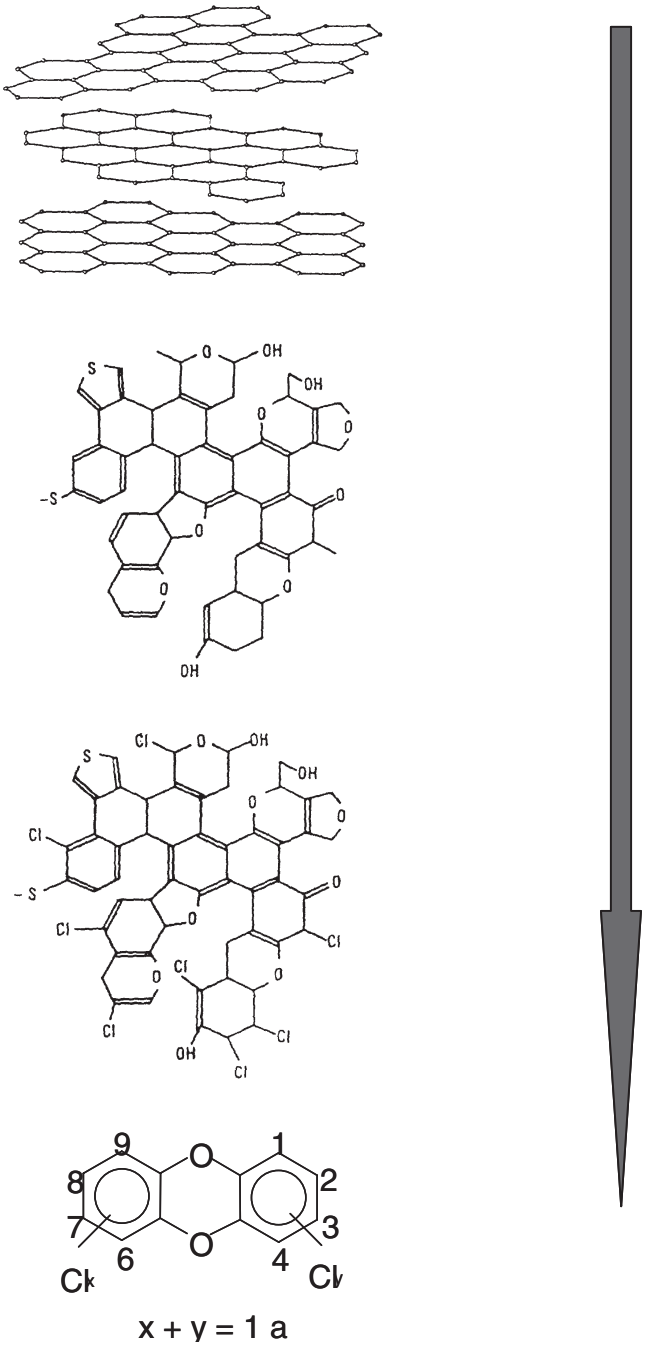

Fig. 4: Supposed path for the transformation of the hexagonal structure of the coal PCDD for oxidation of the peripheral aromatic and chlorination-breaking of the turbo-graphite layer

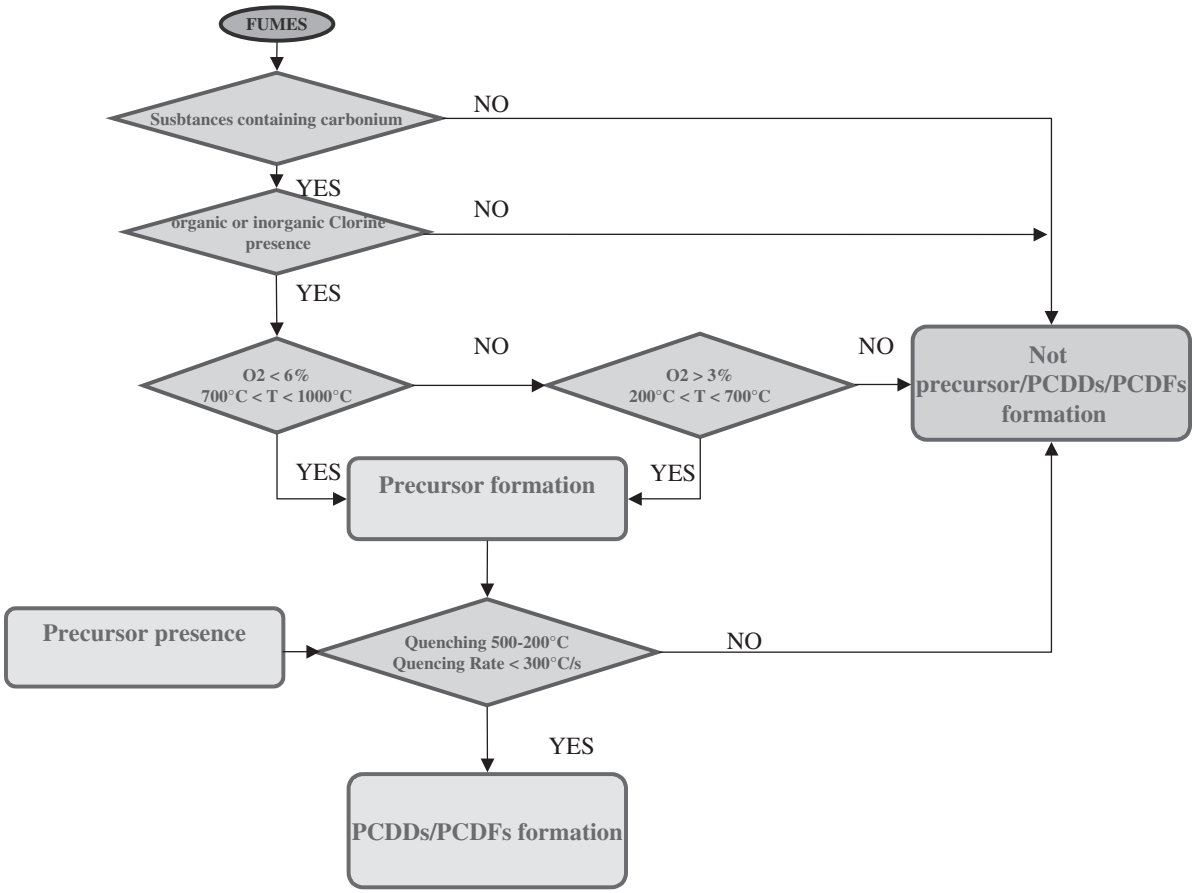

Fig. 5: Flowsheet showing conditions necessary for PCDD/F formation

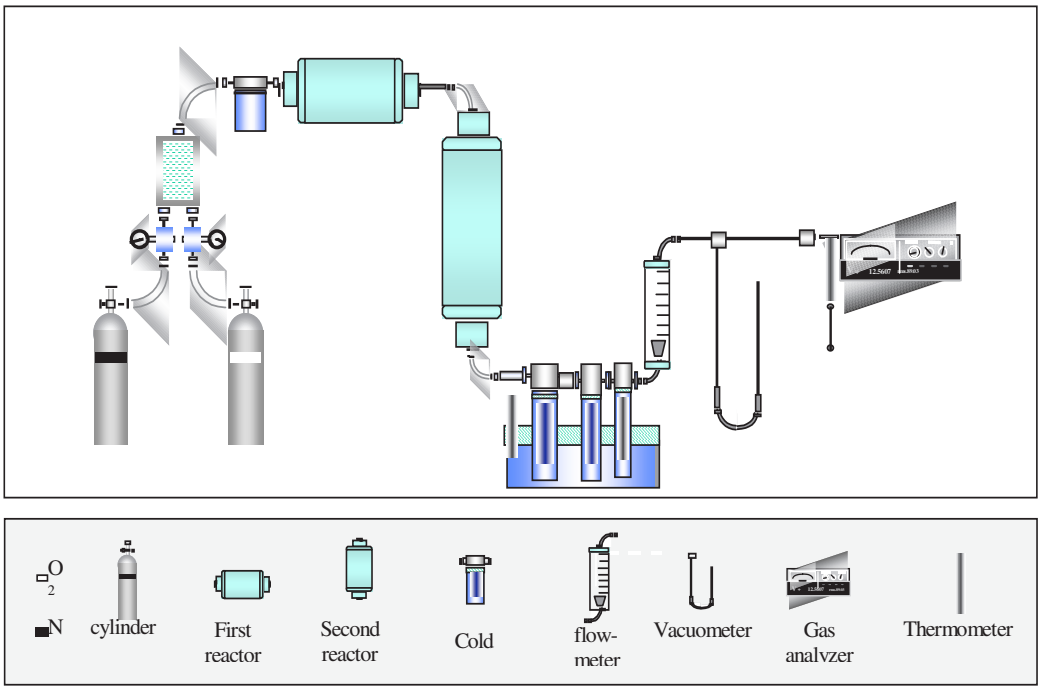

Fig. 6: Schematic arrangement of the HEART experimental system

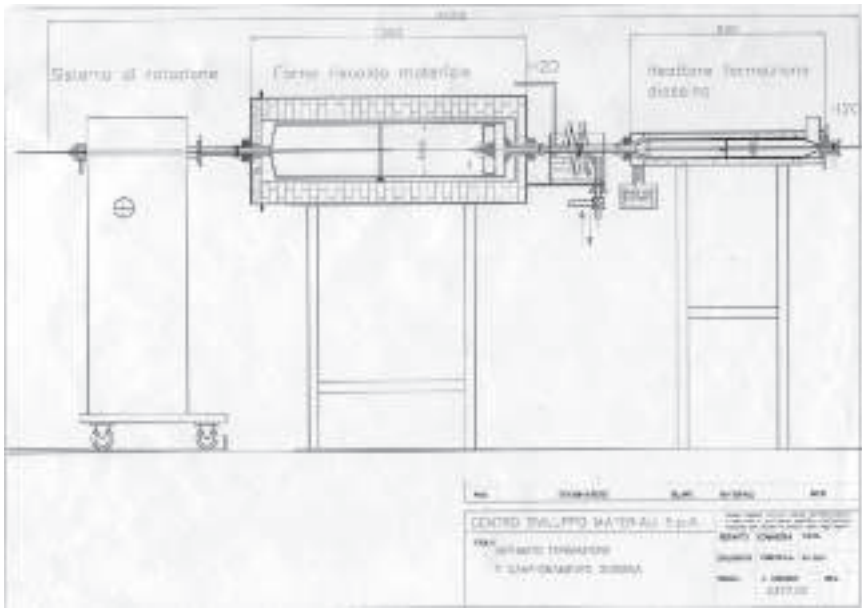

Fig. 7: Schematic arrangement of the HEART system

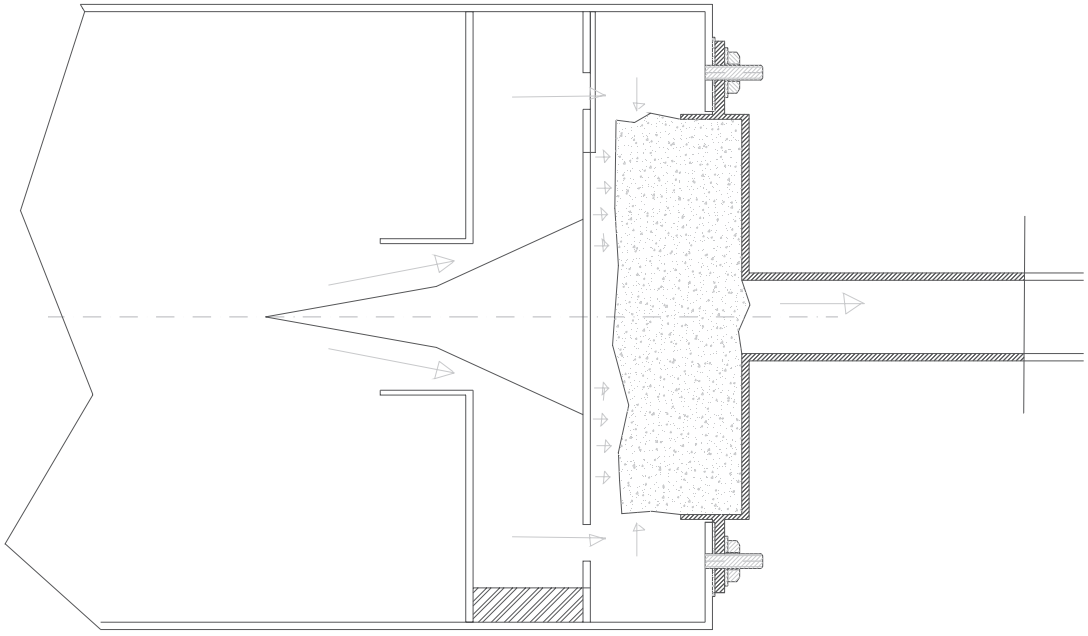

Fig. 8: Modified connection between heating chambers in HEART system

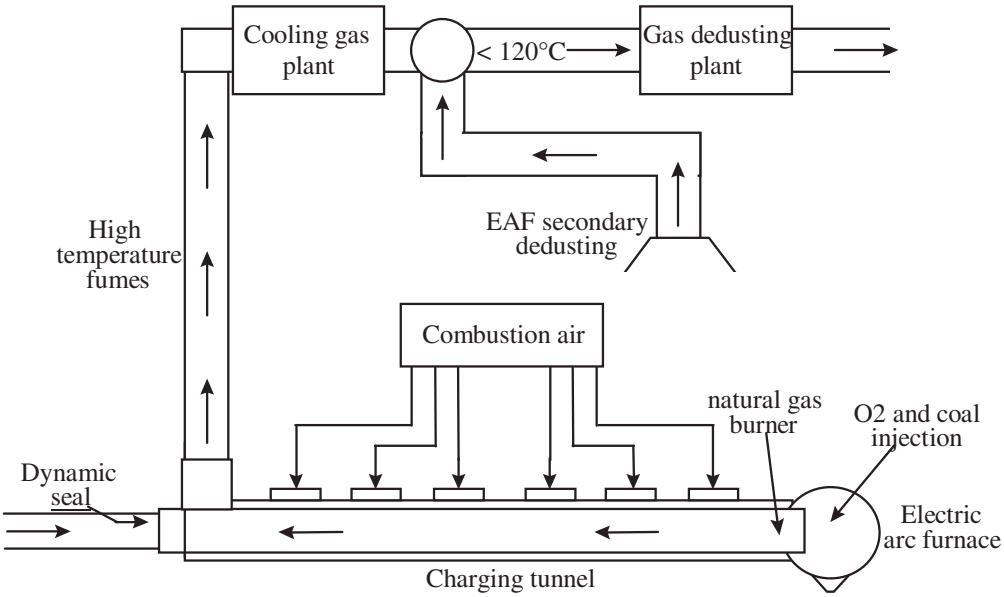

Fig. 9: Schematic arrangement of EAF equipped with a tunnel pre-heater

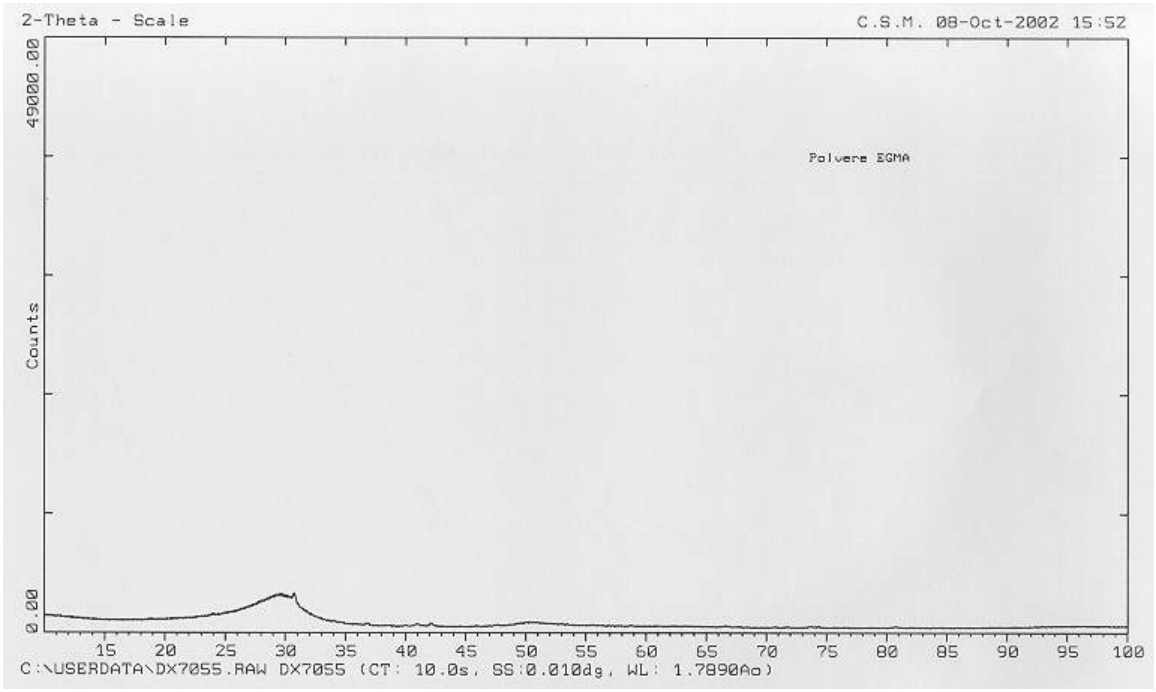

(a) Low resolution

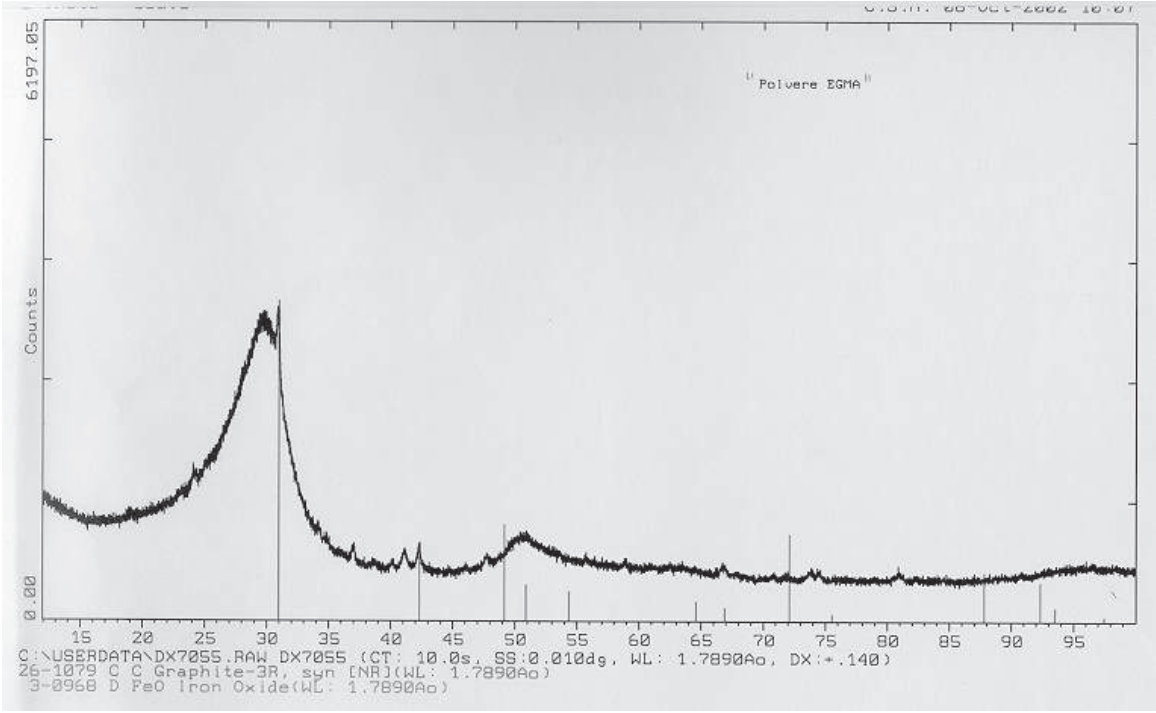

(b) High resolution

Fig. 10(a and b): X-ray diffraction pattern of carbon injected in EAF

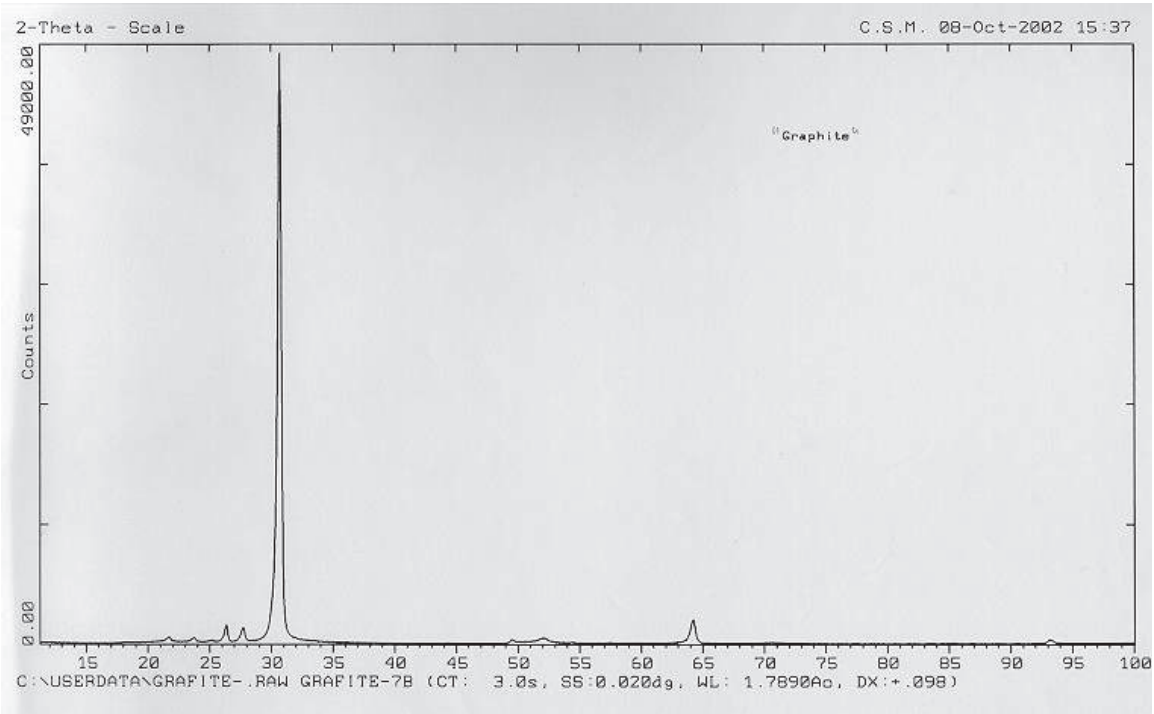

Fig. 11: Graphite X-ray diffraction pattern

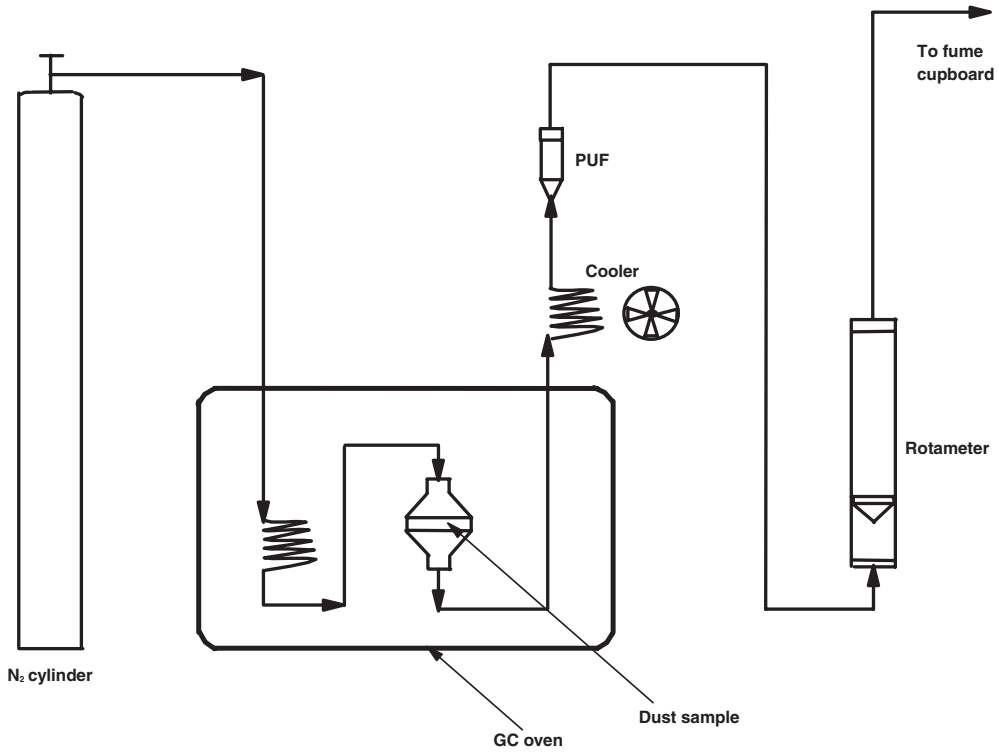

Fig. 12: Schematic of experimental system used for PCDD/F volatility studies

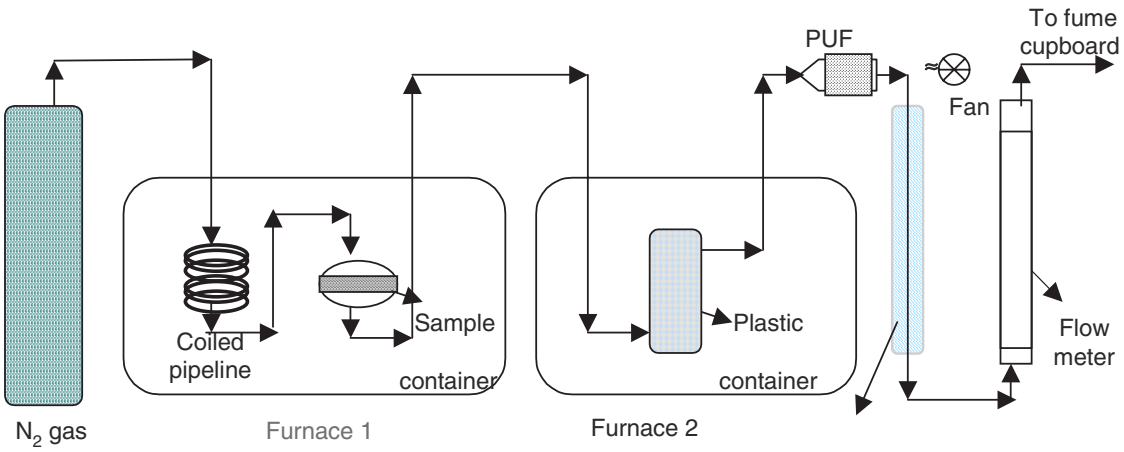

Fig. 13: Schematic of experimental system used for studies of adsorption and desorption of PCDD/Fs on plastics

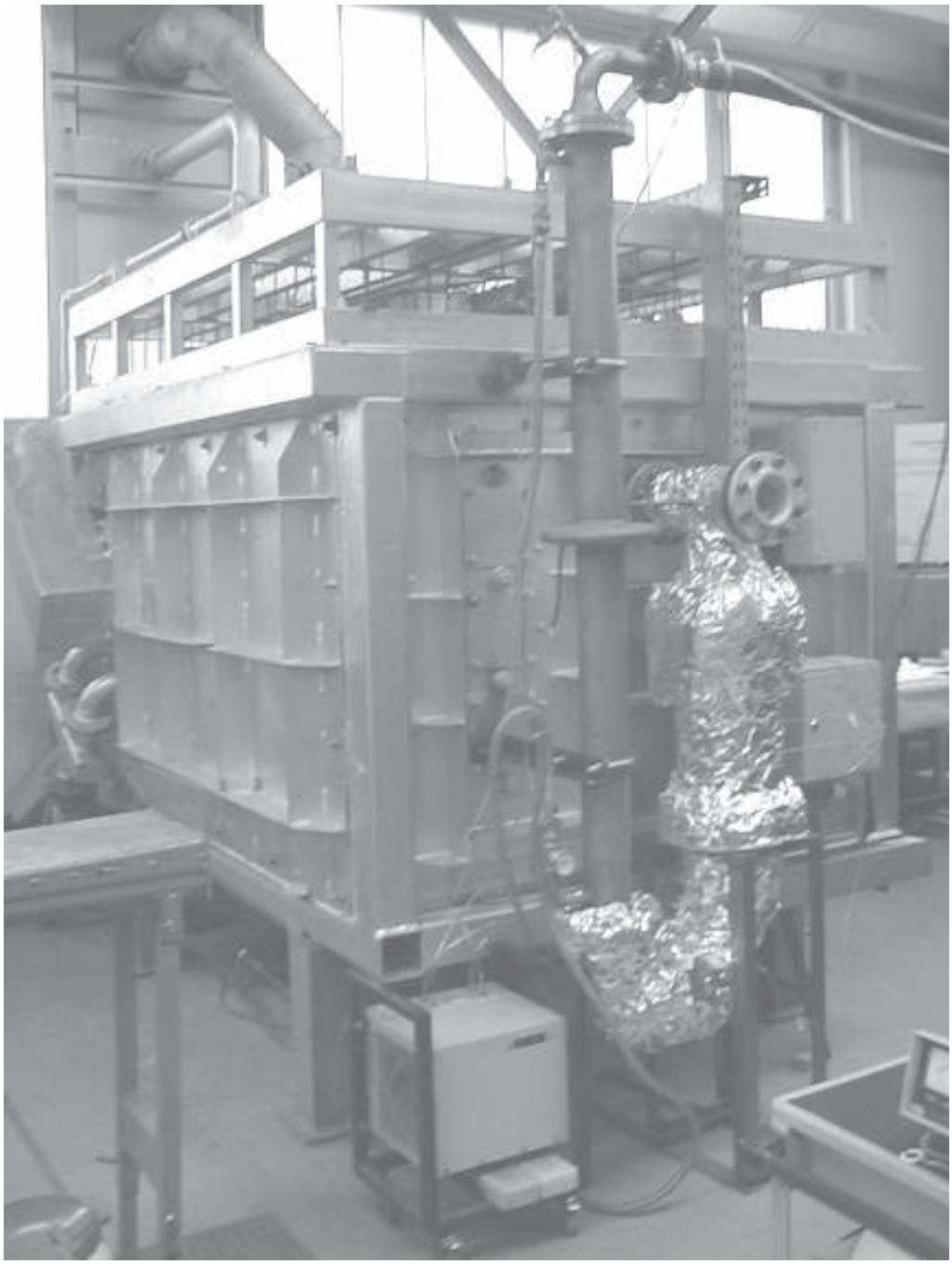

Fig. 14: The experimental shaft furnace at BFI

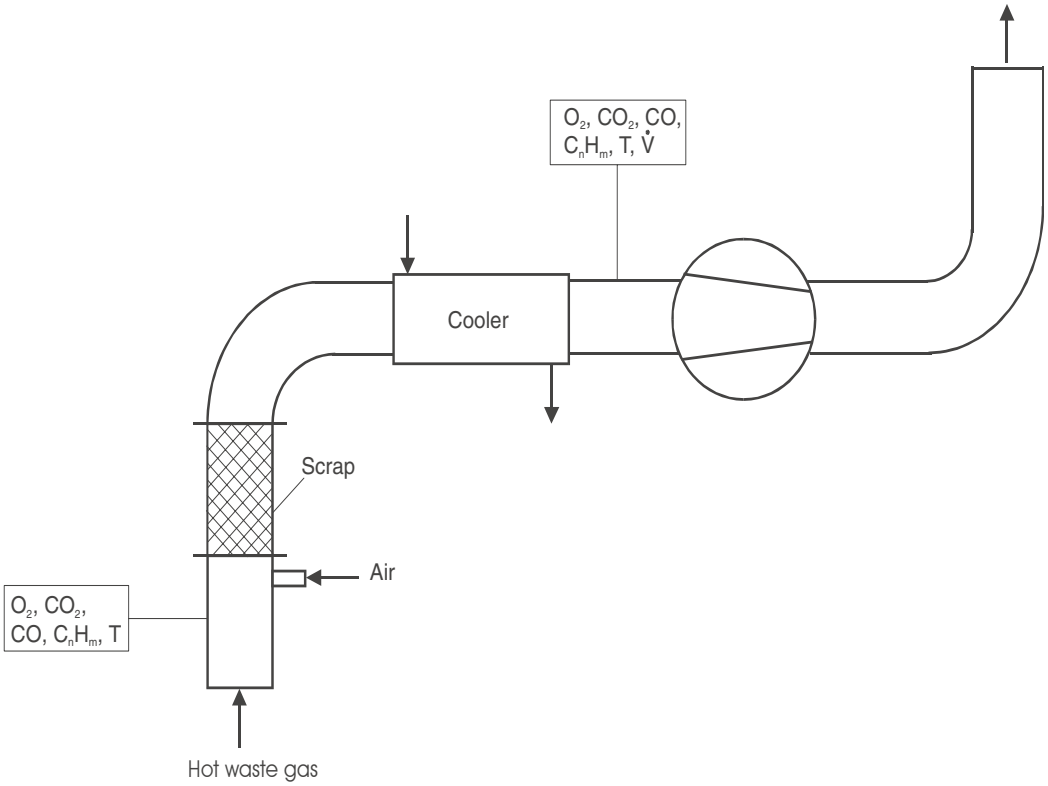

Fig. 15: Experimental pre-heating shaft system at BFI

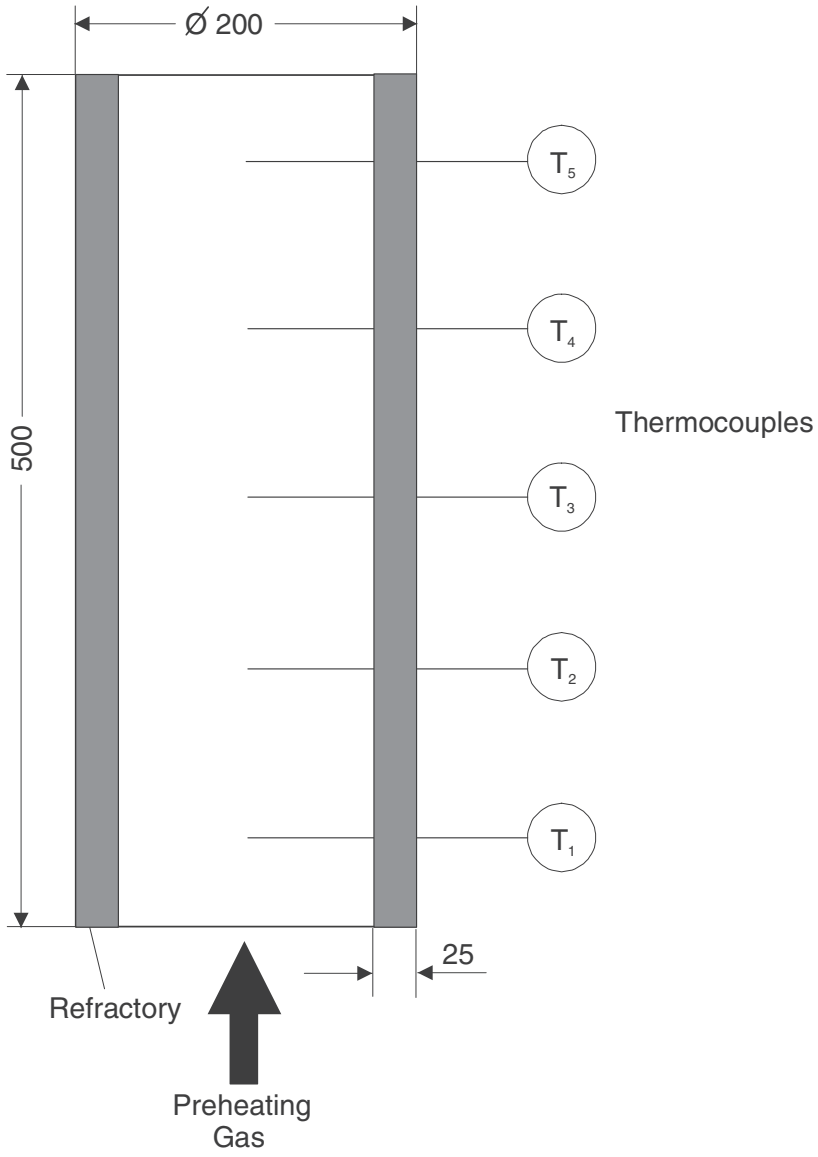

Fig. 16: Schematic of the scrap pre-heating chamber (all dimensions shown in mm)

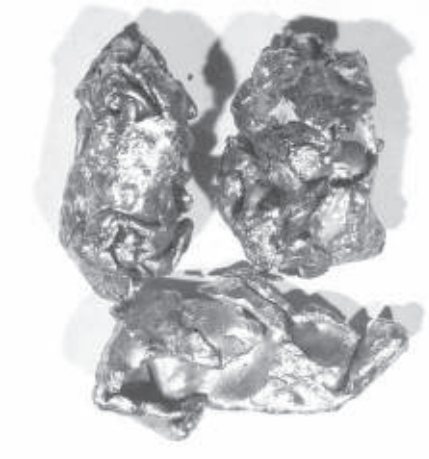

Fig. 17: Double shredded scrap

Fig. 18: Tin scrap

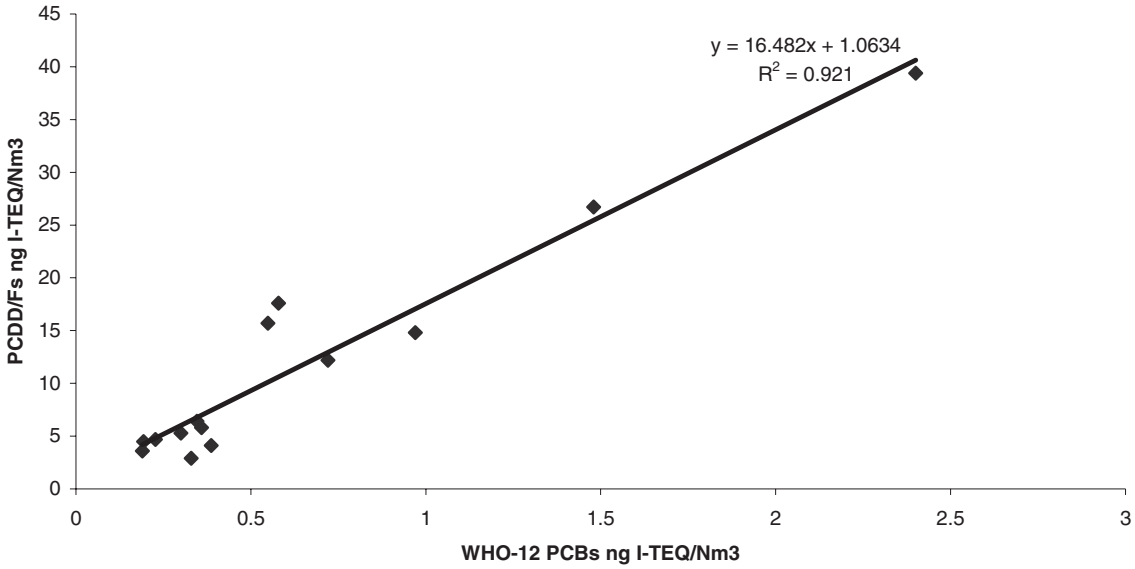

Fig. 19: Correlation between PCDD/Fs and WHO-12 PCBs in EAF off-gas

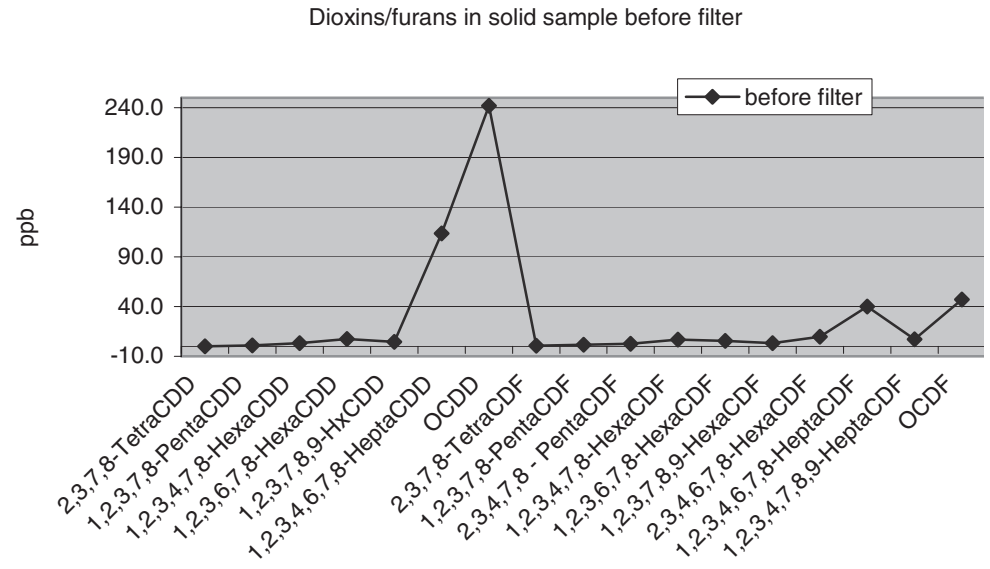

Fig. 20: PCDD/F profile in dust before the bag filter at SN's Long Product Plant at Maia

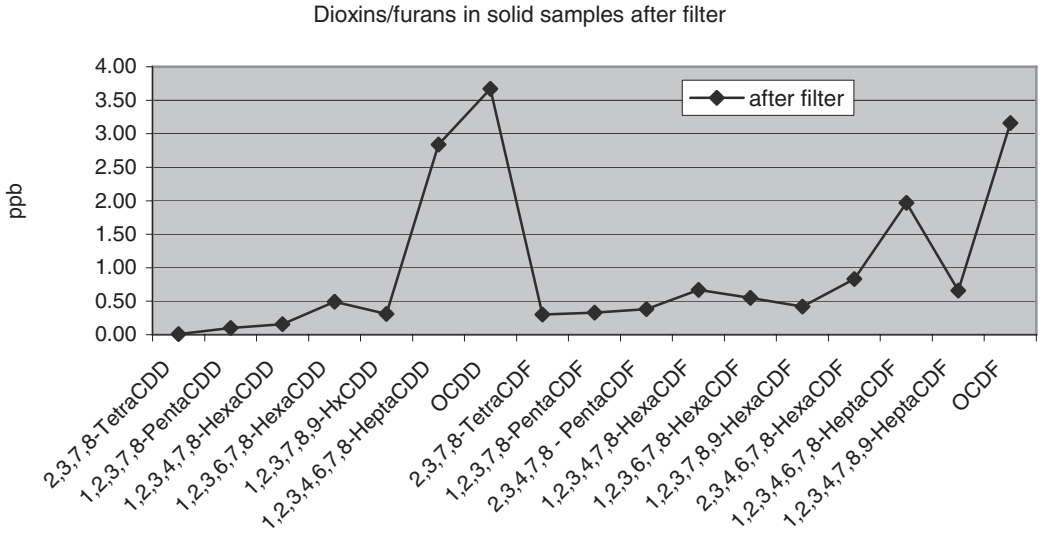

Fig. 21: PCDD/F profile in dust after the bag filter at SN's Long Product Plant at Maia

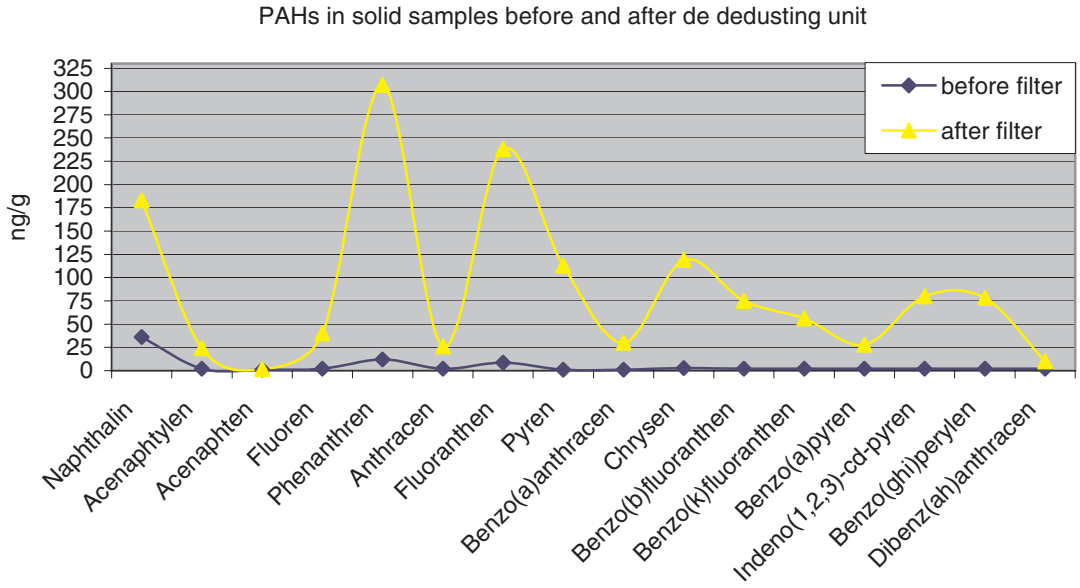

Fig. 22: PAH profile in dust before and after the bag filter
at SN's Long Product Plant at Maia

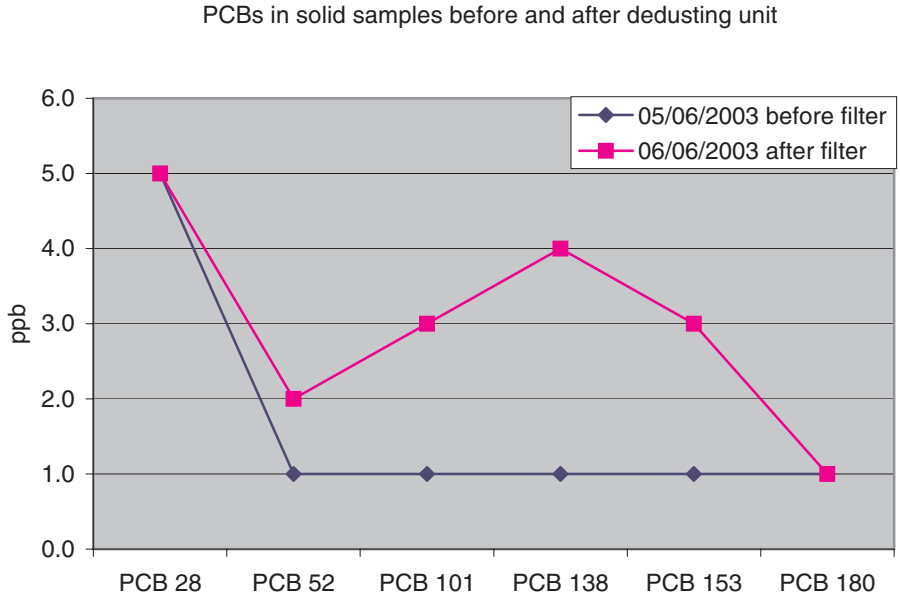

Fig. 23: EC7-PCB profile in dust before and after the bag filter
at SN's Long Products Plant at Maia

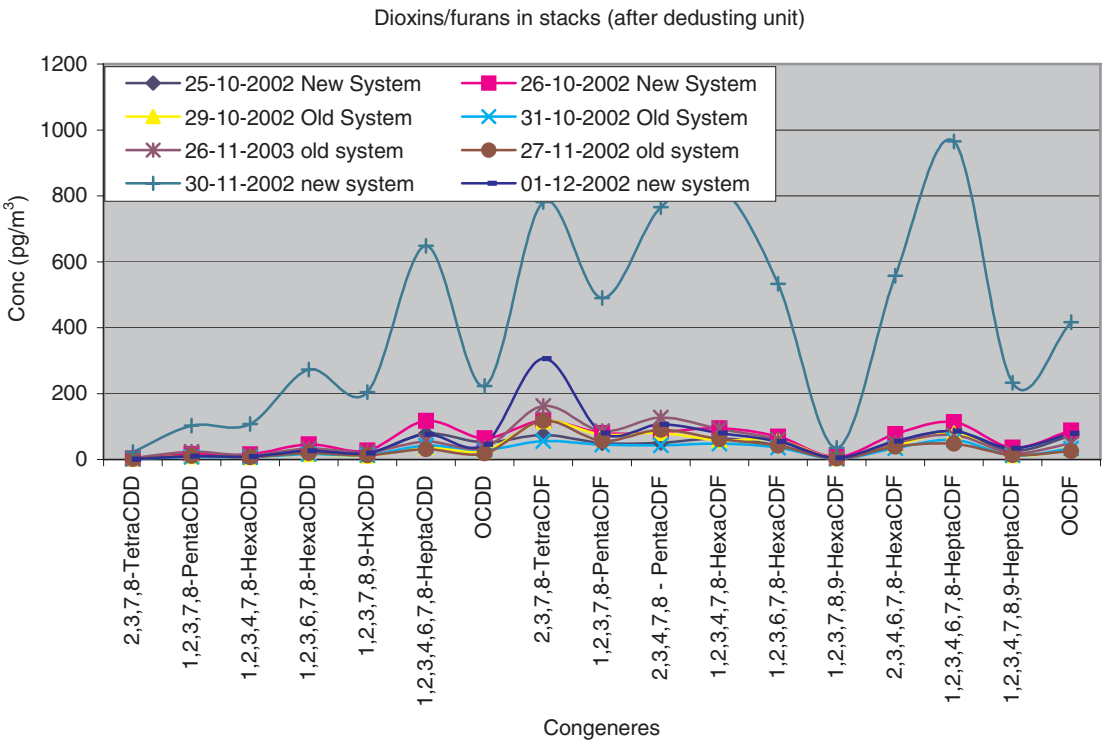

Fig. 24: PCDD/F profile in waste gas after de-dusting at SN's Long Products Plant at Maia

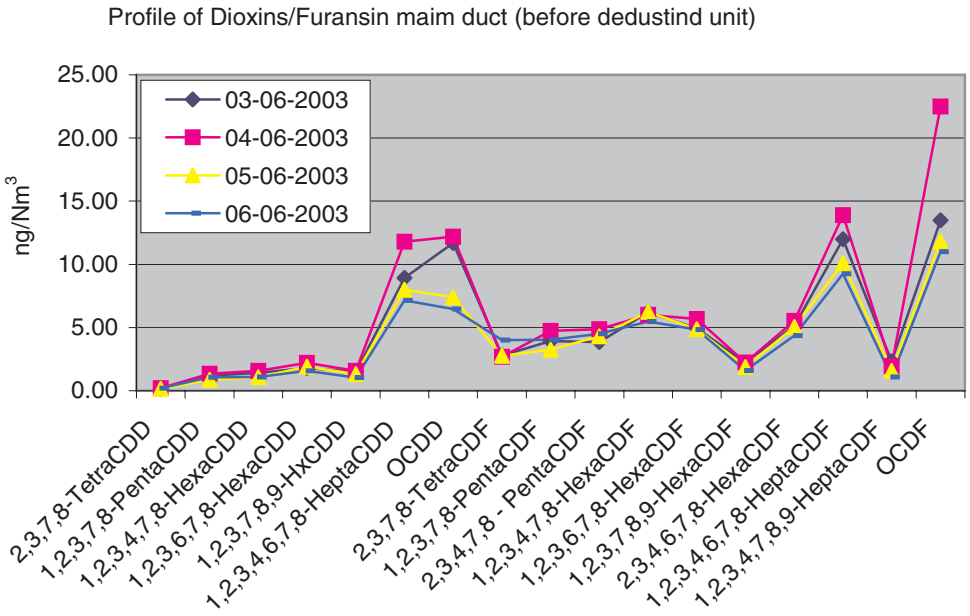

Fig. 25: PCDD/F profile in waste gas before de-dusting at SN's Long Products Plant at Maia

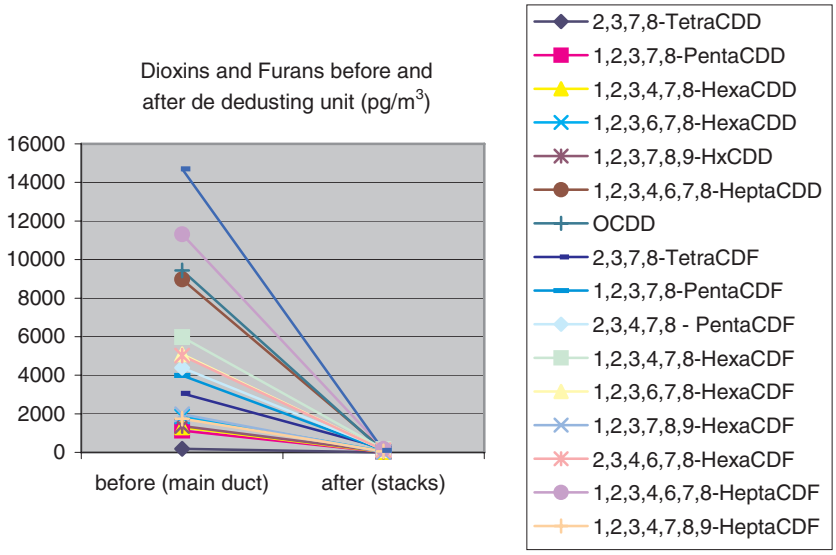

Fig. 26: Comparison between PCDD/F concentrations in waste gas before and after de-dusting at SN's Long Products Plant at Maia

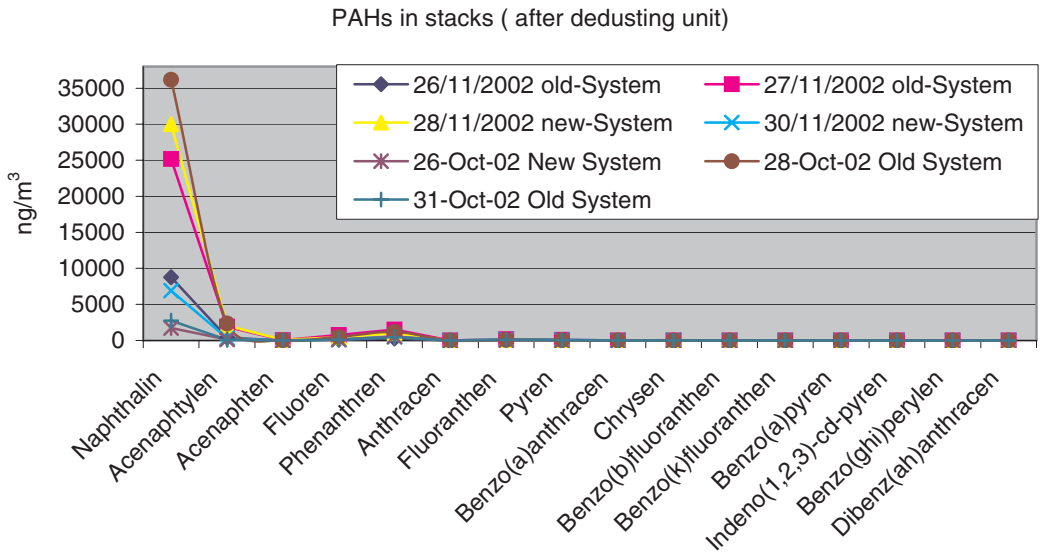

Fig. 27: PAH profile in waste gas after de-dusting at SN's Long Products Plant at Maia

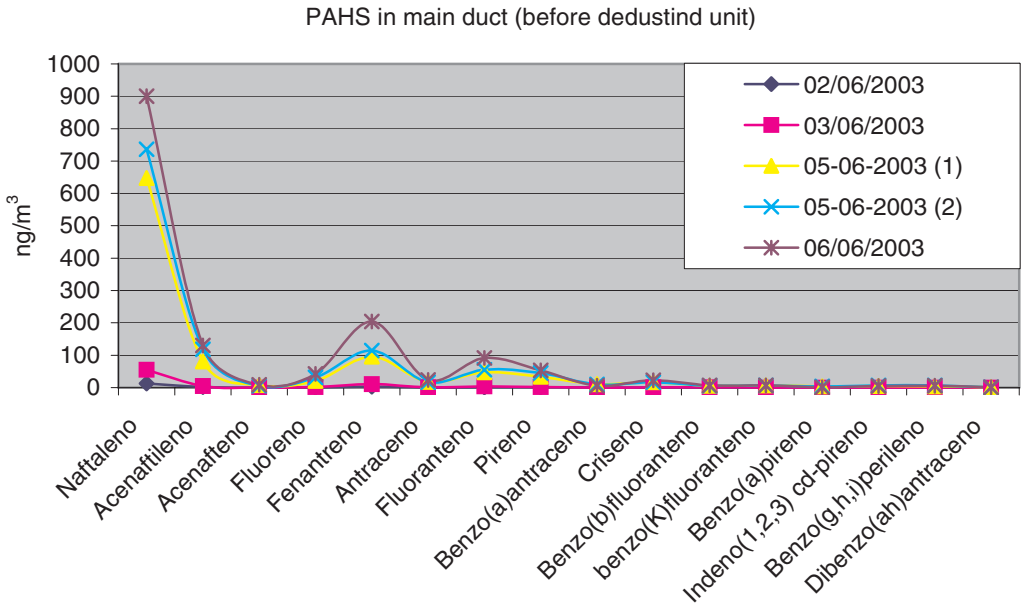

Fig. 28: PAH profile in waste gas before de-dusting at SN's Long Products Plant at Maia

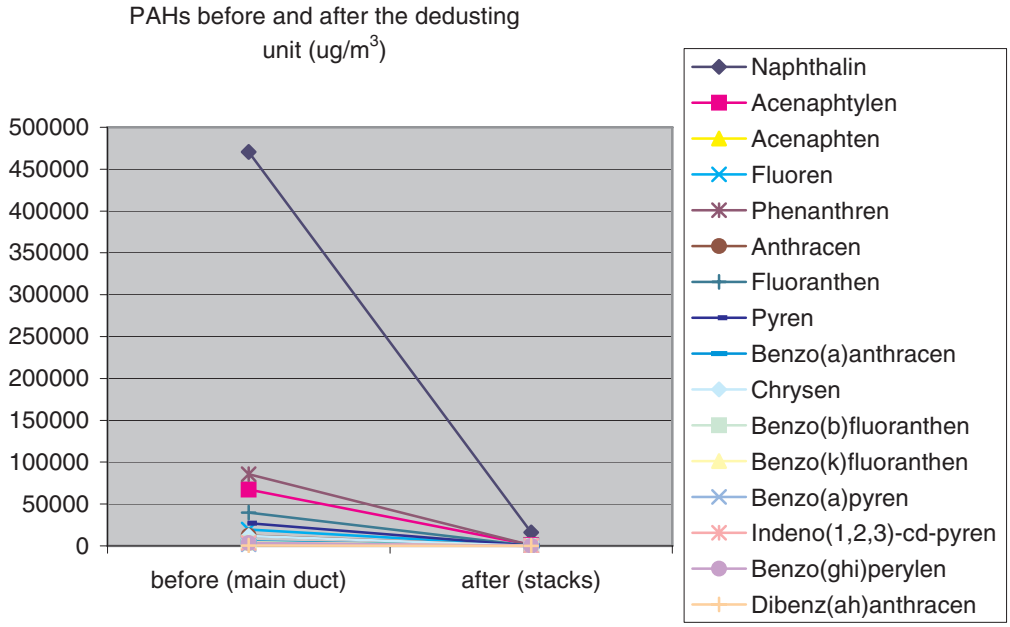

Fig. 29: Comparison between PAH concentrations in waste gas before and after de-dusting at SN's Long Products Plant at Maia

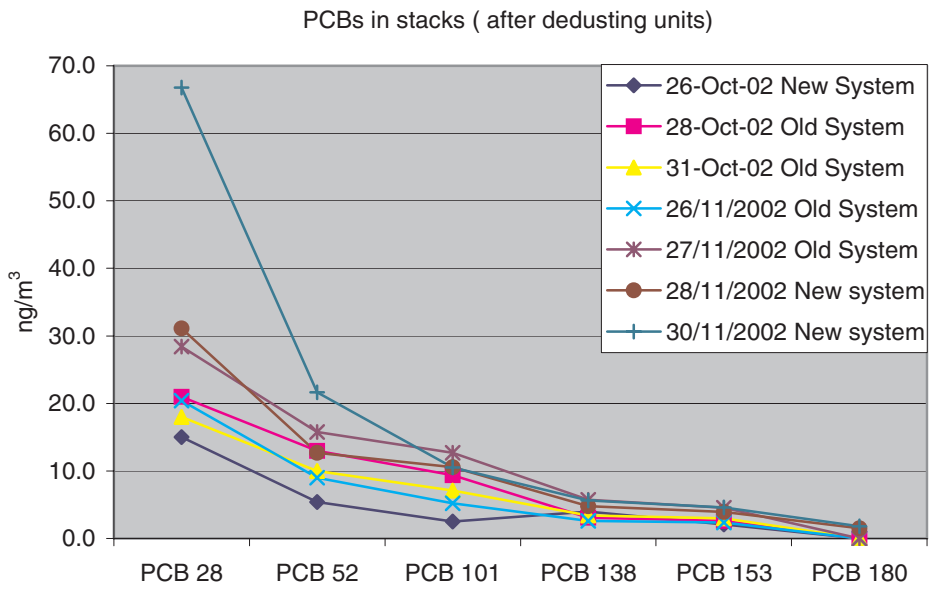

Fig. 30: EC7-PCB profile in waste gas after de-dusting at SN's Long Products Plant at Maia

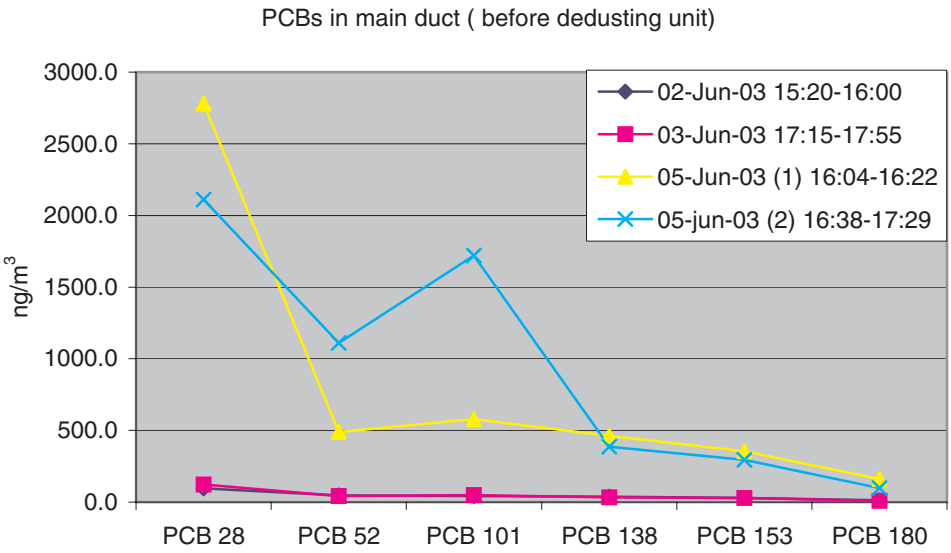

Fig. 31: EC7-PCB profile in waste gas before de-dusting at SN's Long Products Plant at Maia

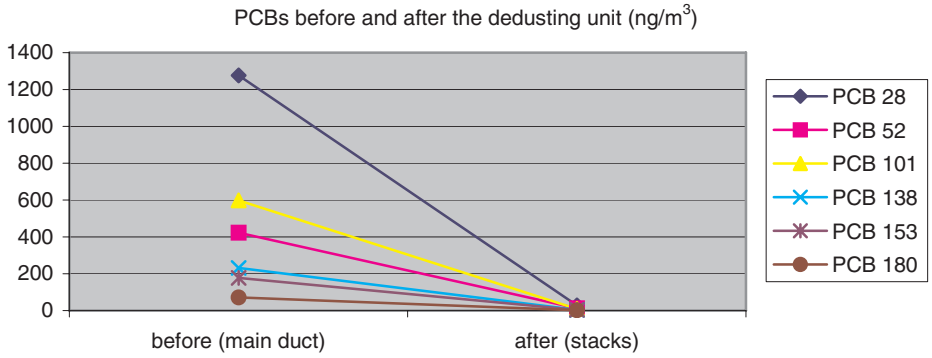

Fig. 32: Comparison between EC7-PCB concentrations in waste gas before and after dedusting at SN's Long Products Plant at Maia

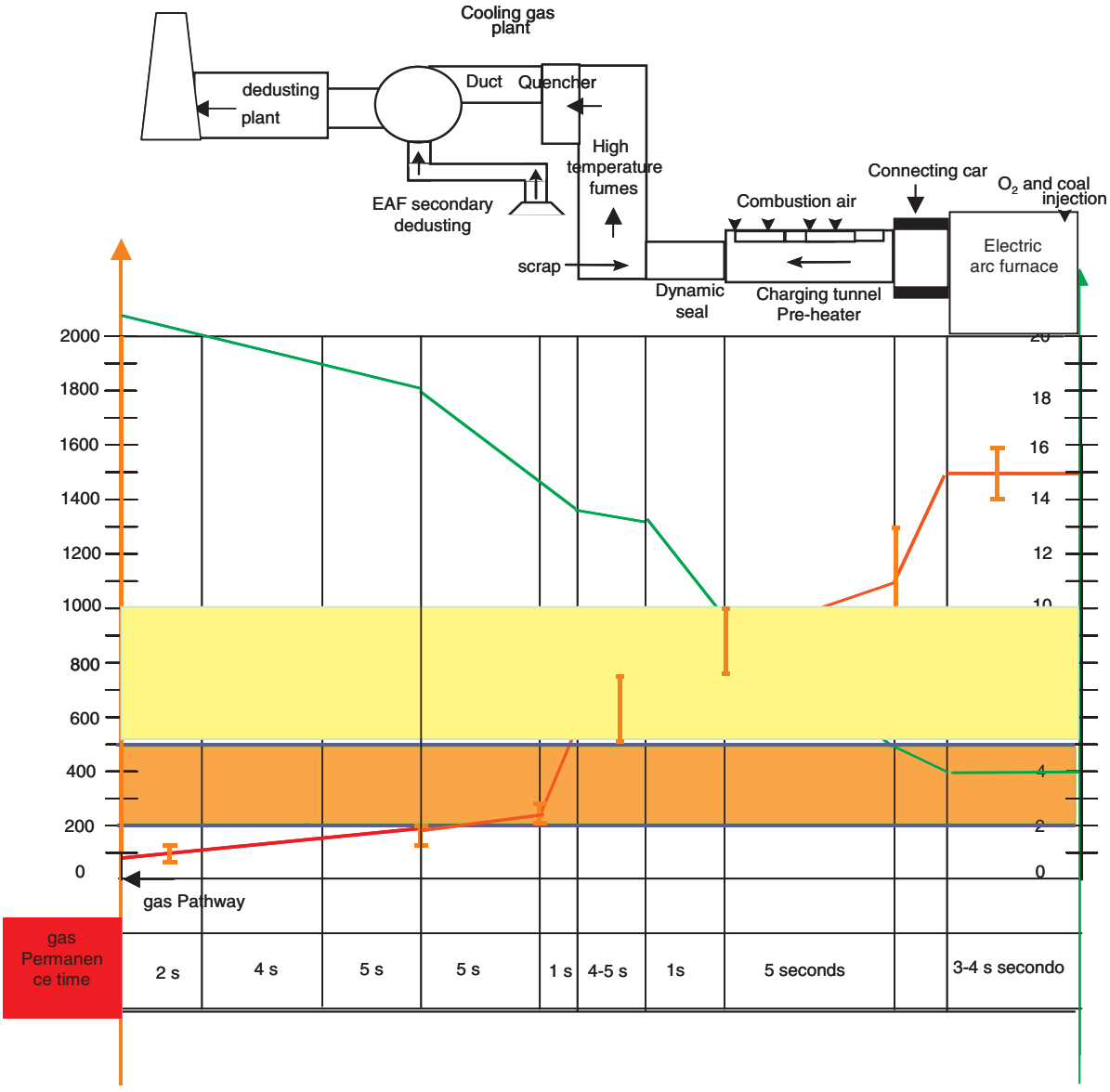

Fig. 33: Plant scheme, oxygen and temperature trends

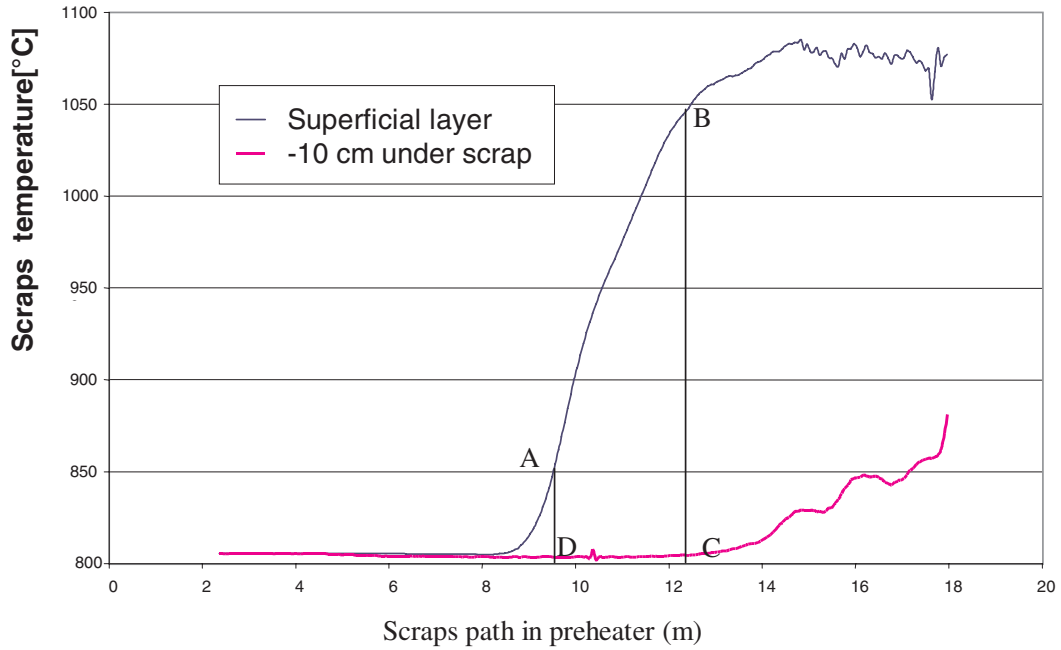

Fig. 34: Example of probable zone (ABCD area) to control for avoiding PCDD/F formation

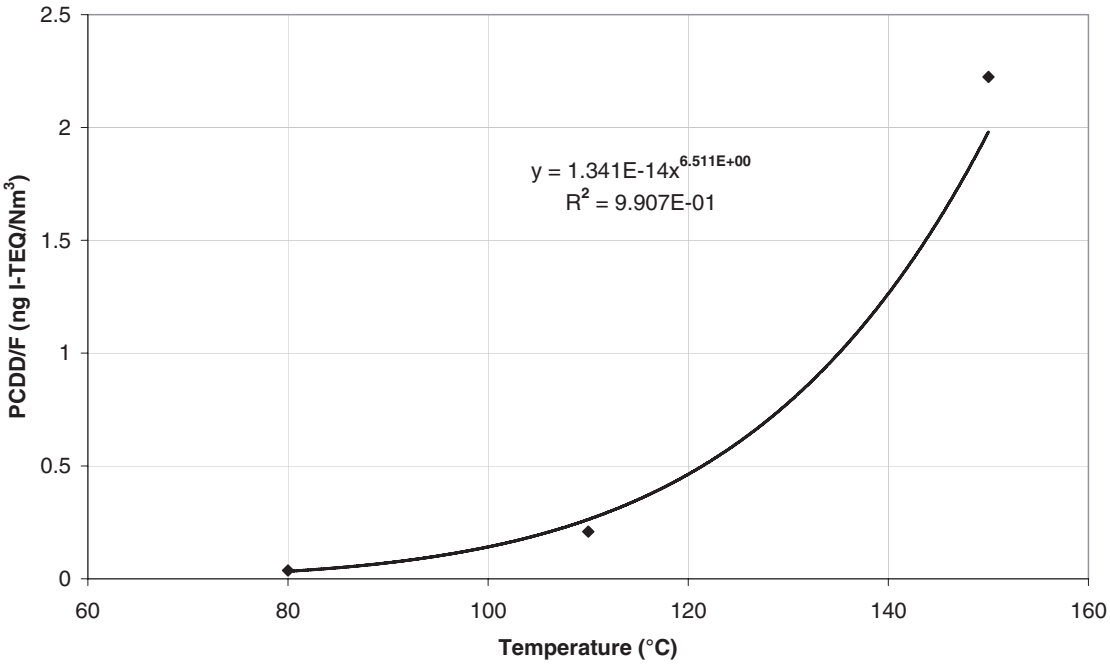

Fig. 35: Average concentration of PCDD/F in gas exit from 20 h laboratory test

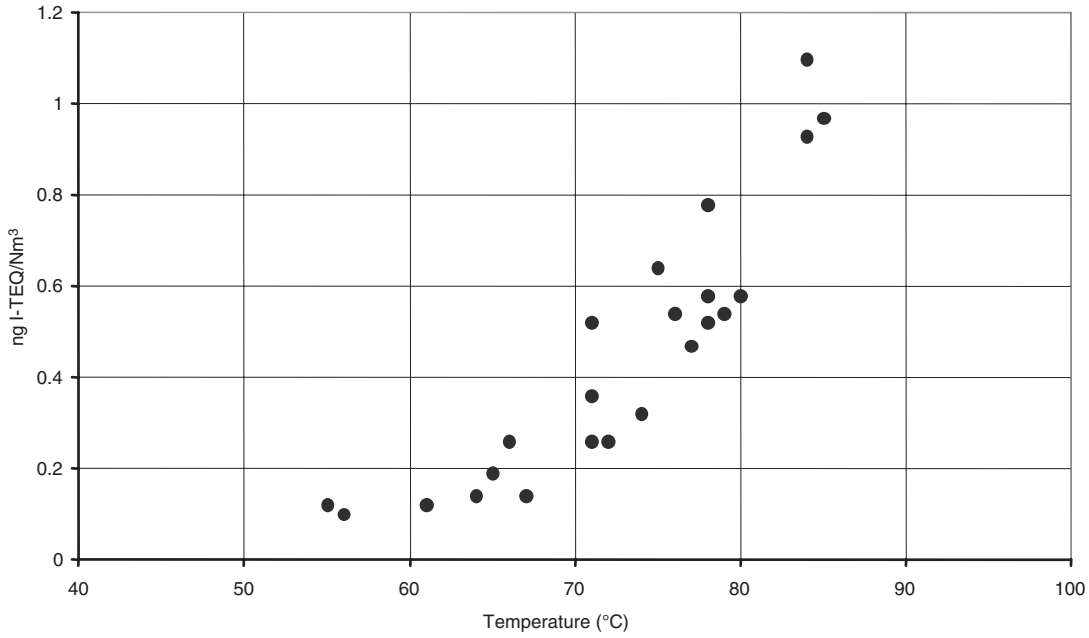

Fig. 36: Plot of PCDD/F concentration against temperature for short-term samples

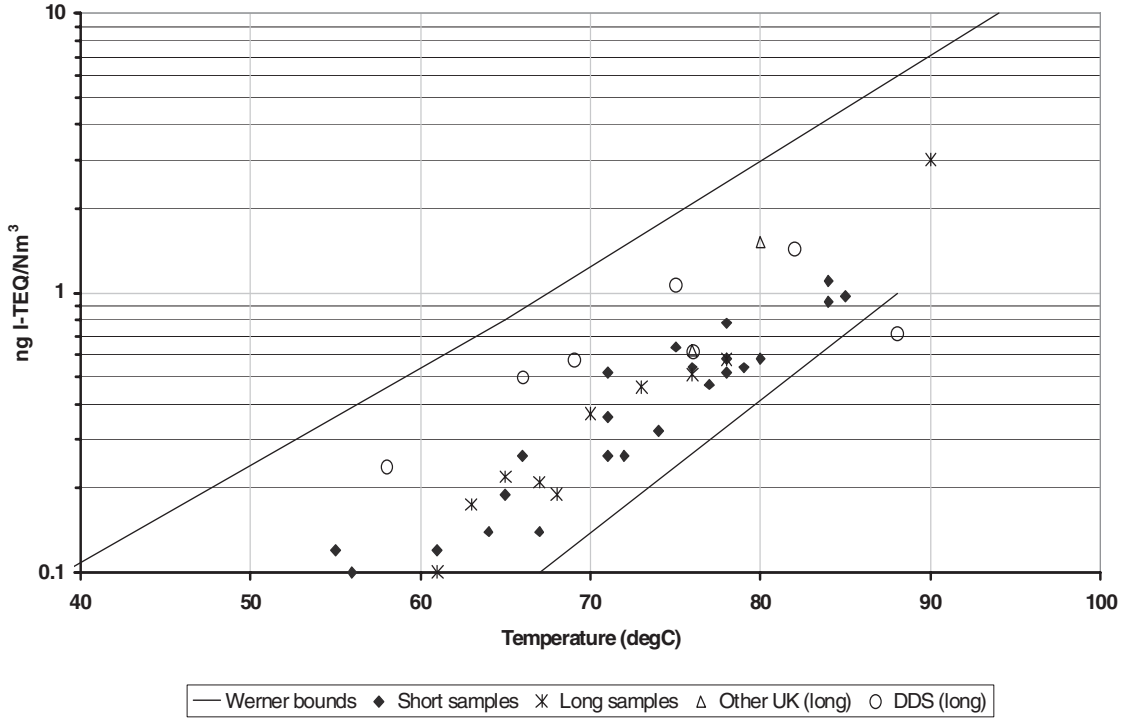

Fig. 37: Log-linear plot of PCDD/F concentration against temperature for samples from Aldwarke Melting Shop - comparison with data of Werner and other workers

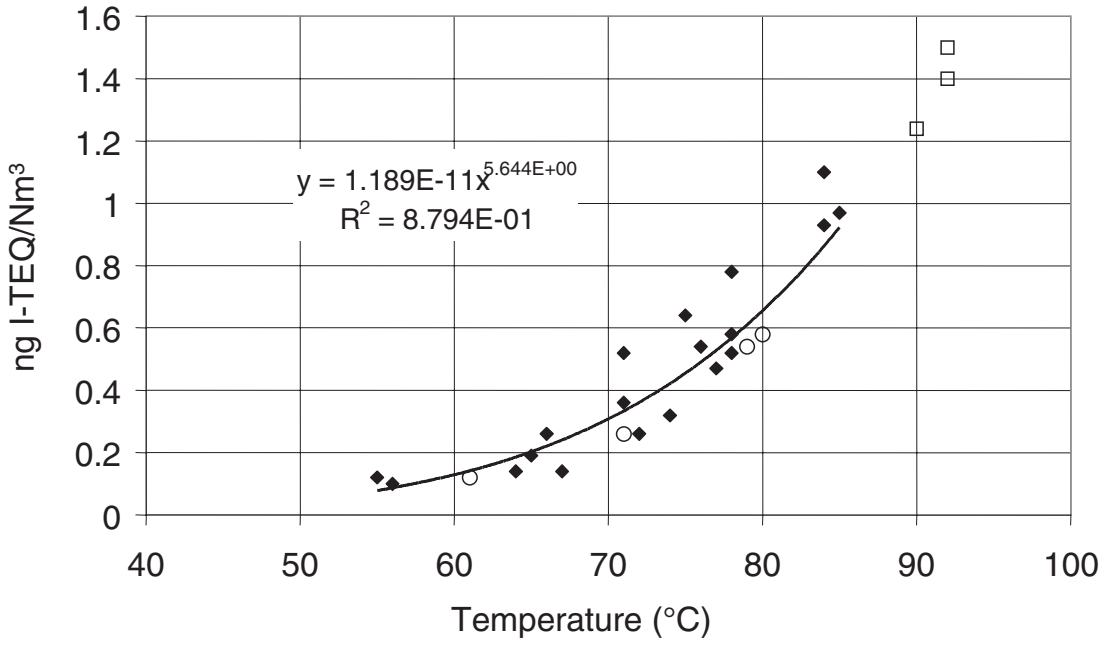

Fig. 38: Correlation between PCDD/F concentration and temperature for short-term samples

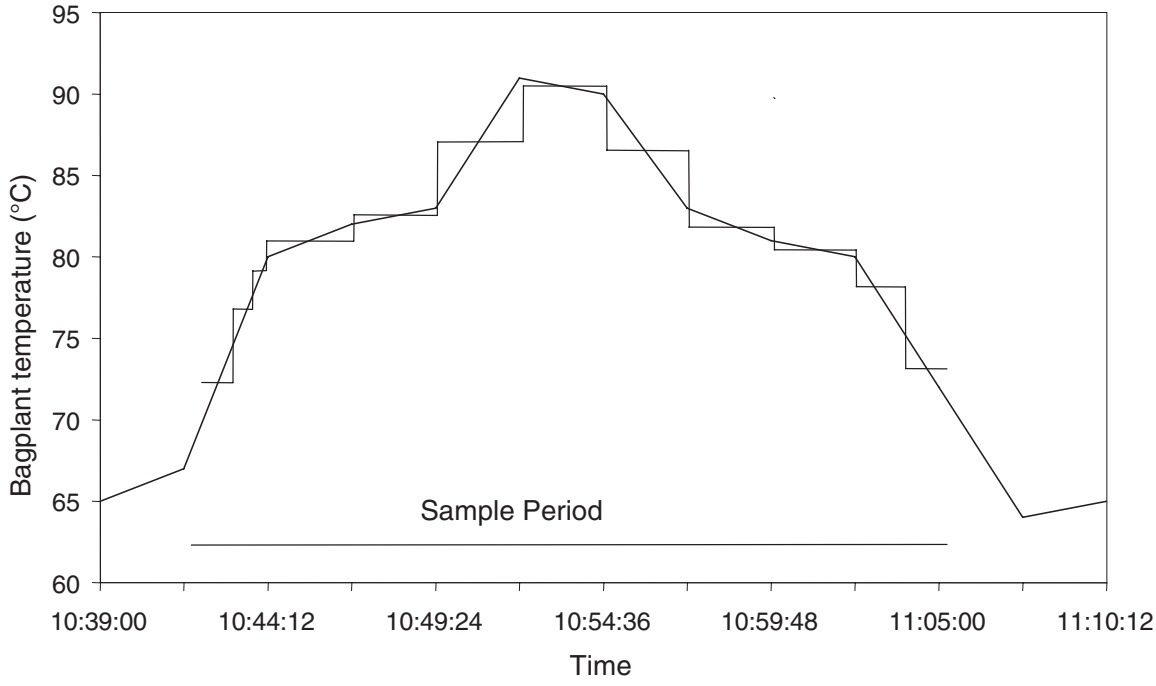

Fig. 39: Illustration of temperature approximation

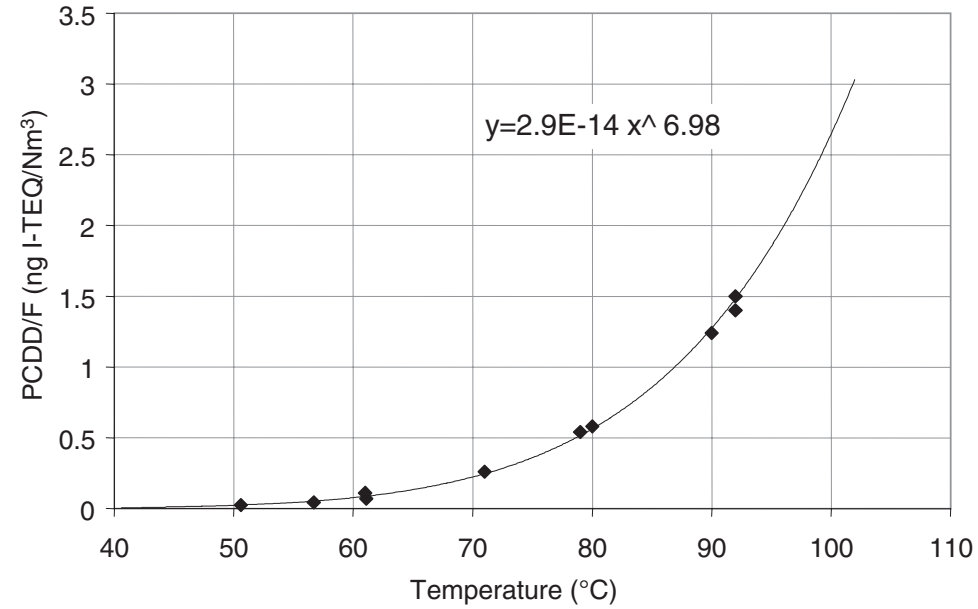

Fig. 40: 'True' temperature relationship between PCDD/F concentration and temperature

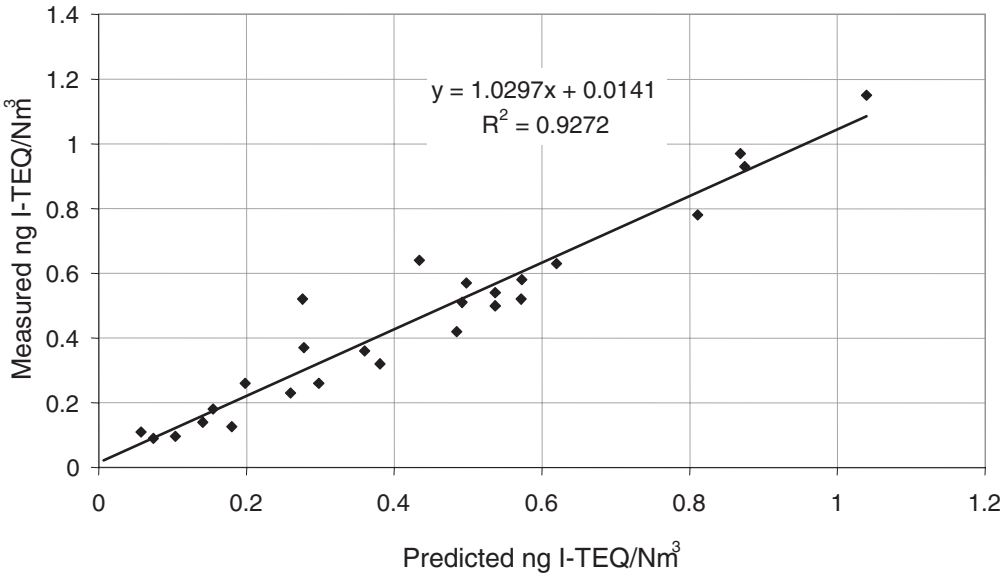

Fig. 41: Measured v predicted PCDD/F concentration

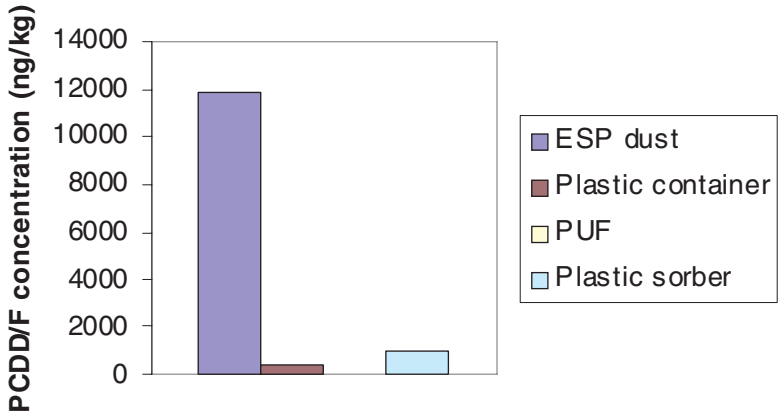

(a) 5 mm polypropylene spheres

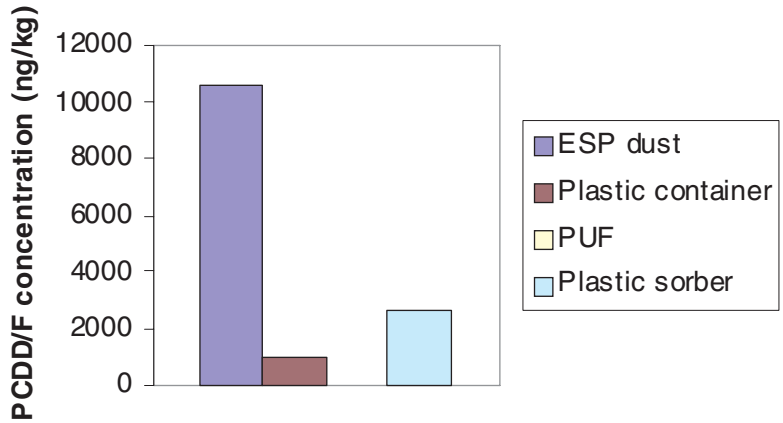

(b) Commercial powder

Fig. 42(a and b): The partitioning of the sum of all targeted PCDD/F to the ESP dust, plastic container, PUF and plastic absorber of the experimental apparatus using 5 and 10 mm spheres

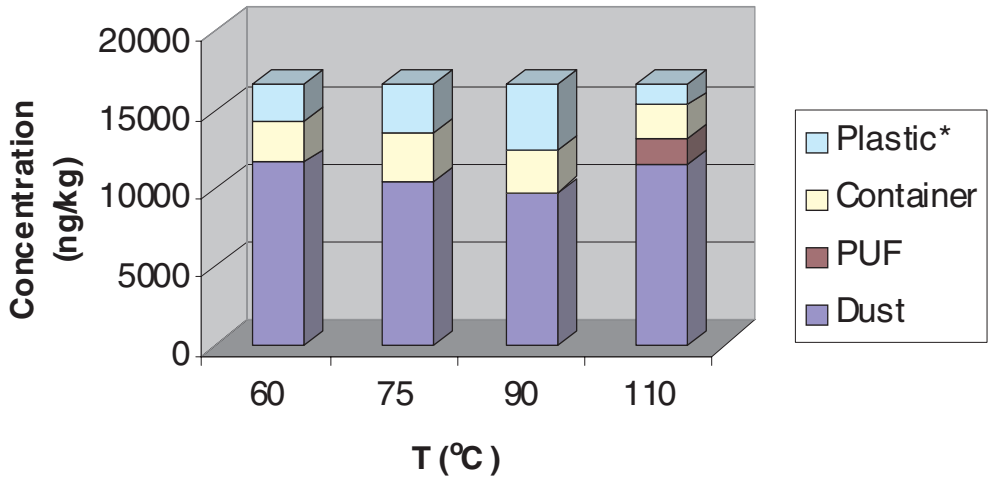

(a) ng/kg

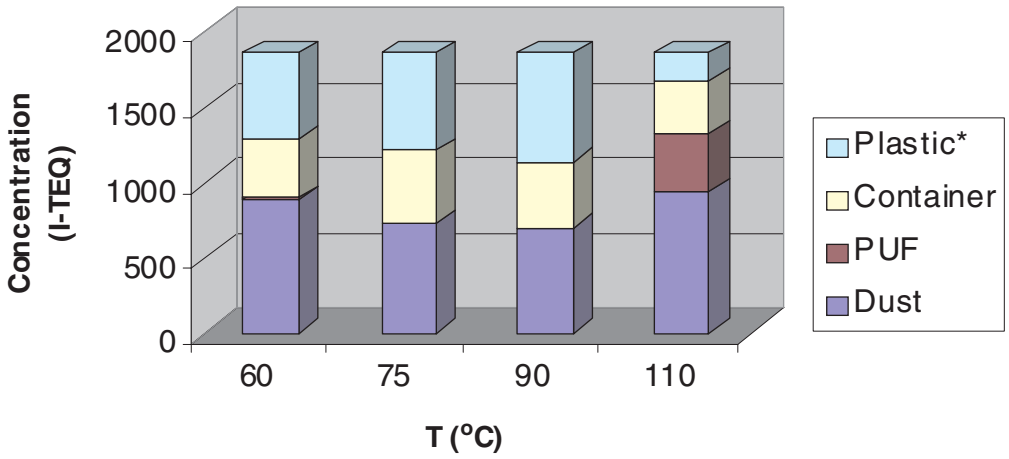

(b) ng I-TEQ/kg

Fig. 43(a and b): The effect of polypropylene temperature on PCDD/F absorption

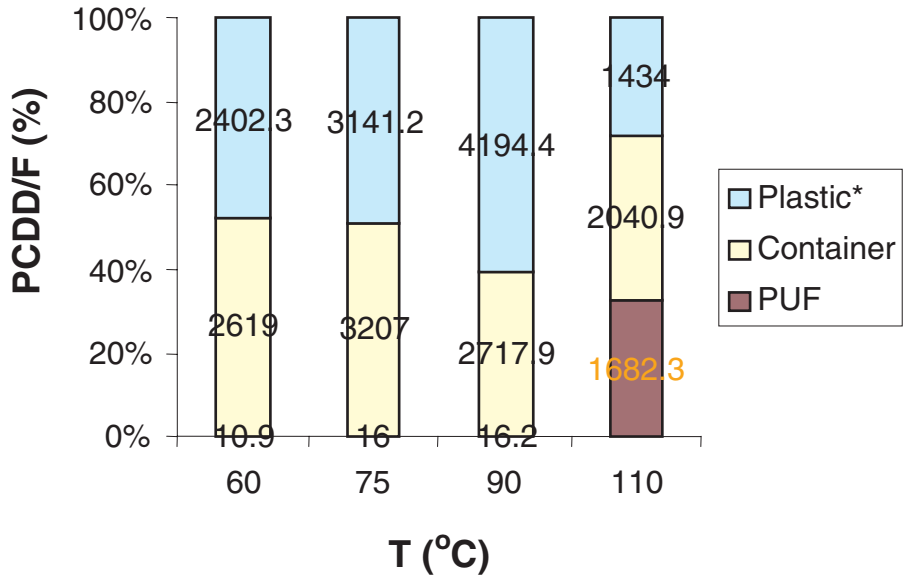

(a) ng/kg

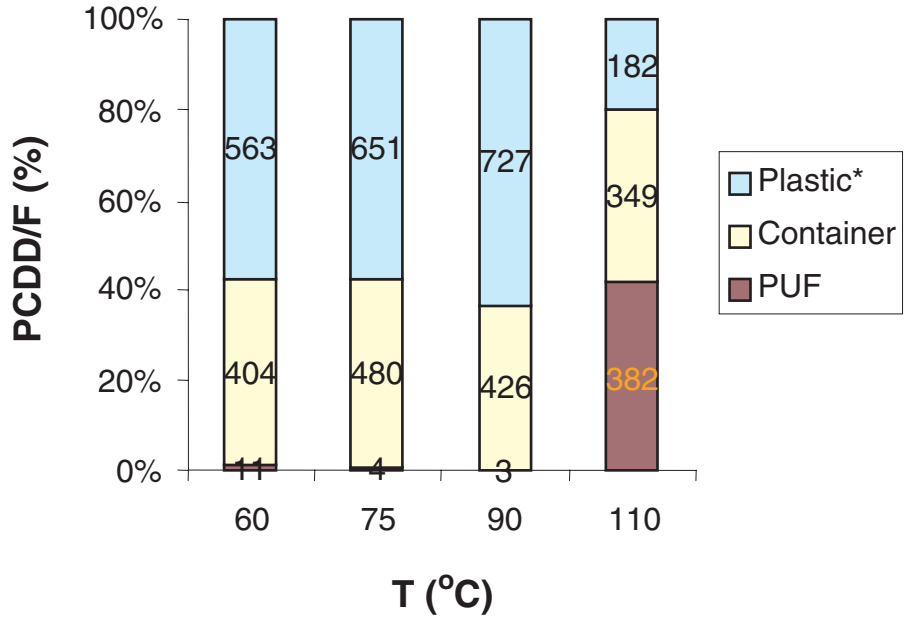

(b) ng I-TEQ/kg

Fig. 44(a and b): The effect of polypropylene temperature on PCDD/F absorption

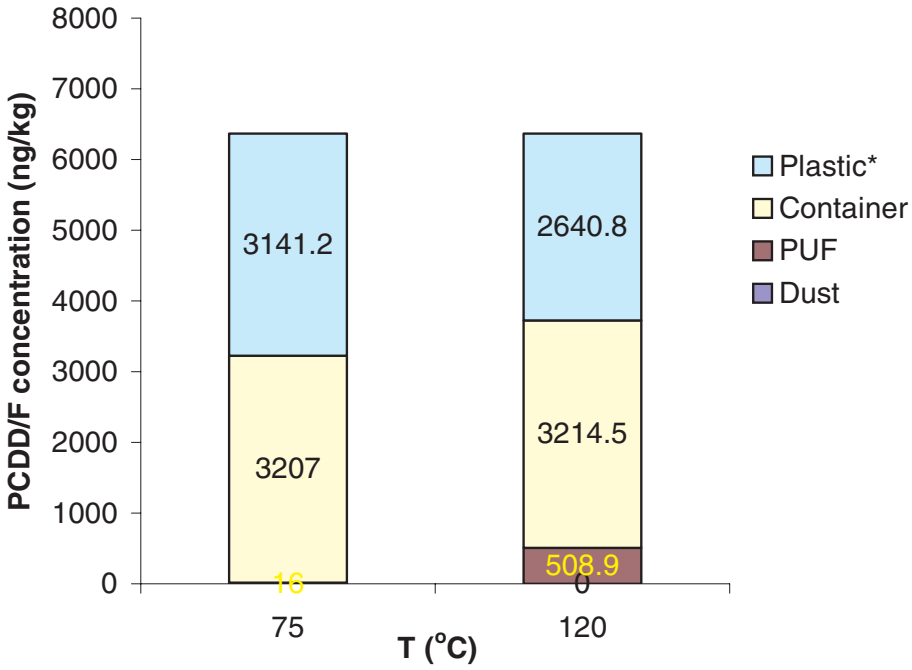

Fig. 45: PCDD/F distribution in desorption experiments

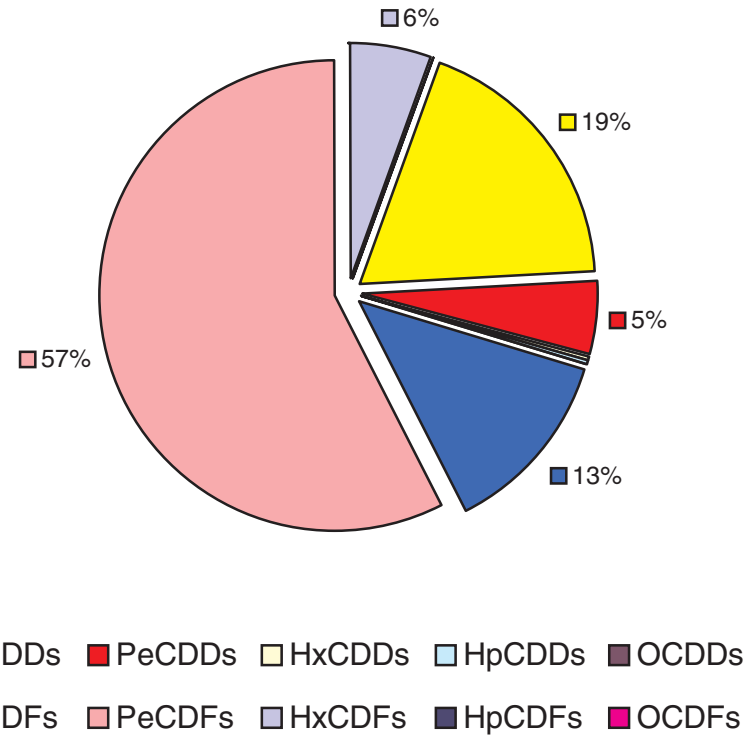

Fig. 46: Homologue proportion of vapour PCDD/F, I-TEQ/kg in desorption experiment conducted at 120°C

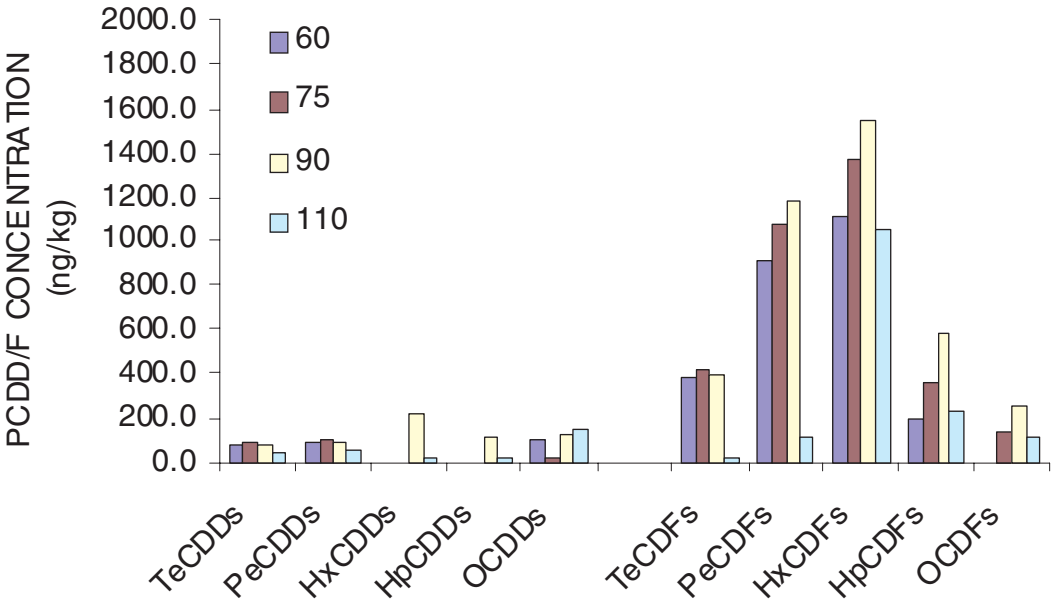

(a) ng/kg

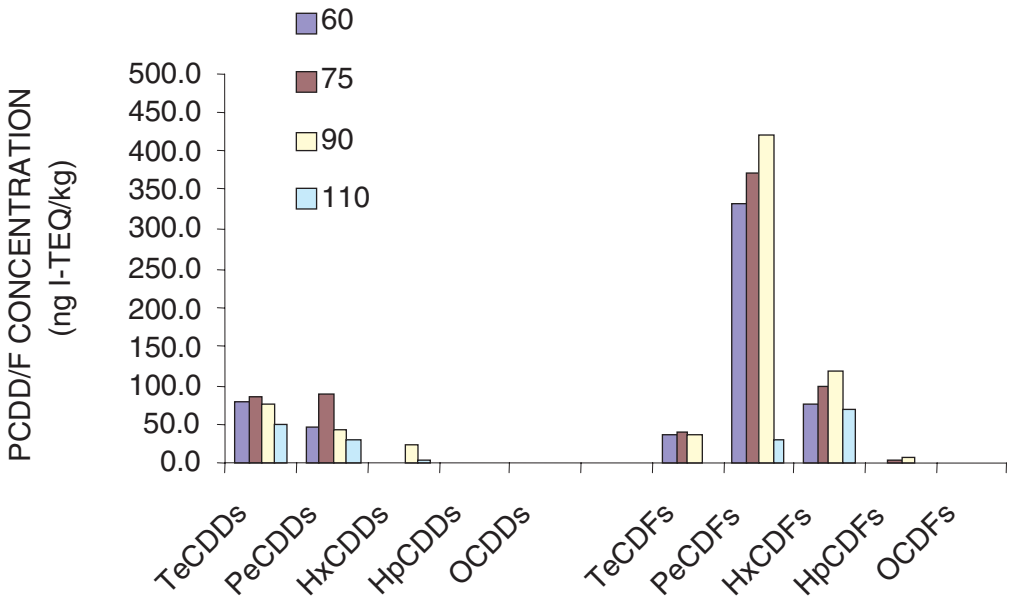

(b) ng I-TEQ/kg

Fig. 47(a and b): Estimated PCDD/F homologue loading profile in polypropylene

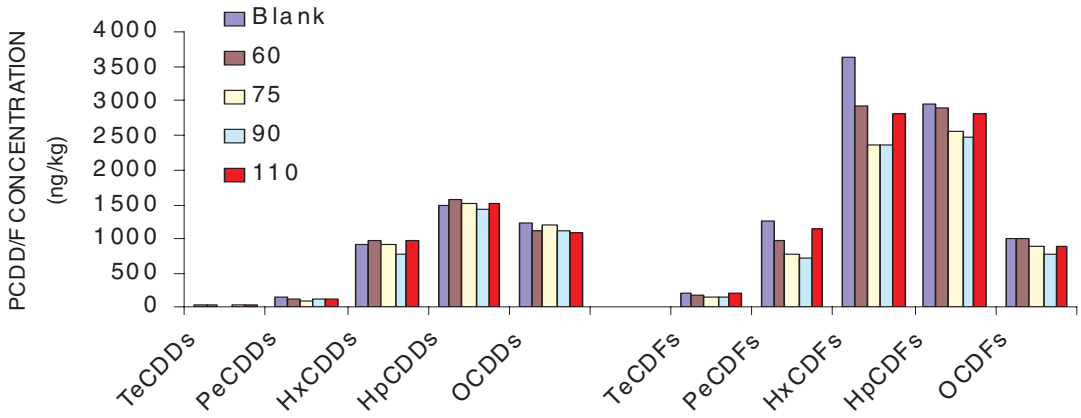

(a) Dust

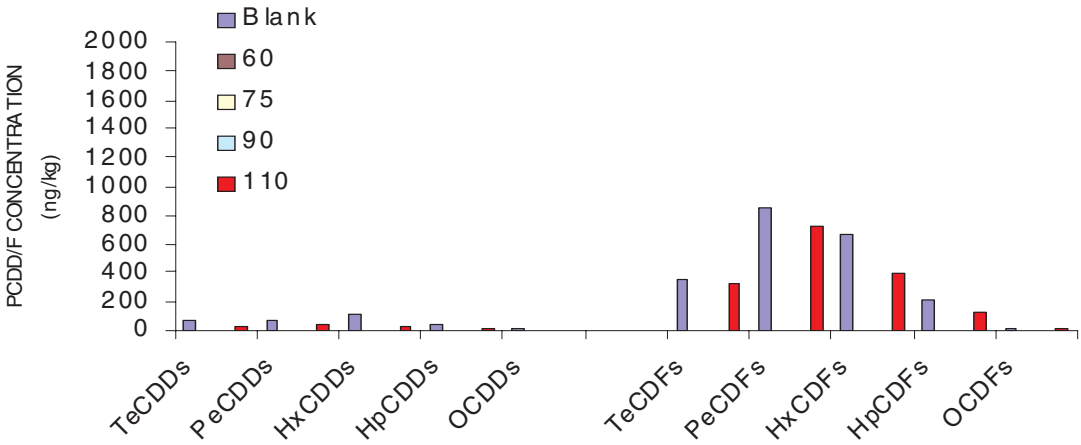

(b) PUF

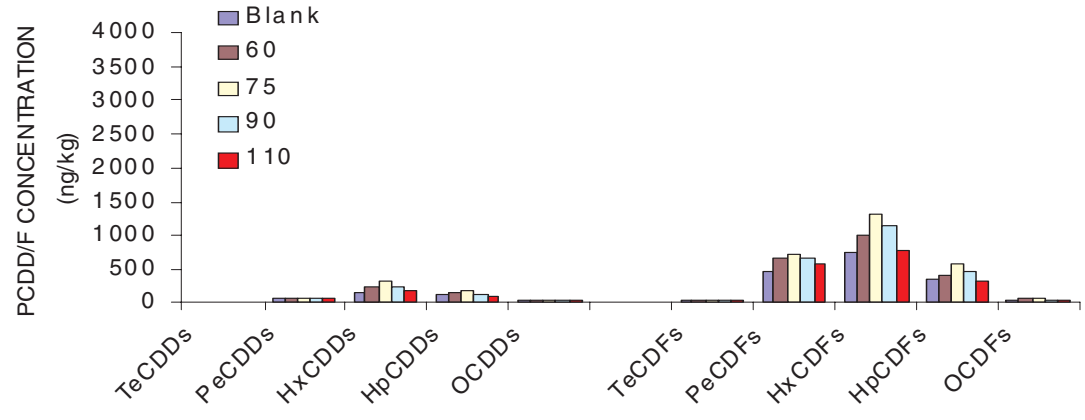

(c) Container

Fig. 48(a-c): The effect of polypropylene temperature on PCDD/F homologue distribution in ng/kg

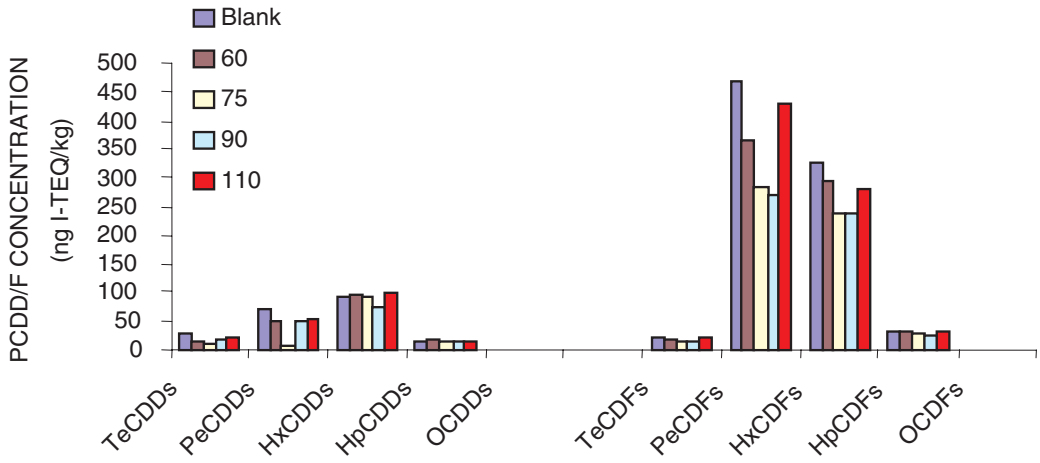

(a) Dust

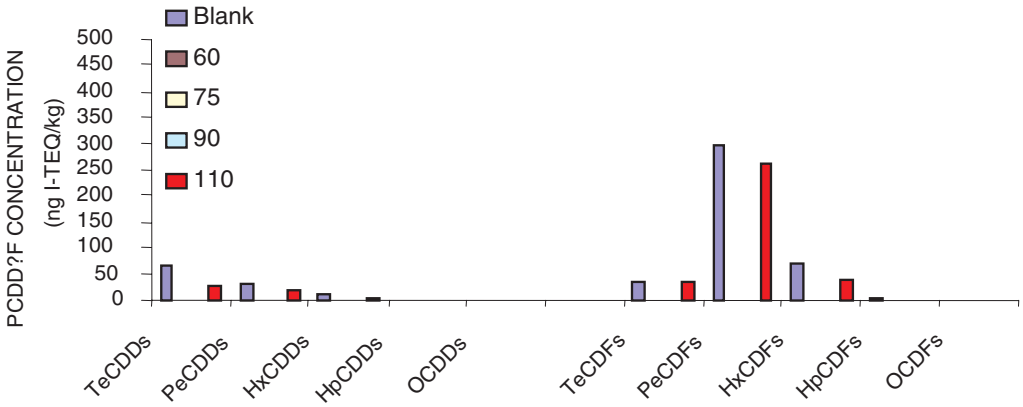

(b) PUF

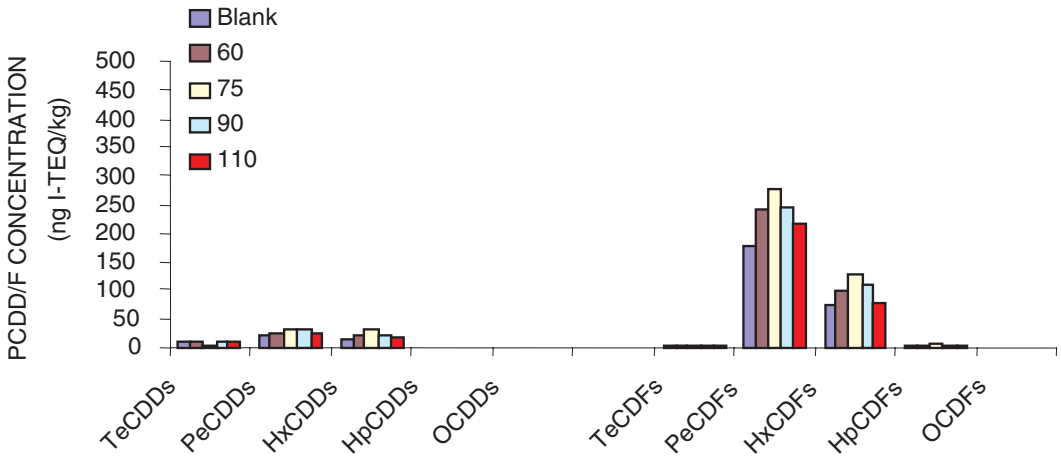

(c) Container

Fig. 49(a-c): The effect of polypropylene temperature on PCDD/F homologue distribution in ng I-TEQ/kg

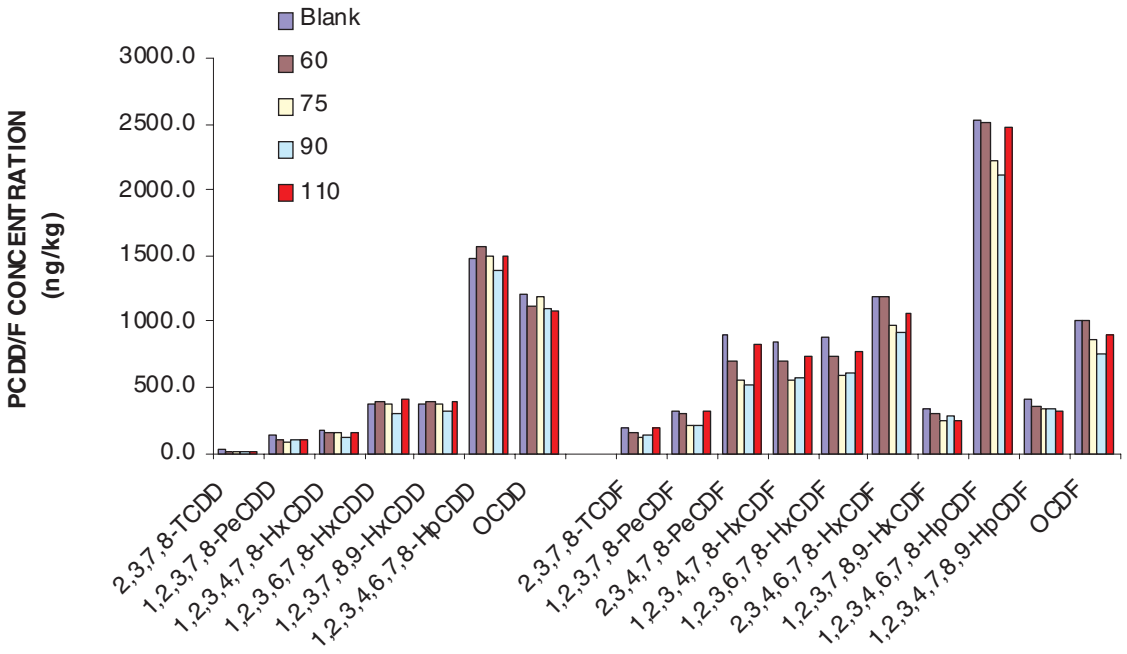
PCDD/F CONCENTRATION (ng/kg)
Blank
60
75
90
110
3000.0
2500.0
2000.0
1500.0
1000.0
500.0
0.0
2,3,7,8-TCDD
1,2,3,7,8-PeCDD
1,2,3,4,7,8-HxCDD
1,2,3,6,7,8-HxCDD
1,2,3,7,8,9-HxCDD
1,2,3,4,6,7,8-HpCDD
OCDD
2,3,7,8-TCDF
1,2,3,7,8-PeCDF
2,3,4,7,8-PeCDF
1,2,3,4,7,8-HxCDF
1,2,3,6,7,8-HxCDF
2,3,4,6,7,8-HxCDF
1,2,3,7,8,9-HxCDF
1,2,3,4,6,7,8-HpCDF
1,2,3,4,7,8,9-HpCDF
OCDF

(a) Dust

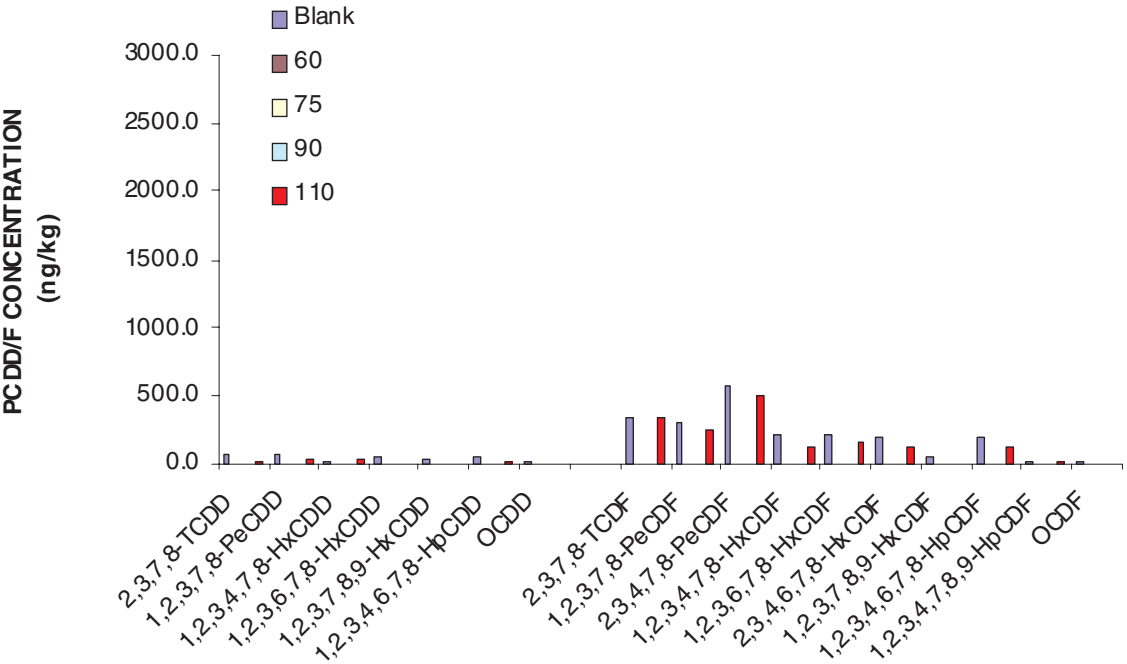
PCDD/F CONCENTRATION (ng/kg)
Blank
60
75
90
110
3000.0
2500.0
2000.0
1500.0
1000.0
500.0
0.0
2,3,7,8-TCDD
1,2,3,7,8-PeCDD
1,2,3,4,7,8-HxCDD
1,2,3,6,7,8-HxCDD
1,2,3,7,8,9-HxCDD
1,2,3,4,6,7,8-HpCDD
OCDD
2,3,7,8-TCDF
1,2,3,7,8-PeCDF
2,3,4,7,8-PeCDF
1,2,3,4,7,8-HxCDF
1,2,3,6,7,8-HxCDF
2,3,4,6,7,8-HxCDF
1,2,3,7,8,9-HxCDF
1,2,3,4,6,7,8-HpCDF
1,2,3,4,7,8,9-HpCDF
OCDF

(b) PUF

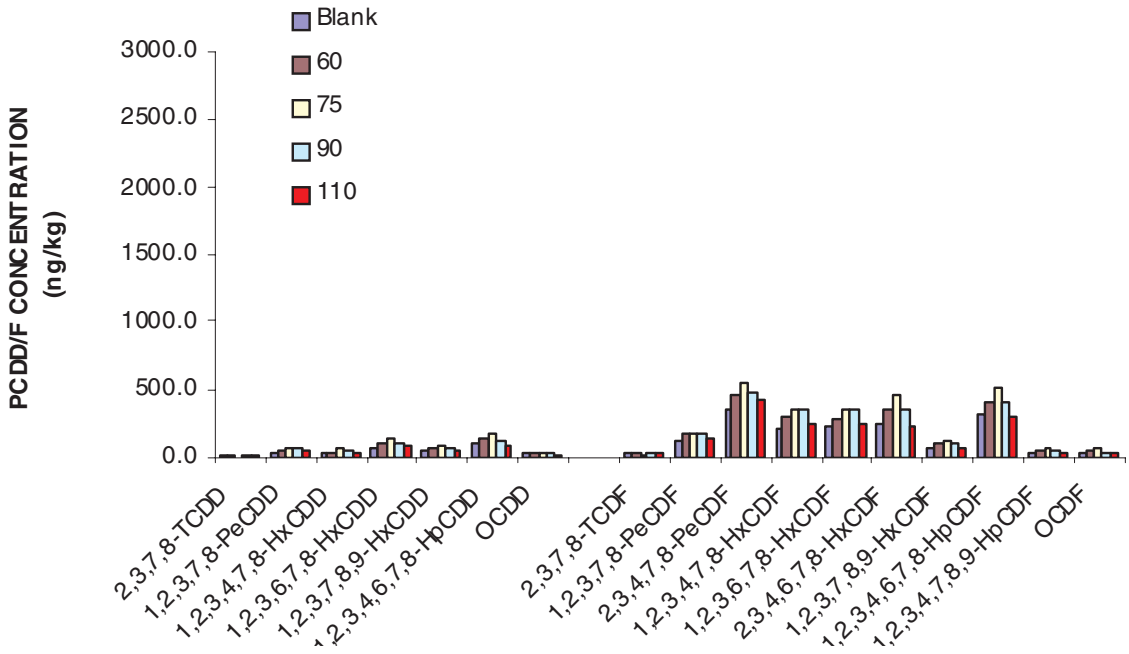

(c) Container

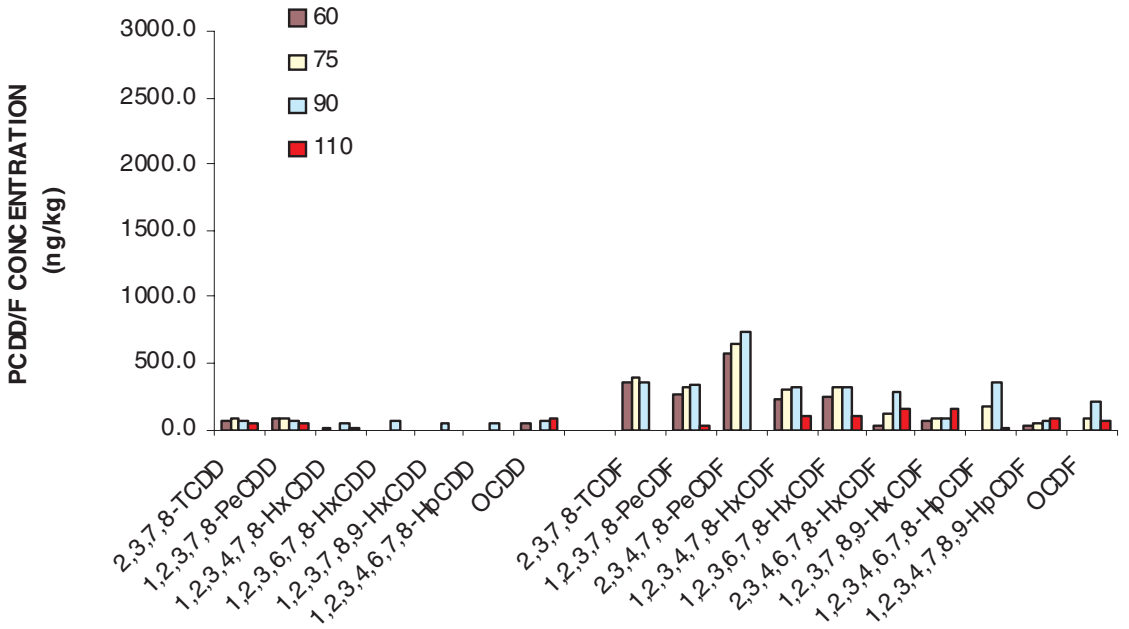

(d) Plastic

Fig. 50(a-d): The effect of polypropylene temperature on PCDD/F congener distribution in ng/kg

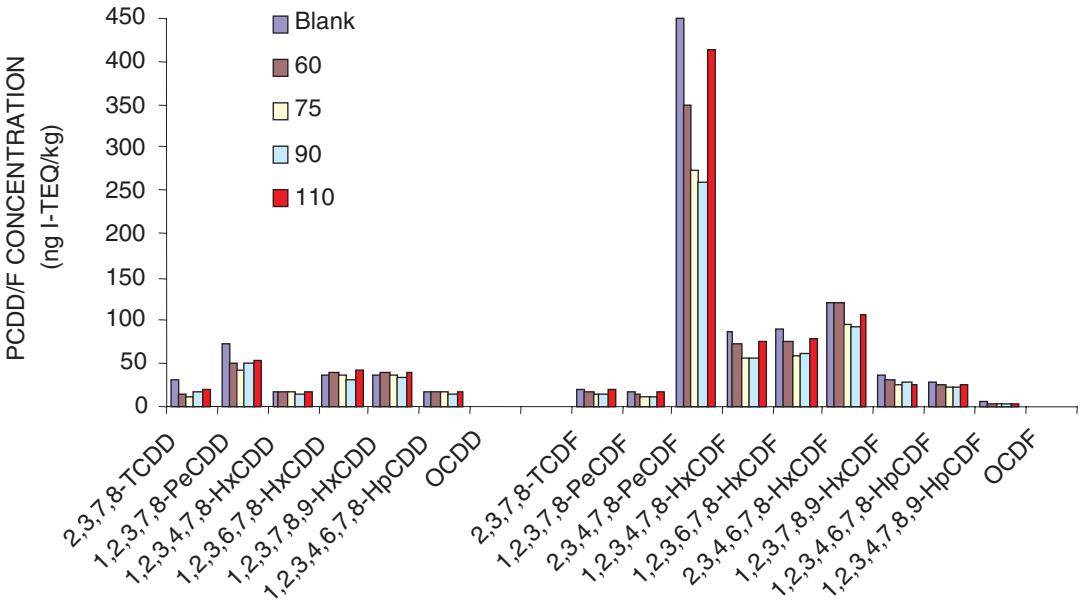
PCDD/F CONCENTRATION
(ng I-TEQ/kg)
450
400
350
300
250
200
150
100
50
0
Blank
60
75
90
110
2,3,7,8-TCDD
1,2,3,7,8-PeCDD
1,2,3,4,7,8-HxCDD
1,2,3,6,7,8-HxCDD
1,2,3,7,8,9-HxCDD
1,2,3,4,6,7,8-HpCDD
OCDD
2,3,7,8-TCDF
1,2,3,7,8-PeCDF
2,3,4,7,8-PeCDF
1,2,3,4,7,8-HxCDF
1,2,3,6,7,8-HxCDF
2,3,4,6,7,8-HxCDF
1,2,3,7,8,9-HxCDF
1,2,3,4,6,7,8-HpCDF
1,2,3,4,7,8,9-HpCDF
OCDF

(a) Dust

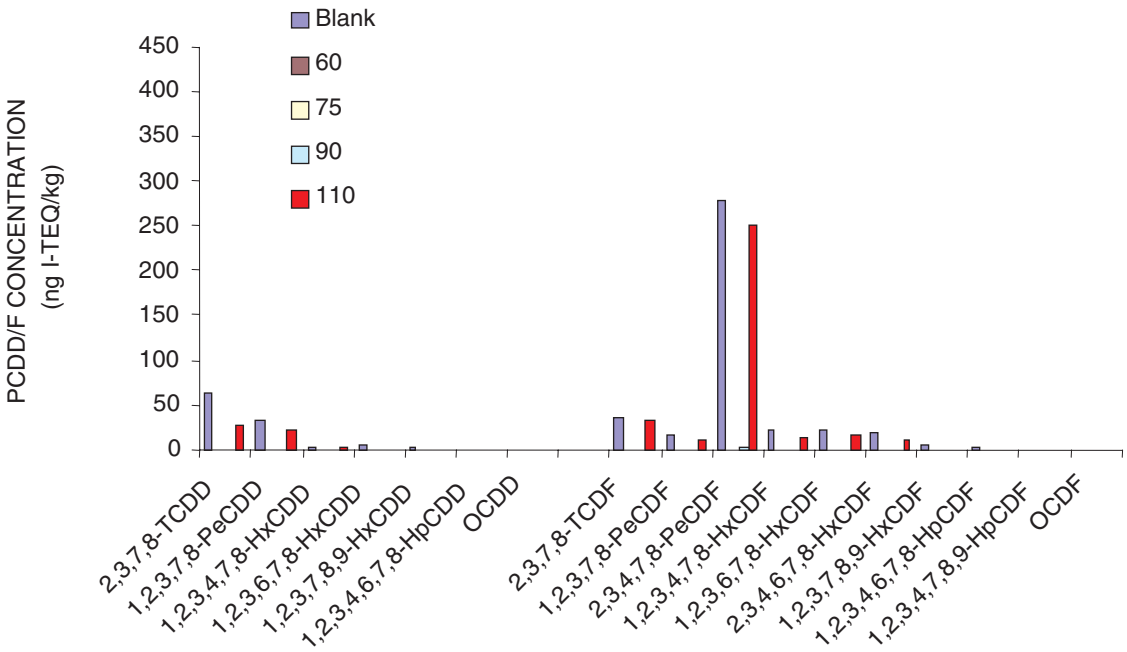
PCDD/F CONCENTRATION
(ng I-TEQ/kg)
450
400
350
300
250
200
150
100
50
0
Blank
60
75
90
110
2,3,7,8-TCDD
1,2,3,7,8-PeCDD
1,2,3,4,7,8-HxCDD
1,2,3,6,7,8-HxCDD
1,2,3,7,8,9-HxCDD
1,2,3,4,6,7,8-HpCDD
OCDD
2,3,7,8-TCDF
1,2,3,7,8-PeCDF
2,3,4,7,8-PeCDF
1,2,3,4,7,8-HxCDF
1,2,3,6,7,8-HxCDF
2,3,4,6,7,8-HxCDF
1,2,3,7,8,9-HxCDF
1,2,3,4,6,7,8-HpCDF
1,2,3,4,7,8,9-HpCDF
OCDF

(b) PUF

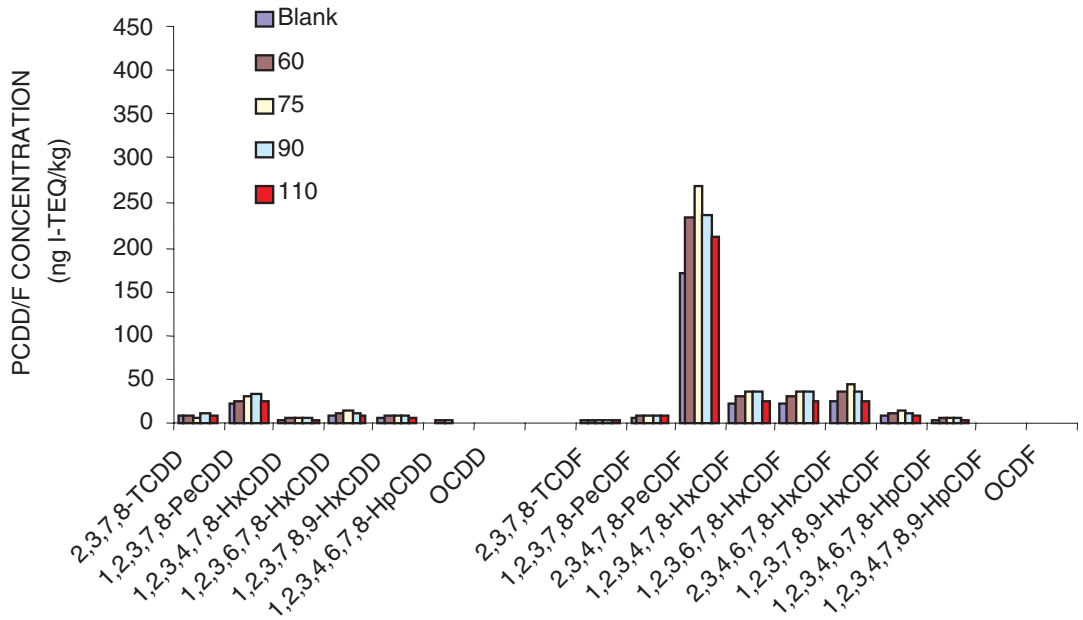

(c) Container

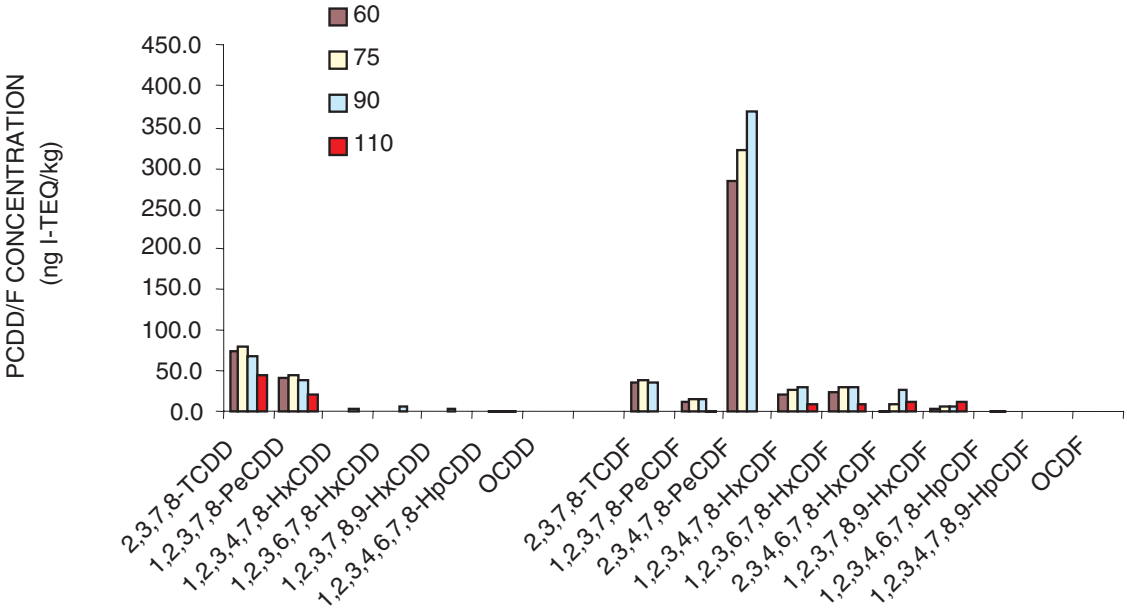

(d) Plastic

Fig. 51(a-d): The effect of polypropylene temperature on PCDD/F congener distribution in ng I-TEQ/kg

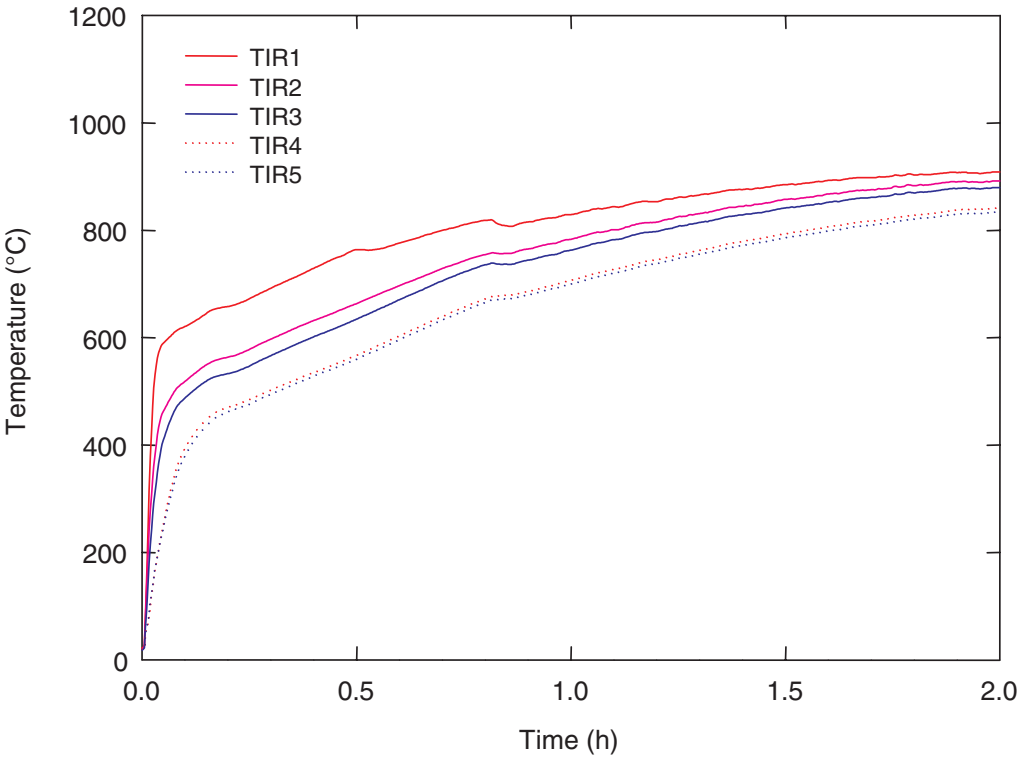

Fig. 52: Scrap temperature profile in the scrap pre-heating chamber for a selected scrap pre-heating trial

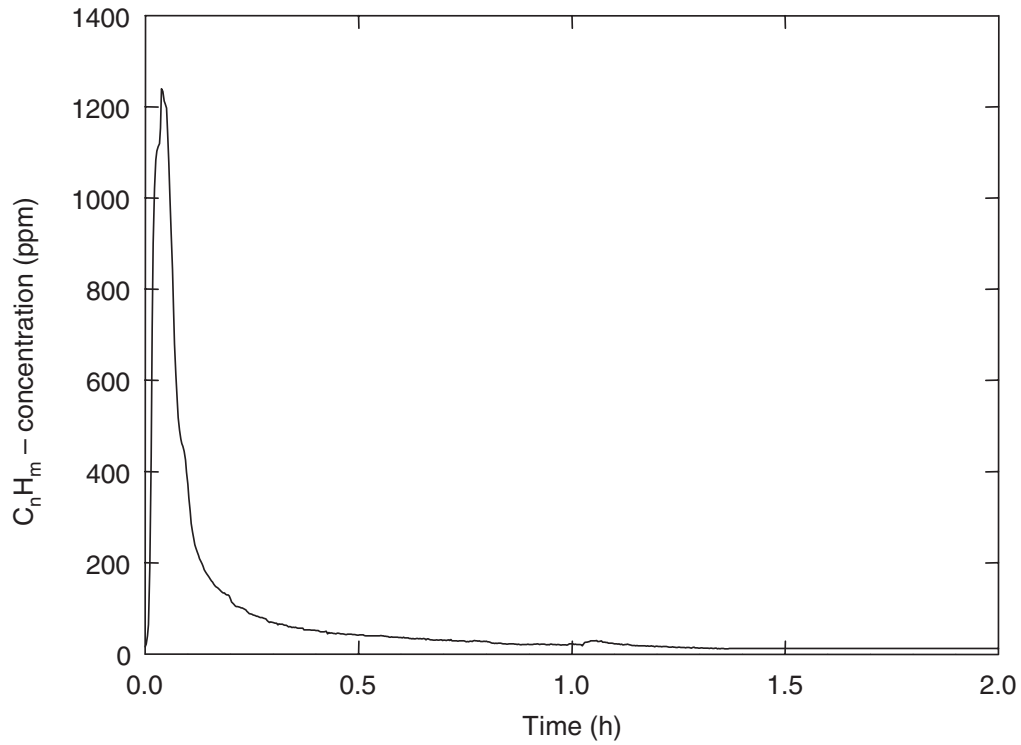

Fig. 53: VOC-concentration (CnHm) at the exit of the scrap pre-heating chamber for a selected pre-heating trial with oil contaminated scrap

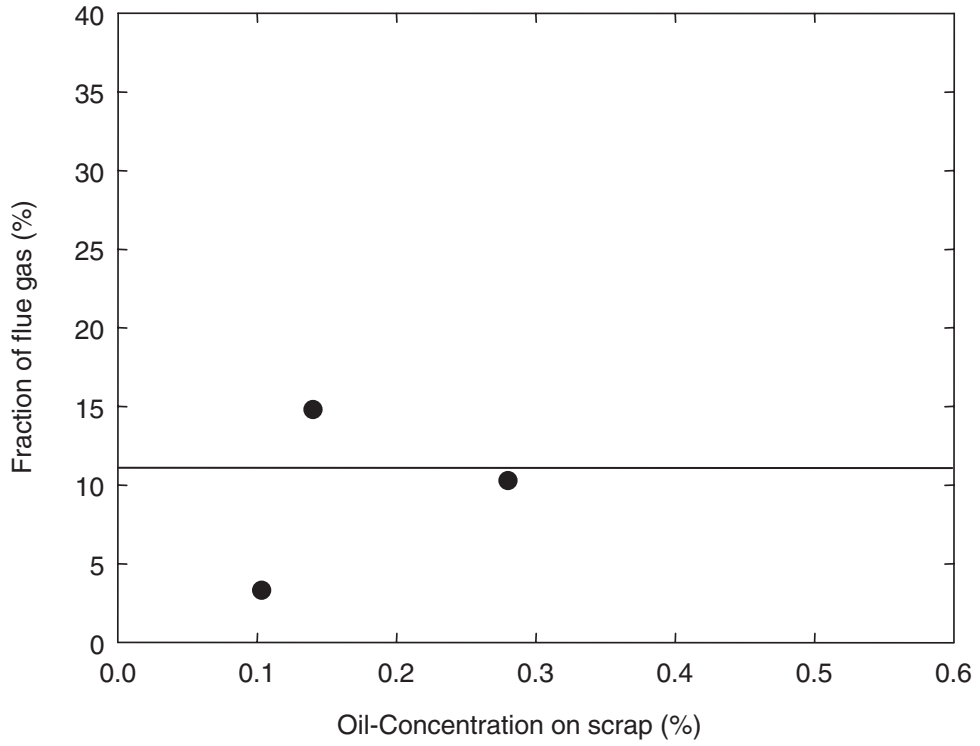

Fig. 54: Relative VOC amount on scrap pre-heating with oxygen-free pre-heating gas with varying the oil concentration on scrap

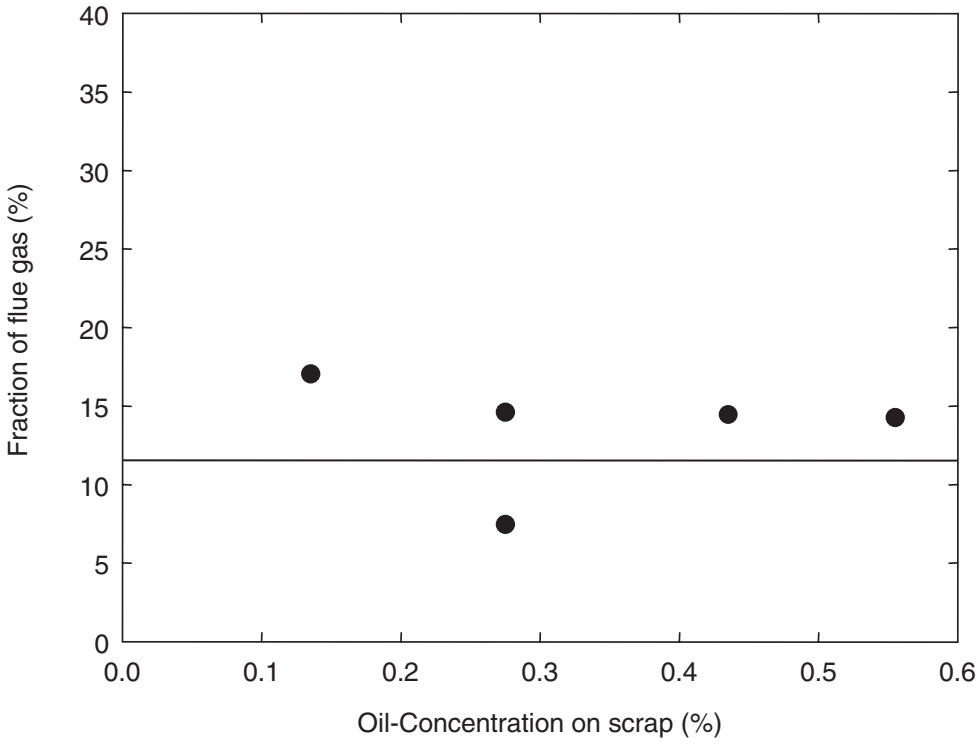

Fig. 55: Relative VOC amount with varying oil concentration on scrap (10% O_2 in pre-heating gas)

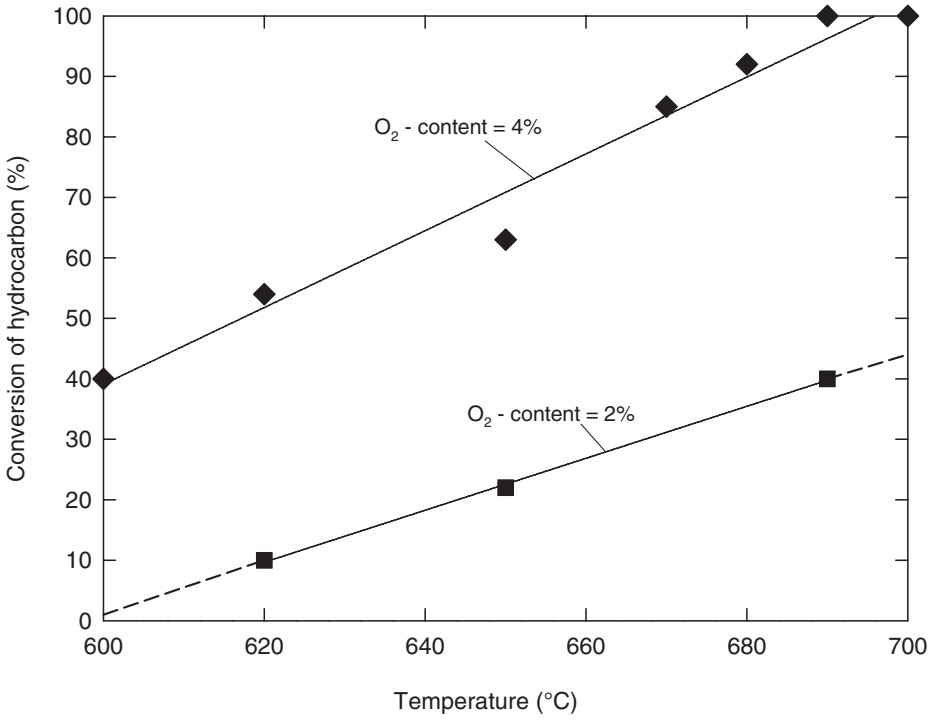

Fig. 56: Conversion of hydrocarbon versus temperature
(hydrocarbon amount: 2500 ppm)

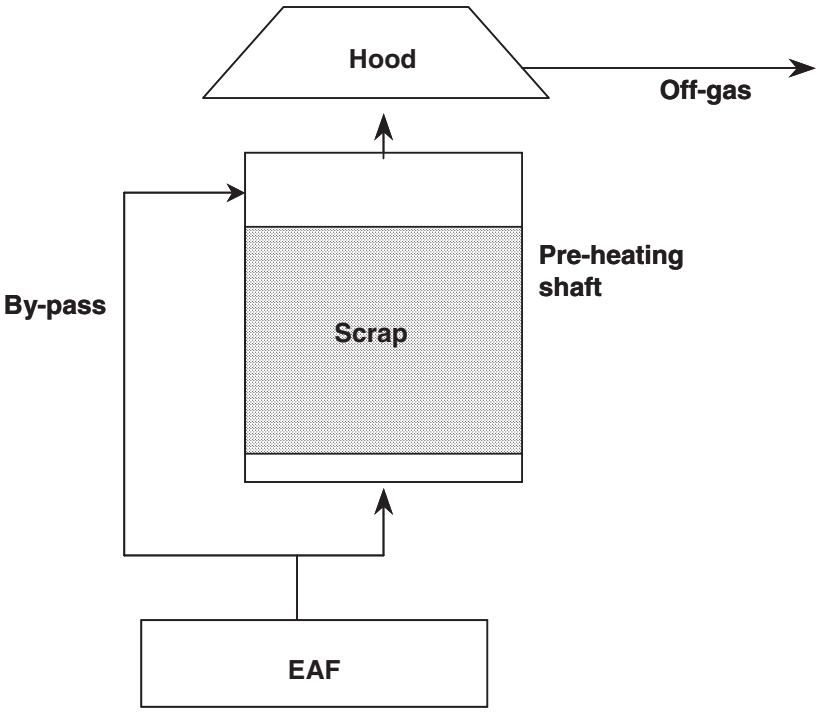

Fig. 57: Scheme of post-combustion in a shaft

Appendix 1

Terminology and structure of trace organic pollutants

A1.1 Introduction

Emissions from iron and steelmaking processes contain trace amounts of organic pollutants. In several instances these trace organic pollutants belong to families of compounds that are referred to by generic names or abbreviations. However, in discussing the formation, quantification and effects of trace organic compounds it is often necessary to refer to specific members or subgroups of the parent families of compounds. This Appendix presents general information on the nomenclature, terminology, chemical structures and important subgroups of three important families of trace organic pollutants viz., dioxins (polychlorinated dibenzo-p-dioxins and polychlorinated dibenzofurans), PCBs (polychlorinated biphenyls) and PAHs (polycyclic aromatic hydrocarbons).

A1.2 Structure and composition of dioxins (PCDD/Fs)

'Dioxin' is a collective noun that is applied to the members of two closely related families of chlorinated tricyclic organic compounds, namely, polychlorinated dibenzo-p-dioxins (PCDDs) and polychlorinated dibenzofurans (PCDFs). The parent compounds from which PCDDs and PCDFs are derived are shown in Fig. A1.1, together with the numbering convention that is used for denoting the positions on the two benzenoid rings where substituent chlorine atoms may be placed. In each series the number of chlorine substituents may vary from 1 to 8 giving rise to 75 PCDDs and 135 PCDFs. Each individual PCDD or PCDF is termed a congener, while members within a given level of chlorination are referred to as homologues. Each homologue group is made up of a number of positional isomers as indicated in Table A1.1. Dioxins have no known uses and are not manufactured intentionally. However, they are formed as unwanted by-products in the chlorinated organ chemical industry and in combustion processes associated with industry, manufacturing and waste incineration. In particular, dioxins are formed and emitted from certain iron and steelmaking processes, such as iron ore sintering and EAF steelmaking.

A1.2.1 International toxic equivalents

The chemical toxicities of PCDDs and PCDFs vary both with the number and configuration of the chlorine substituents and only those compounds having chlorine atoms in the 2,3,7 and 8 positions are regarded as being toxicologically important. The analysis is therefore directed towards the quantification of the 17 target congeners that possess the 2,3,7,8-configuration of chlorine atoms. Of the 17 target compounds, 2,3,7,8-tetrachlorodibenzo-p-dioxin (2,3,7,8-TCDD) is the most toxic and is assigned a toxicity rating (referred to as an International Toxic Equivalent Factor or I-TEF, also known as International Toxic Equivalency Factor) of 1. The remaining 2, 3, 7, 8 - congeners are assigned lower TEFs relative to that of 2, 3, 7, 8 - TCDD as shown in Table A1.2. The structures are shown in Figs. A1.2 and A1.3.

The overall toxicity of a sample containing a mixture of PCDDs and PCDFs is obtained using a procedure developed by NATO-CCMS (North Atlantic Treaty Organisation's Committee on Challenges of Modern Society) in 1998 to promote international consistency in reporting PCDD/F data. The overall toxicity (I-TEQ, International Toxic Equivalent, or Equivalence) is calculated by firstly, multiplying the concentrations of the individual target compounds by their respective TEFs. The resulting values are referred to as TEQs (or Toxic Equivalents). Secondly, the individual TEQs are summed to provide the overall I-TEQ of the sample. The I-TEQ value is used to compare the PCDD/F concentrations of different samples and is required

essentially for regulatory purposes and for assessing the environmental impact of emissions. However, for fundamental studies concerning the formation, transport and fate of PCDD/Fs it is necessary to have detailed information on the congener profile of the sample.

A1.3 Structure and composition of polychlorinated biphenyls (PCBs)

PCBs are based on the biphenyl structure (Fig. A1.4), a molecule composed of two benzene rings joined together by a single carbon bond, and are derived by systematically substituting the hydrogen atoms by chlorine atoms to give a family of 209 compounds containing between 1 and 10 chlorine substituents. The full list is given in Table A1.3 together with their IUPAC identification numbers. Unlike PCDD/Fs, PCBs were produced commercially, principally for use as dielectric fluids and coolants in transformers and electrical capacitors. They were also used as plasticisers, in 'carbonless' copy paper and as deinking solvents for recycling newsprints. PCBs are produced by heating biphenyl and chlorine with ferric chloride as catalyst and this reaction produces a mixture of many of the 209 congeners; the exact proportions depend upon the ratio of chlorine to biphenyl, and the reaction time and temperature. Biphenyl is prepared by heating benzene to 750°C in the presence of lead as a catalyst. Commercially, individual PCB compounds were not isolated but sold as partially separated mixtures with the average chlorine content ranging from 21 to 68% in different products. These mixtures were sold under trade names such as Aroclors (Monsanto) and Clophen (Bayer). Although the manufacture and use of PCBs is no longer permitted in the UK under The Control of Pollution (Supply and Use of Injurious Substances Regulations 1986, as amended), use of PCBs in certain existing equipment was exempted from the ban. However, concern about the effects of PCBs on sea mammals led to agreement by the Third North Sea Conference in 1990 to phase out and destroy remaining identifiable PCBs by the end of 1999. Total world production of PCBs since 1930 has been estimated to be between 1 and 2 million tonnes and although their use is now severely restricted, these substances are widely distributed in the environment and foods owing to their resistance to degradation by normal environmental processes. PCBs are also formed inadvertently and are emitted at trace levels in certain industrial and combustion processes and they are known to be chemical precursors in the synthesis of PCDFs.

The tricyclic structure of PCDFs results in flat molecules in which all the atoms (C, H, O and Cl) lie in the same place. In PCBs, however, the two benzene rings are connected by a carbon - carbon single band so that they are free to rotate with respect to each other. When the so-called ortho-position (2, 2', 6 and 6') are occupied by bulky groups or atoms, such as chlorine, steric interactions between the substituent groups force the benzene rings to adopt a skew conformation where they lie in different planes with respect of each other. However, in PCBs that have no chlorine atoms (or at most two chlorine) in the ortho-position, the two benzene rings can adopt an almost co-planar (i.e. flat) configuration which is similar in size and shape to that of PCDD/Fs. At a molecular level it is the size and shape of the molecule that is important in determining the toxicity of PCDD/Fs and PCBs owing to their ability to fit into the cavity in a specific biological receptor. Those PCBs which can adopt a co-planar configuration and that have chlorine substituted in the 3, 3', 4 and 4' position have molecular characteristics similar to those of the 2,3,7,8-substituted PCDD/Fs and are more toxic than other PCB congeners.

The 'dioxin-like PCBs' or 'co-planar PCBs' include:

(i) 3 non-ortho PCBs: 77, 126 and 169. These have no chlorine atoms substituted in the ortho position, i.e. on the carbon atom adjacent to the carbon to carbon bond that links the two benzene molecules, i.e. in the 2, 2', 6 or 6' positions.

(ii) 8 mono-ortho PCBs: 105, 114, 118, 123, 156, 167, 189. These have only one chlorine atom substituted in the ortho position.

(iii) 2 di-ortho PCBs: 170 and 180. These have two chlorine atoms in the ortho position.

Recently, the World Health Organisation (WHO) assigned toxic equivalent factors to twelve of these PCBs relative to 2, 3, 7, 8-TCDD, as for the PCDD/Fs.

Unfortunately there is no universally accepted set of PCBs similar to the 17 targeted PCDD/Fs and hence different sub-sets tend to be used in environmental studies depending upon the main focus of the work. At least five sub-sets of the 209 congeners are used by different groups of workers as follows:

1. The twelve congeners regarded as 'dioxin-like' by the international community which have now been assigned toxic equivalent factors (TEFs) (see Table A1.4, Figs. A1.5 and A1.6) by the World Health Organisation (WHO) (PCBs 77, 81, 105, 114, 118, 123, 126, 156, 157, 167, 169 and 189). These TEFs are relative to 2, 3, 7, 8 - TCDD as for PCDD/Fs;

2. seventeen congeners with reported toxicological effects (PCBs 4, 18, 28, 31, 47, 49, 51, 52, 77, 81, 105, 118, 126, 153, 156, 157 and 169);

3. seven congeners selected by the International Committee for the Exploration of the Sea for analysis in marine fish (PCBs 28, 52, 101, 118, 138, 153 and 180), same set as EC7 below;

4. thirty-four congeners commonly found to occur in food or human milk (PCBs 28, 33, 37, 41, 44, 49, 52, 60, 66, 74, 87, 99, 101, 105, 110, 114, 118, 141, 151, 153, 156, 157, 180, 183, 185, 187, 189, 191, 193, 194, 201, 203, 206 and 209);

5. the so-called EC7 (Fig. A1.7), which is a set of seven PCBs that are typically found in Aroclors which were used as transformer oils and which were commonly found in soils that had been contaminated as a result of leakage from transformers (PCBs 28, 52, 101, 118, 138, 153 and 180).

As is evident from the above listings there is considerable overlap between the various sub-sets so that the total number of PCBs that is required for analysis to cover all these groups is 46. Additionally, the UK Food Standard Agency also includes PCBs 61, 80, 128, 129, 149, 170, 202 and 209 in its suite of PCBs to be determined in milk.

A1.4 Structure and composition of polycyclic aromatic hydrocarbons (PAHs)

Polycyclic aromatic hydrocarbons (PAHs) are ring compounds wherein two or more aromatic rings are fused together in the ortho-positions (Fig. A1.8). PAHs are constituents of coal tar and some of the lighter compounds such as naphthalene and anthracene were industrially important as intermediates in the coal chemicals industry in the past. Apart from these two compounds other PAHs have no commercial importance. PAHs are commonly found in combustion waste gases as products of incomplete combustion of organic compounds. Although about 500 PAHs have been detected in air, environmentally the most significant group is the sixteen PAHs of the US EPA Priority PAHs. These are listed in Table A1.5 and with physical data in Table A1.6.

Subsets of the USA EPA 16 PAHs are shown in Table A1.5 and include:

1. The UK Committee on Carcinogenicity (COC), part of the Department of Health, allocated a Toxic Equivalency Factor (TEF) to each of the US EPA Priority 16 PAHs, based on carcinogenic potential and not related to the PCDD/F I-TEQ system.

2. The International Agency for Research on Cancer (IARC) has classified many PAHs according to their likely carcinogenic hazard for humans. The UK Expert Panel on Air Quality Standards (EPAQS) group listed the IARC classifications for most of the US EPA Priority 16 PAHs, Table A1.5. Group 2A compounds are 'probably carcinogenic to humans', group 2B are 'possibly carcinogenic to humans' and group 3 are 'not classifiable'. IARC class chrysene as group 3, but the EPAQS report states that the UK Committee on Carcinogenicity regards chrysene as a possible human carcinogen, group 2B.

3. EPAQS Seven. The UK Expert Panel on Air Quality Standards (EPAQS) allocated weighting factors to the seven PAHs defined as probable or possible human carcinogens (IARC groups 2A and 2B). These factors were determined from animal experiments and indicate the carcinogenic potency relative to benzo(a)pyrene.

4. Borneff Six. These are also part of the World Health Organisation drinking water standard and there is a Borneff Four subset, which is the same as the POPS 4, below.

5. UNICE POPs 4 (Persistent Organic Pollutants). The United Nations/Economic Commission for Europe (UN/ECE) protocol on Persistent Organic Pollutants (the POPS Protocol, June 1998) requires each signatory to 'Reduce its total annual emissions of each of the substances listed in Annex III...' {Article 3, paragraph 5(a)}. Annex III specifies just four PAHs for the purposes of creating emissions inventories and these are indicated in the table.

6. B[a]P (Benzo[a]pyrene). Although the EPAQS (UK Expert Panel on Air Quality Standards) group allocated weighting factors to seven PAHs, their final recommendation for an air quality standard was based on only one of these, benzo(a)pyrene (B[a]P). Although B[a]P is neither the most carcinogenically potent PAH, nor the one found at the highest concentration, it was found that B[a]P contributed around 40 - 50% of the total carcinogenic potency of ambient mixtures of PAHs in the UK when the EPAQS weighting factors were used. The suggested standard is an annual average of 0.25 ng/m^3.

7. B[a]P Equivalent (Benzo[a]pyrene). The Environment Agency has adopted this reporting standard based on molecular weight and requests PAH data in terms of B[a]P equivalent. The equivalent is based on molecular weight, for example, to convert a value for naphthalene (molecular weight 128. 19) to B[a]P (m.w. 252. 32), the multiplication factor is 252/128 = 1.97. This equivalent is calculated for each of the 16 US EPA Priority PAHs and these values summed to provide a total PAH concentration expressed as B[a]P equivalent. This weighting method therefore gives more weight to the lighter compounds, whereas other methods tend to give more weight to the heavier compounds which have greater carcinogenic potential. This method is used by Corus and other companies to report data to the Environment Agency.

Although the PAHs differ in toxicity, there is no commonly accepted method of expressing concentrations in terms of toxic equivalent concentrations similar to those used for PCDD/Fs and PCBs. It is also important to note that the total PAH concentration of a sample i.e. the sum of the US EPA 16, will depend upon the method used to calculate the sum. For example, when calculated as B[a]P equivalent, the PAH concentration in a typical steel industry emission is about fifteen times greater than a POPS 4 estimate. This is because the POPS 4 constitute only 10% of the total PAH emission and because of the large contribution of naphthalene, the predominant species in steel industry sources of PAHs, which carries a weighting factor of 1.97 when expressed as B[a]P equivalent.

Table A1.1: Number of PCDD and PCDF isomers

Chlorine atoms	Number of isomers	
	Dioxin	Furan
1	2	4
2	10	16
3	14	28
4	22	38
5	14	28
6	10	16
7	2	4
8	1	1
Total	75	135

Table A1.2: International toxic equivalent factors (I-TEQ) for PCDD and PCDF compounds

Congener	Dibenzo-p-dioxin	Dibenzofuran
2,3,7,8 - tetrachoro-	1	0.1
2,3,4,7,8 - pentachloro-	No congener	0.5
1,2,3,7,8 - pentachloro-	0.5	0.05
1,2,3,4,7,8 - hexachloro-	0.1	0.1
1,2,3,7,8,9 - hexachloro-	0.1	0.1
1,2,3,6,7,8 - hexachloro-	0.1	0.1
2,3,4,6,7,8 - hexachloro-	No congener	0.1
1,2,3,4,6,7,8 - heptachloro-	0.01	0.01
1,2,3,4,7,8,9 - heptachloro-	No congener	0.01
octachloro-	0.001	0.001

Table A1.3: List of the 209 PCB congeners with the corresponding IUPAC number

IUPAC Number	PCB Compound
1	2 - Monochlorobiphenyl
2	3 - Monochlorobiphenyl
3	4 - Monochlorobiphenyl
4	2,2' - Dichlorobiphenyl
5	2,3 - Dichlorobiphenyl
6	2,3' - Dichlorobiphenyl
7	2,4 - Dichlorobiphenyl
8	2,4' - Dichlorobiphenyl
9	2,5 - Dichlorobiphenyl
10	2,6 - Dichlorobiphenyl
11	3,3' - Dichlorobiphenyl
12	3,4 - Dichlorobiphenyl
13	3,4' - Dichlorobiphenyl
14	3,5 - Dichlorobiphenyl
15	4,4' - Dichlorobiphenyl
16	2,2',3 - Trichlorobiphenyl
17	2,2',4 - Trichlorobiphenyl
18	2,2',5 - Trichlorobiphenyl
19	2,2',6 - Trichlorobiphenyl
20	2,3,3' - Trichlorobiphenyl
21	2,3,4 - Trichlorobiphenyl
22	2,3,4' - Trichlorobiphenyl
23	2,3,5' - Trichlorobiphenyl
24	2,3,6 - Trichlorobiphenyl
25	2,3',4 - Trichlorobiphenyl
26	2,3',5 - Trichlorobiphenyl
27	2,3',6 - Trichlorobiphenyl
28	2,4,4' - Trichlorobiphenyl
29	2,4,5 - Trichlorobiphenyl
30	2,4,6 - Trichlorobiphenyl
31	2,4',5 - Trichlorobiphenyl
32	2,4',6 - Trichlorobiphenyl
33	2',3,4 - Trichlorobiphenyl
34	2',3,5 - Trichlorobiphenyl
35	3,3',4 - Trichlorobiphenyl
36	3,3',5 - Trichlorobiphenyl
37	3,4,4' - Trichlorobiphenyl
38	3,4,5 - Trichlorobiphenyl
39	3,4',5 – Trichlorobiphenyl
40	2,2',3,3' - Tetrachlorobiphenyl
41	2,2',3,4' - Tetrachlorobiphenyl
42	2,2',3,4' - Tetrachlorobiphenyl
43	2,2',3,5 - Tetrachlorobiphenyl
44	2,2',3,5' - Tetrachlorobiphenyl
45	2,2',3,6 - Tetrachlorobiphenyl
46	2,2',3,6' - Tetrachlorobiphenyl
47	2,2',4,4' - Tetrachlorobiphenyl
48	2,2',4,5 - Tetrachlorobiphenyl
49	2,2',4,5' - Tetrachlorobiphenyl
50	2,2',4,6 - Tetrachlorobiphenyl
51	2,2',4,6' - Tetrachlorobiphenyl
52	2,2',5,5' - Tetrachlorobiphenyl
53	2,2',5,6' - Tetrachlorobiphenyl
54	2,2',6,6' - Tetrachlorobiphenyl
55	2,3,3',4 - Tetrachlorobiphenyl

56	2,3,3',4 - Tetrachlorobiphenyl
58	2,3,3',5' - Tetrachlorobiphenyl
57	2,3,3',5' - Tetrachlorobiphenyl
59	2,3,3',6 - Tetrachlorobiphenyl
60	2,3,4,4' - Tetrachlorobiphenyl
61	2,3,4,5 - Tetrachlorobiphenyl
62	2,3,4,6 - Tetrachlorobiphenyl
63	2,3,4,5 - Tetrachlorobiphenyl
64	2,3,4',6 - Tetrachlorobiphenyl
65	2,3,5,6 - Tetrachlorobiphenyl
66	2,3',4,4' - Tetrachlorobiphenyl
67	2,3',4,5' - Tetrachlorobiphenyl
68	2,3',4,5' - Tetrachlorobiphenyl
69	2,3',4,6' - Tetrachlorobiphenyl
70	2,3',4',5 - Tetrachlorobiphenyl
71	2,3',4',6 - Tetrachlorobiphenyl
72	2,3',5,5' - Tetrachlorobiphenyl
73	2,3',5',6 - Tetrachlorobiphenyl
74	2,4,4',5 - Tetrachlorobiphenyl
75	2,4,4',6 - Tetrachlorobiphenyl
76	2,3,4',5 - Tetrachlorobiphenyl
77	3,3',4,4' - Tetrachlorobiphenyl
78	3,3',4,5 - Tetrachlorobiphenyl
79	3,3',4,5' - Tetrachlorobiphenyl
80	3,3',5,5' - Tetrachlorobiphenyl
81	3,4,4',5 – Tetrachlorobiphenyl
82	2,2',3,3',4 - Pentachlorobiphenyl
83	2,2',3,3',5 - Pentachlorobiphenyl
84	2,2',3,3',6 - Pentachlorobiphenyl
85	2,2',3,4,4' - Pentachlorobiphenyl
86	2,2',3,4,5 - Pentachlorobiphenyl
87	2,2',3,4,5' - Pentachlorobiphenyl
88	2,2',3,4,6 - Pentachlorobiphenyl
89	2,2',3,4,6' - Pentachlorobiphenyl
90	2,2',3,4',5 - Pentachlorobiphenyl
91	2,2',3,4',6 - Pentachlorobiphenyl
92	2,2',3,5',5 - Pentachlorobiphenyl
93	2,2',3,5,6 - Pentachlorobiphenyl
94	2,2',3,5,6' - Pentachlorobiphenyl
95	2,2',3,5',6 - Pentachlorobiphenyl
96	2,2',3,6,6' - Pentachlorobiphenyl
97	2,2',3',4,5 - Pentachlorobiphenyl
98	2,2',3',4,6 - Pentachlorobiphenyl
99	2,2',4,4',5 - Pentachlorobiphenyl
100	2,2',4,4',6 - Pentachlorobiphenyl
101	2,2',4,5,5' - Pentachlorobiphenyl
102	2,2',4,5',6 - Pentachlorobiphenyl
103	2,2',4,5',6 - Pentachlorobiphenyl
104	2,2',4,6,6' - Pentachlorobiphenyl
105	2,3,3',4,4' - Pentachlorobiphenyl
106	2,3,3',4,5 - Pentachlorobiphenyl
107	2,3,3',4,5' - Pentachlorobiphenyl
108	2,3,3',4,5' - Pentachlorobiphenyl
109	2,3,3',4,6 - Pentachlorobiphenyl
110	2,3,3',4',6 - Pentachlorobiphenyl
111	2,3,3',5,5' - Pentachlorobiphenyl
112	2,3,3',5,6 - Pentachlorobiphenyl
113	2,3,3',5',6 - Pentachlorobiphenyl

114	2,3,4,4',5 - Pentachlorobiphenyl
115	2,3,4,4',6 - Pentachlorobiphenyl
116	2,3,4,5,6 - Pentachlorobiphenyl
117	2,3,4',5,6 - Pentachlorobiphenyl
118	2,3',4,4',5 - Pentachlorobiphenyl
119	2,3',4,4',6 - Pentachlorobiphenyl
120	2,3',4,5',5 - Pentachlorobiphenyl
121	2,3',4,5',6 - Pentachlorobiphenyl
122	2',3,3',4,5 - Pentachlorobiphenyl
123	2',3,4,4',5 - Pentachlorobiphenyl
124	2',3,4,5,5' - Pentachlorobiphenyl
125	2',3,4,5,6' - Pentachlorobiphenyl
126	3,3',4,4',5 - Pentachlorobiphenyl
127	3,3',4,5,5' - Pentachlorobiphenyl
128	2,2',3,3',4,4' - Hexachlorobiphenyl
129	2,2',3,3',4,5 - Hexachlorobiphenyl
130	2,2',3,3',4,5' - Hexachlorobiphenyl
131	2,2',3,3',4,6 - Hexachlorobiphenyl
132	2,2',3,3',4,6 - Hexachlorobiphenyl
133	2,2',3,3',5,5' - Hexachlorobiphenyl
134	2,2',3,3',5,6 - Hexachlorobiphenyl
135	2,2',3,3',5,6' - Hexachlorobiphenyl
136	2,2',3,3',6,6' - Hexachlorobiphenyl
137	2,2',3,4,4',5 - Hexachlorobiphenyl
138	2,2',3,4,4',5' - Hexachlorobiphenyl
139	2,2',3,4,4',6 - Hexachlorobiphenyl
140	2,2',3,4,4',6 - Hexachlorobiphenyl
141	2,2',3,4,5,5' - Hexachlorobiphenyl
142	2,2',3,4,5,6 - Hexachlorobiphenyl
143	2,2',3,4,5,6' - Hexachlorobiphenyl
144	2,2',3,4,5',6 - Hexachlorobiphenyl
145	2,2',3,4,6,6' - Hexachlorobiphenyl
146	2,2',3,4,5,5' - Hexachlorobiphenyl
147	2,2',3,4',5,6 - Hexachlorobiphenyl
148	2,2',3,4',5,6' - Hexachlorobiphenyl
149	2,2',3,4',5',6 - Hexachlorobiphenyl
150	2,2',3,4',6,6' - Hexachlorobiphenyl
151	2,2',3,5,5',6 - Hexachlorobiphenyl
152	2,2',3,5,6,6' - Hexachlorobiphenyl
153	2,2',4,4’5,5' - Hexachlorobiphenyl
154	2,2',4,4',5,6' - Hexachlorobiphenyl
155	2,2',4,4',6,6' - Hexachlorobiphenyl
156	2,3,3',4,4',5 - Hexachlorobiphenyl
157	2,3,3',4,4',5' - Hexachlorobiphenyl
158	2,3,3',4,4',6 - Hexachlorobiphenyl
159	2,3,3',4,5,5' - Hexachlorobiphenyl
160	2,3,3',4,5,6 - Hexachlorobiphenyl
161	2,3,3',4,5,6 - Hexachlorobiphenyl
162	2,3,3',4',5,5' - Hexachlorobiphenyl
163	2,3,3',4,5',6 - Hexachlorobiphenyl
164	2,3,3',4,5',6 - Hexachlorobiphenyl
165	2,3,3',5,5',6 - Hexachlorobiphenyl
166	2,3,4,4',5,6 - Hexachlorobiphenyl
167	2,3',4,4',5,5' - Hexachlorobiphenyl
168	2,3,4,4',5,6 - Hexachlorobiphenyl
169	3,3',4,4',5,5' - Hexachlorobiphenyl
170	2,2',3,3',4,4',5 - Heptachlorobiphenyl
171	2,2',3,3',4,4',6 - Heptachlorobiphenyl

172	2,2',3,3',4,5,5' - Heptachlorobiphenyl
173	2,2',3,3',4,5,6 - Heptachlorobiphenyl
174	2,2',3,3',4,5,6' - Heptachlorobiphenyl
175	2,2',3,3',4',5,6 - Heptachlorobiphenyl
176	2,2',3,3',4',6,6 - Heptachlorobiphenyl
177	2,2',3,3',4',5,6 - Heptachlorobiphenyl
178	2,2',3,3',5,5',6 - Heptachlorobiphenyl
179	2,2',3,3',5',6,6 - Heptachlorobiphenyl
180	2,2',3,4,4',5,5' - Heptachlorobiphenyl
181	2,2',3,4,4',5,6 - Heptachlorobiphenyl
182	2,2',3,4,4',5,6' - Heptachlorobiphenyl
183	2,2',3,4,4',5',6 - Heptachlorobiphenyl
184	2,2',3,4,4',6,6' - Heptachlorobiphenyl
185	2,2',3,4,5,5',6 - Heptachlorobiphenyl
186	2,2',3,4,5,6,6' - Heptachlorobiphenyl
187	2,2',3,4',5,5',6 - Heptachlorobiphenyl
188	2,2',3,4',5,6,6' - Heptachlorobiphenyl
189	2,3,3',4,4',5,5' - Heptachlorobiphenyl
190	2,3,3',4,4',5,6 - Heptachlorobiphenyl
191	2,3,3',4,4',5,6 - Heptachlorobiphenyl
192	2,3,3',4,5',5,6 - Heptachlorobiphenyl
193	2,3,3',4,5',5,6 - Heptachlorobiphenyl
194	2,2',3,3',4,4',5,5' - Octachlorobiphenyl
195	2,2',3,3',4,4',5,6 - Octachlorobiphenyl
196	2,2',3,3',4,4',5,6 - Octachlorobiphenyl
197	2,2',3,3',4,4',6,6 - Octachlorobiphenyl
198	2,2',3,3',4,5,5',6 - Octachlorobiphenyl
199	2,2',3,3',4,5,6,6' - Octachlorobiphenyl
200	2,2',3,3',4,5',6,6' - Octachlorobiphenyl
201	2,2',3,3',4',5,5',6 - Octachlorobiphenyl
202	2,2',3,3',5,5',6,6' - Octachlorobiphenyl
203	2,2',3,4',4,5',5,6' - Octachlorobiphenyl
204	2,2',3,4,4',5,6,6' - Octachlorobiphenyl
205	2,3,3',4,4',5,5'6 - Nonachlorobiphenyl
206	2,2',3,3',4,4',5,5'6 - Nonachlorobiphenyl
207	2,2',3,3',4,4',5,6,6' - Nonachlorobiphenyl
208	2,2',3,3',4,5,5',6,6' - Nonachlorobiphenyl
209	2,2',3,3',4,4',5,5',6,6' - Decachlorobiphenyl

Table A1.4: List of the World Health Organisation PCBs (WHO 12) with corresponding TEF value

IUPAC number	Name	TEF
77	3,3',4,4'-tetrachloro-PCB	0.0001
81	3,4,4',5-tetrachloro-PCB	0.0001
105	2,3,3',4,4'-pentachloro-PCB	0.0001
114	2,3,4,4',5-pentachloro-PCB	0.0005
118	2,3',4,4',5-pentachloro-PCB	0.0001
123	2',3,4,4',5-pentachloro-PCB	0.0001
126	3,3',4,4',5-pentachloro-PCB	0.1
156	2,3,3',4,4',5-hexachloro-PCB	0.0005
157	2,3,3',4,4',5-hexachloro-PCB	0.0005
167	2,3',4,4',5,5'-hexachloro-PCB	0.00001
169	3,3',4,4',5,5'-hexachloro-PCB	0.01
189	2,3,3',4,4',5,5'-heptachloro-PCB	0.0001

Table A1.5: Categories of the sixteen US EPA priority PAHs

PAH compound	COC TEF	IARC group	EPAQS weighting	Borneff six	POPS four	BaP equivalent
Naphthalene	None					1.97
Acenaphthylene	None					1.66
Acenaphthene	None					1.64
Fluorene	None	3				1.52
Phenanthrene	0.001	3				1.42
Anthracene	0.001	3				1.42
Fluoranthene	0.001	3		✓		1.25
Pyrene	0.001	3				1.25
Benz(a)anthracene	0.1	2A	0.10			1.11
Chrysene	0.1	2B/3	0.03			1.11
Benzo(b)fluoranthene	0.1	2B	0.11	✓	✓	1.00
Benzo(k)fluoranthene	0.1	2B	0.03	✓	✓	1.00
Benzo(a)pyrene	1.0	2A	1.00	✓	✓	1.00
Benzo(g,h,i)perylene	0.1	3		✓		0.91
Indeno(1,2,3 - c,d)pyrene	0.1	2B	0.08	✓	✓	0.91
Dibenzo(a,h)anthracene	1.0	2A	1.91			0.91

Table A1.6: List of the sixteen US EPA priority PAHs with physical property data

PAH compound	Formula	Molecular weight	Boiling point (°C)
Naphthalene	$C_{10}H_8$	128.19	218
Acenaphthylene	$C_{12}H_8$	152.21	270
Acenaphthene	$C_{12}H_{10}$	154.21	279
Fluorene	$C_{13}H_{10}$	166.23	294
Phenanthrene	$C_{14}H_{10}$	178.24	340
Anthracene	$C_{14}H_{10}$	178.24	340
Fluoranthene	$C_{16}H_{10}$	202.26	375
Pyrene	$C_{16}H_{10}$	202.26	393
Benz(a)anthracene	$C_{18}H_{12}$	228.30	-
Chrysene	$C_{18}H_{12}$	228.30	448
Benzo(b)fluoranthene	$C_{20}H_{12}$	252.32	480
Benzo(k)fluoranthene	$C_{20}H_{12}$	252.32	480
Benzo(a)pyrene	$C_{20}H_{12}$	252.32	-
Benzo(g,h,i)perylene	$C_{22}H_{12}$	276.36	-
Indeno(1,2,3 - c,d)pyrene	$C_{22}H_{12}$	276.36	-
Dibenzo(a,h)anthracene	$C_{22}H_{14}$	278.36	-

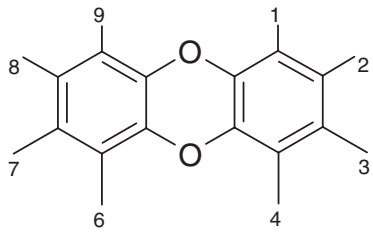

dibenzo-p-dioxin

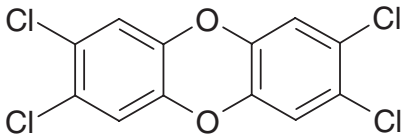

2,3,7,8-tetrachlorodibenzo-p-dioxin

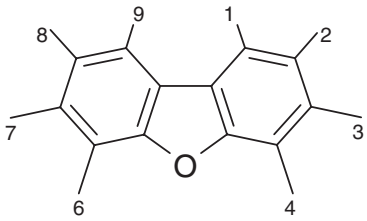

dibenzofuran

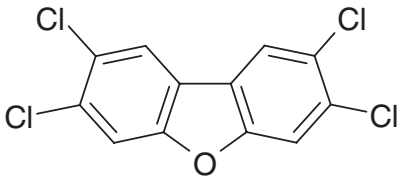

2,3,7,8-tetrachlorodibenzofuran

Fig. A1.1: Structure of selected dioxin compounds

Polychlorinated Dibenzofurans

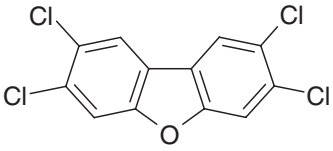

2,3,7,8 - TCDF

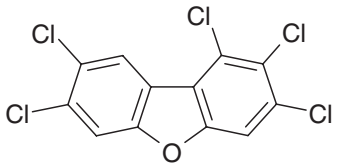

1,2,3,7,8 - PeCDF

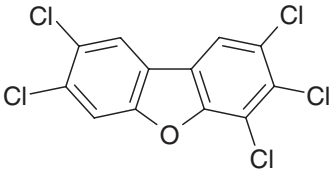

2,3,4,7,8 - PeCDF

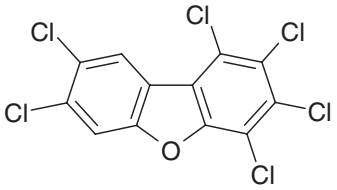

1,2,3,4,7,8 - HxCDF

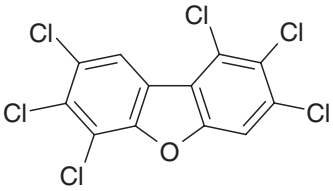

1,2,3,6,7,8 - HxCDF

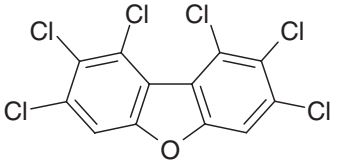

1,2,3,7,8,9 - HxCDF

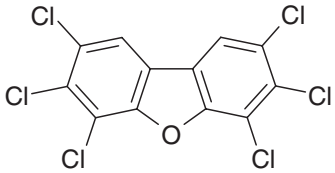

2,3,4,6,7,8 - HxCDF

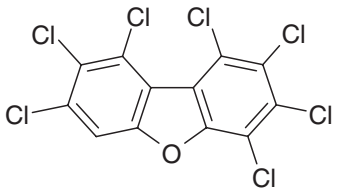

1,2,3,4,7,8,9 - HpCDF

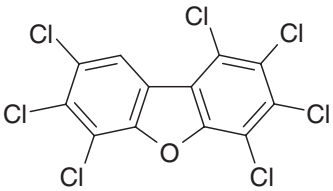

1,2,3,4,6,7,8 - HpCDF

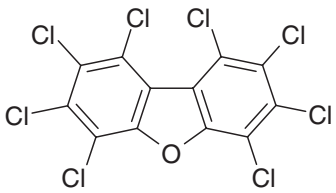

OCDF

Fig. A1.2: Structure of polychlorinated dibenzofuran (PCDF) compounds with chlorine atoms substituted in the 2,3,7,8-positions and assigned TEF values

Polychlorinated Dibenzo-p-dioxins

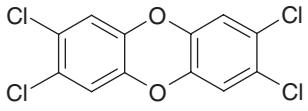

2,3,7,8 - TCDD

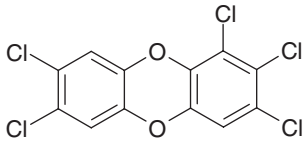

1,2,3,7,8 - PeCDD

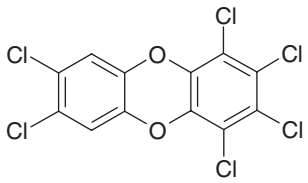

1,2,3,4,7,8 - HxCDD

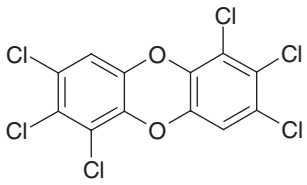

1,2,3,6,7,8 - HxCDD

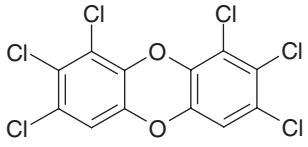

1,2,3,7,8,9 - HxCDD

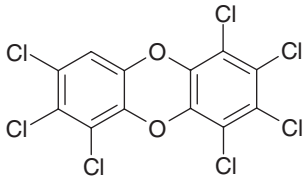

1,2,3,4,6,7,8 - HpCDD

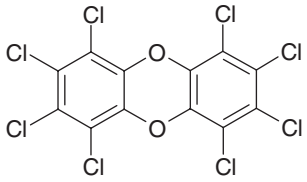

OCDD

Fig. A1.3: Structure of polychlorinated dibenzo-p-dioxin (PCDD) compounds with chlorine atoms substituted in the 2,3,7,8-positions and assigned TEF values

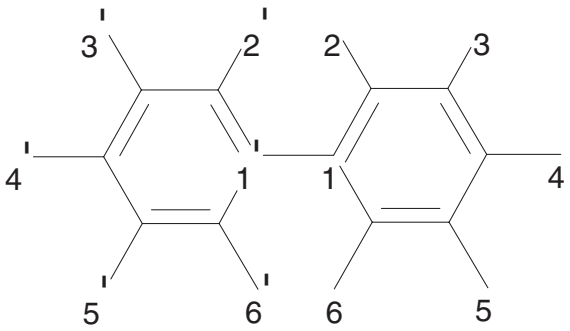

Fig. A1.4: Structure of polychlorinated biphenyl (PCB) parent compound showing the numbering convention

WHO list of PCBs with TEF values

non-ortho co-planar

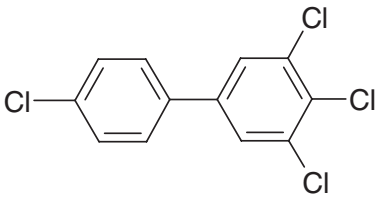

#81 3,4,4',5'-TeCB *TEF 0.0001*

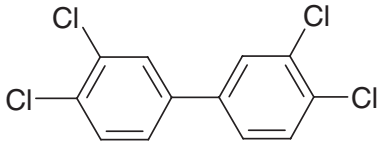

#77 3,3',4,4'-TeCB *TEF 0.0001*

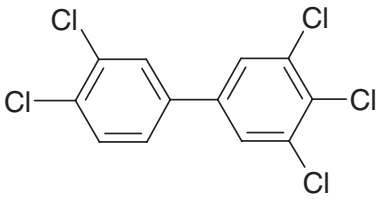

#126 3,3',4,4',5-PeCB ***TEF 0.1***

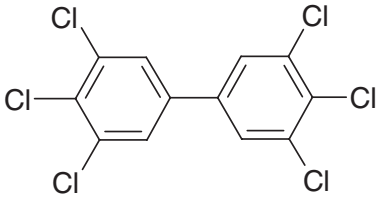

#169 3,3',4,4',5,5'-HxCB *TEF 0.01*

Fig. A1.5: Structure of the non-ortho sub-set of the WHO-12 (World Health Organisation) polychlorinated biphenyls (12 PCBs in total) TEF is the toxic equivalent factor

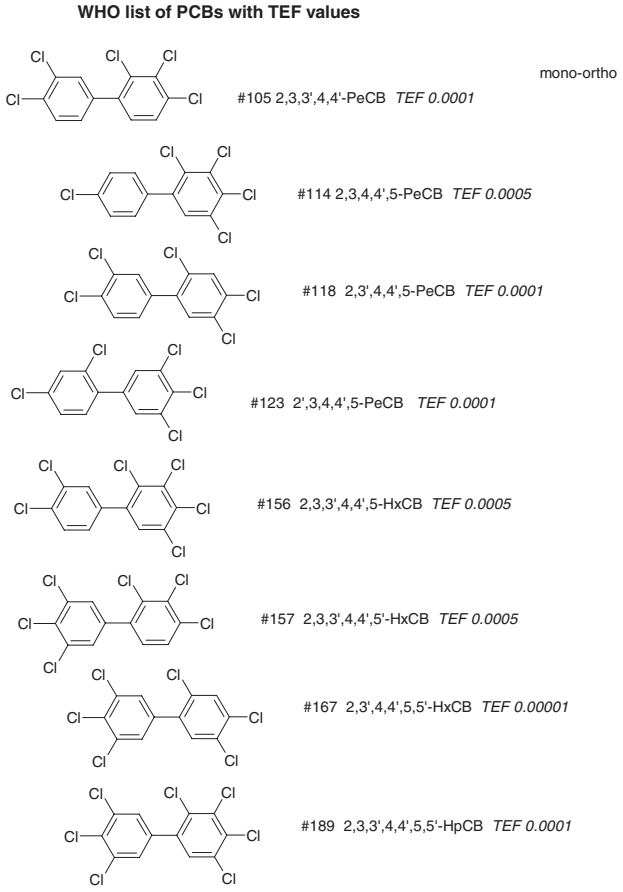

Fig. A1.6: Structure of the mono-ortho sub-set of the WHO-12 (World Health Organisation) polychlorinated biphenyls (12 PCBs in total) TEF is the toxic equivalent factor

Polychlorinated Biphenyls (PCBs) - Targeted EC7 Compounds

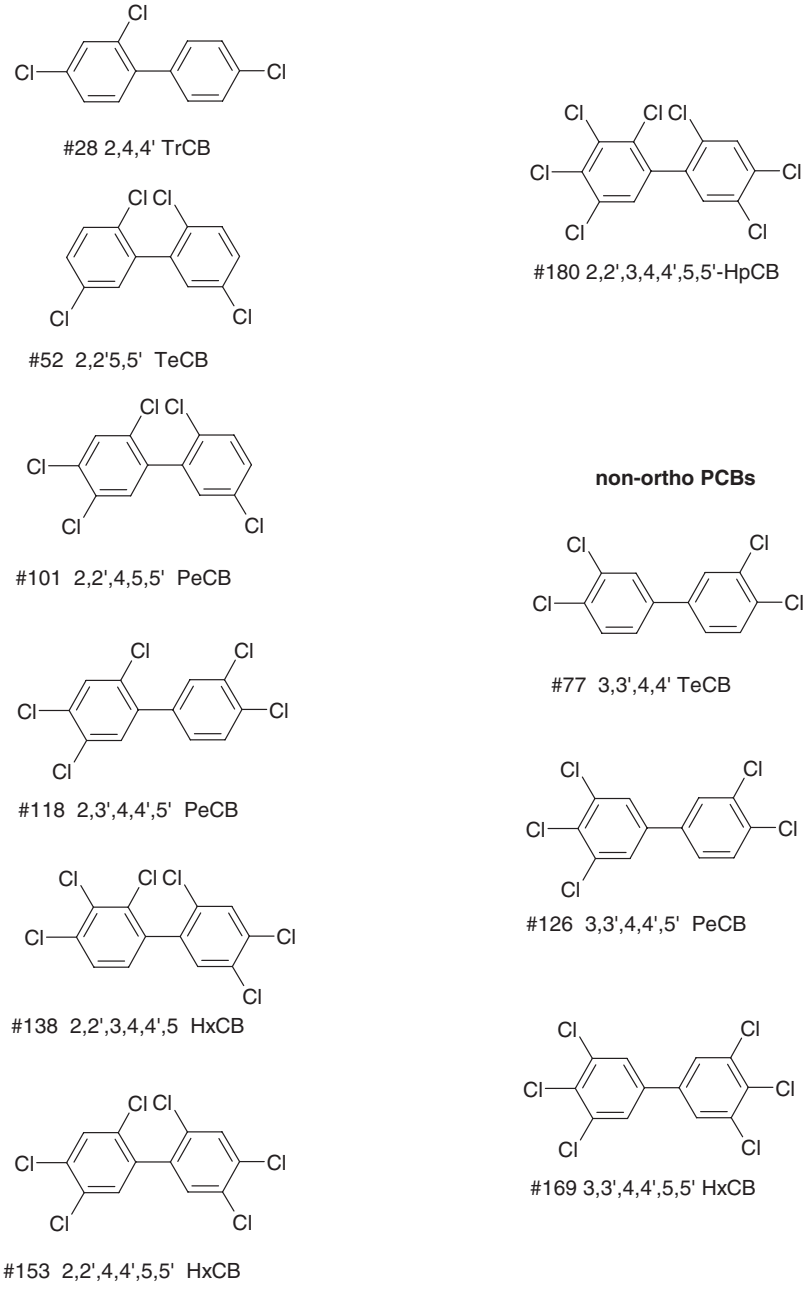

Fig. A1.7: Structure of the EC7 set of polychlorinated biphenyls and the original sub-set of dioxin-like non-ortho PCBs prior to the assignment of the WHO-12

Structure of PAH compounds - EPA16

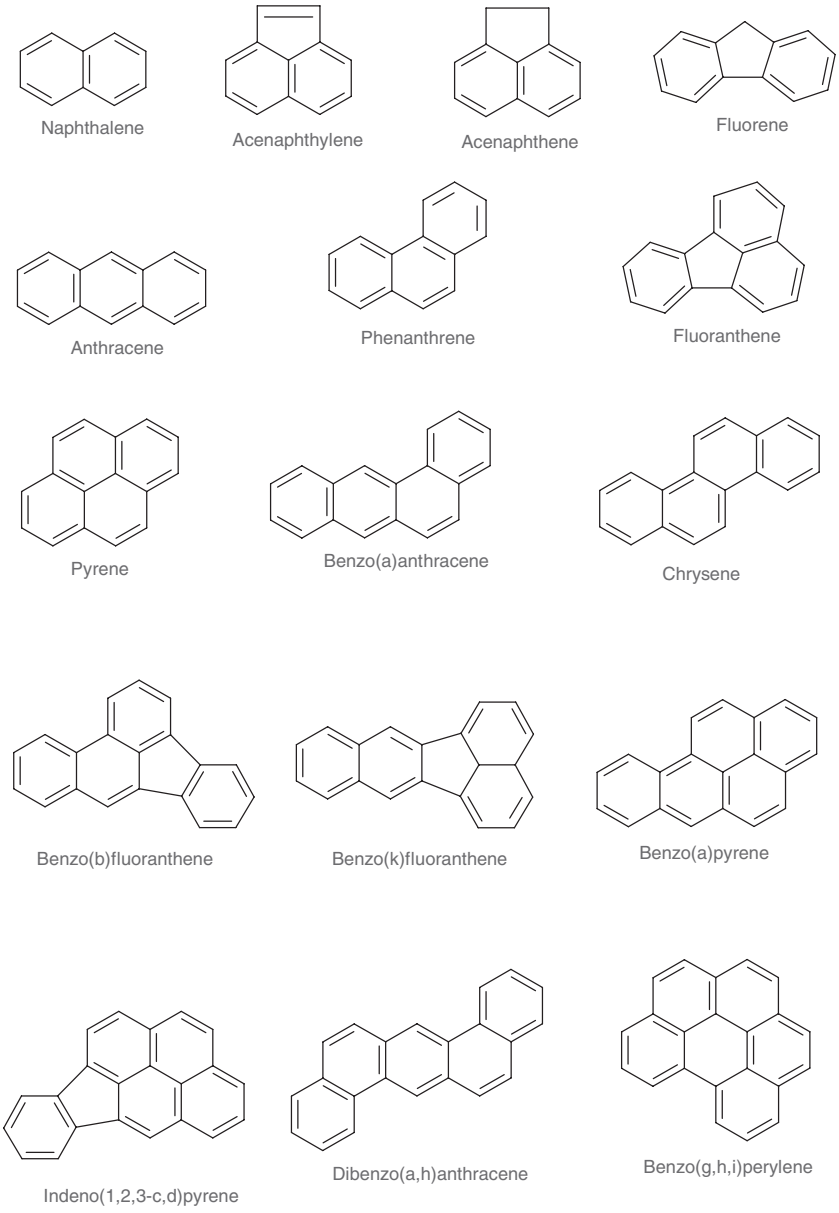

Fig. A1.8: Structure of the sixteen US EPA priority set of polycyclic aromatic hydrocarbons (PAHs) (EPA16)

Appendix 2

HEART: Design and photographic documentation

The following figures and photographs illustrate the design and combustion of the HEART experiment system.

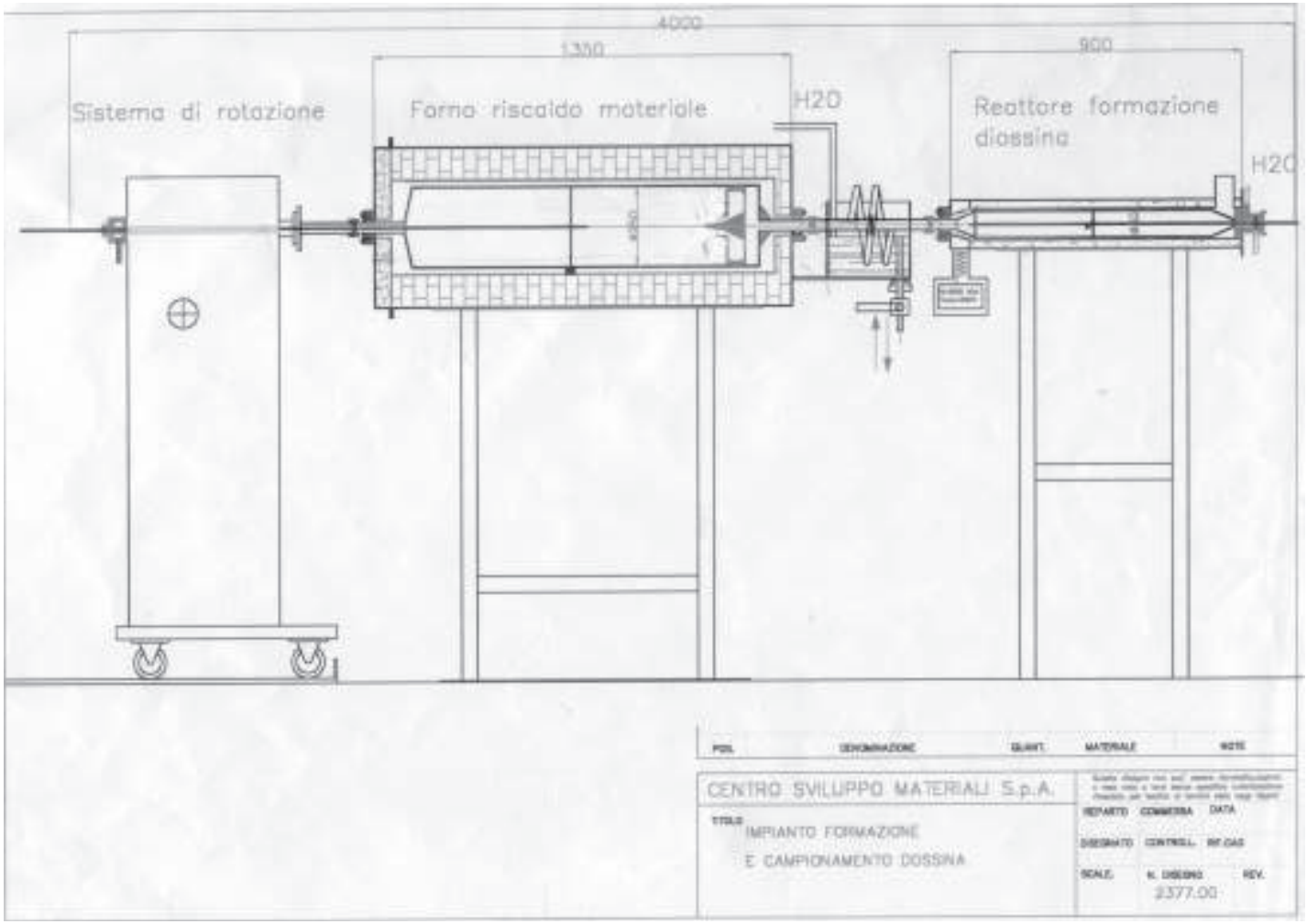

Fig. A2 1:.HEART (Heater apparatus relating toxic-compounds) design

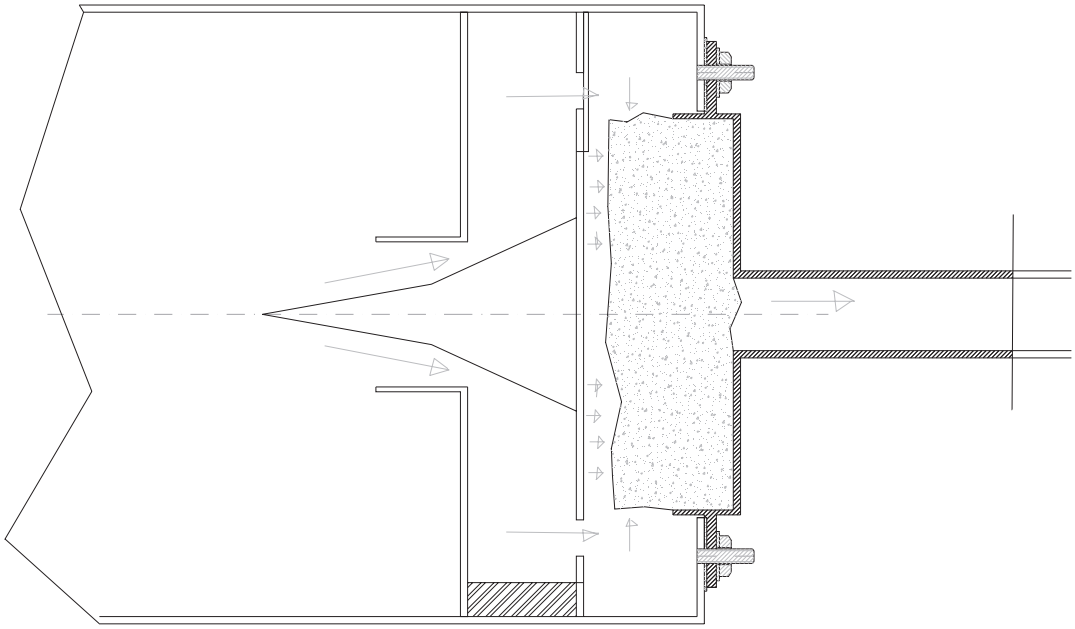

Fig. A2.2: HEART design details: powder filter

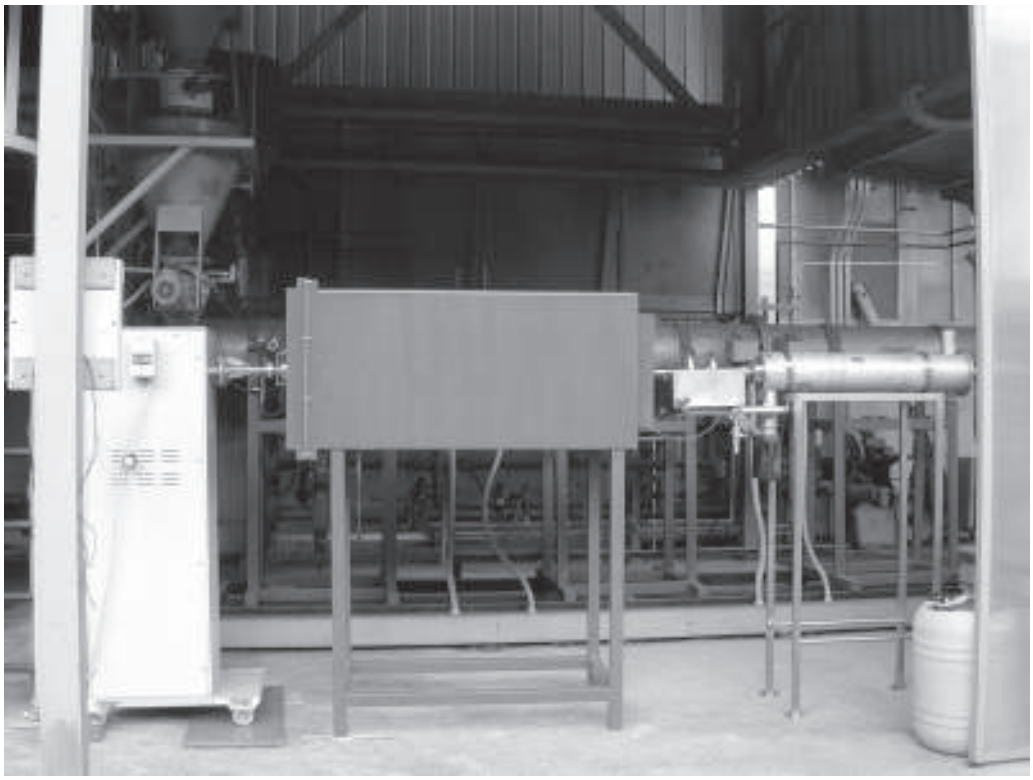

Fig. A2.3: HEART: Heater apparatus relating toxic-compounds

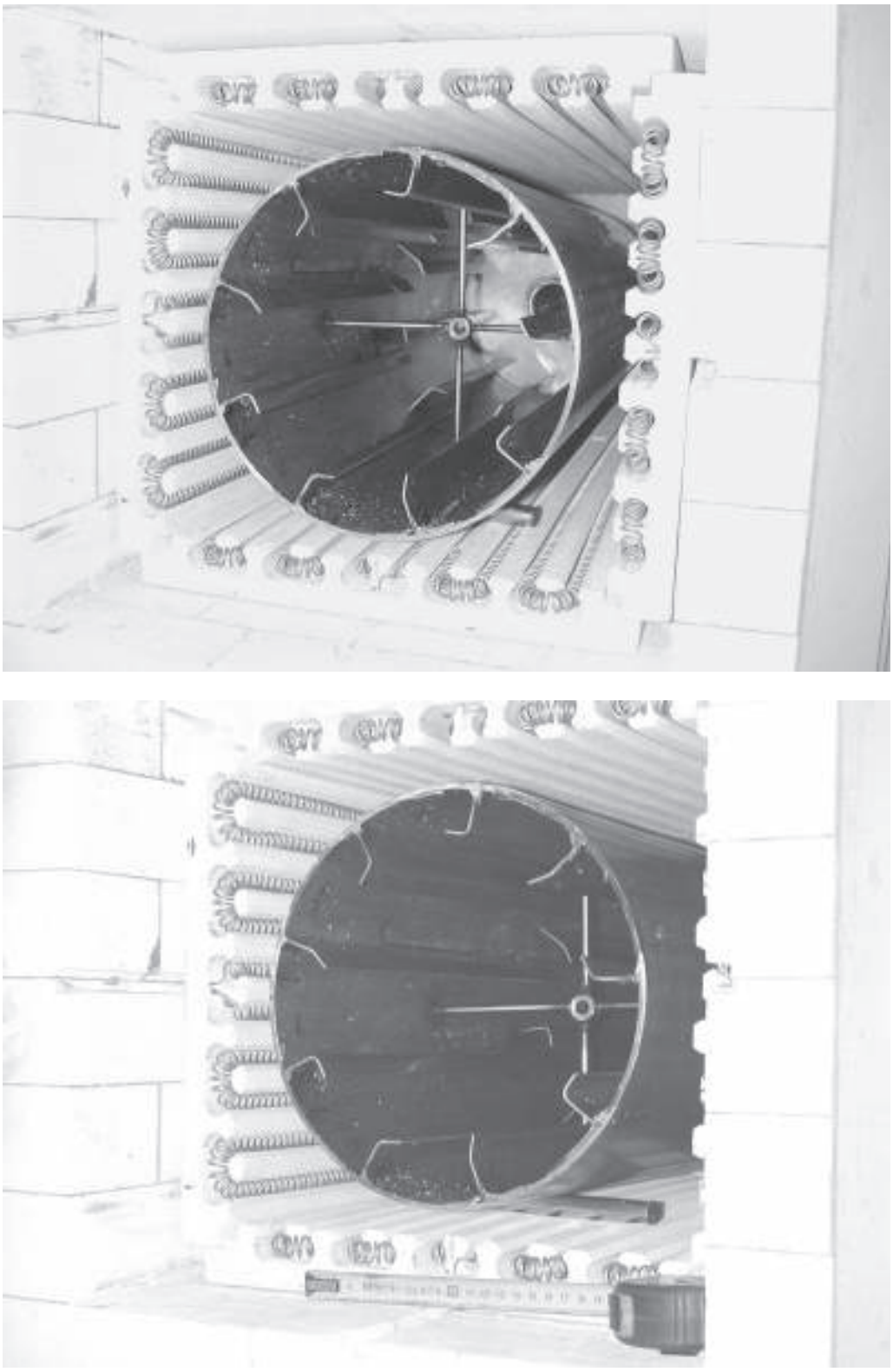

Fig. A2.4: HEART details: Rotary kiln: Internal of first HEART reactor

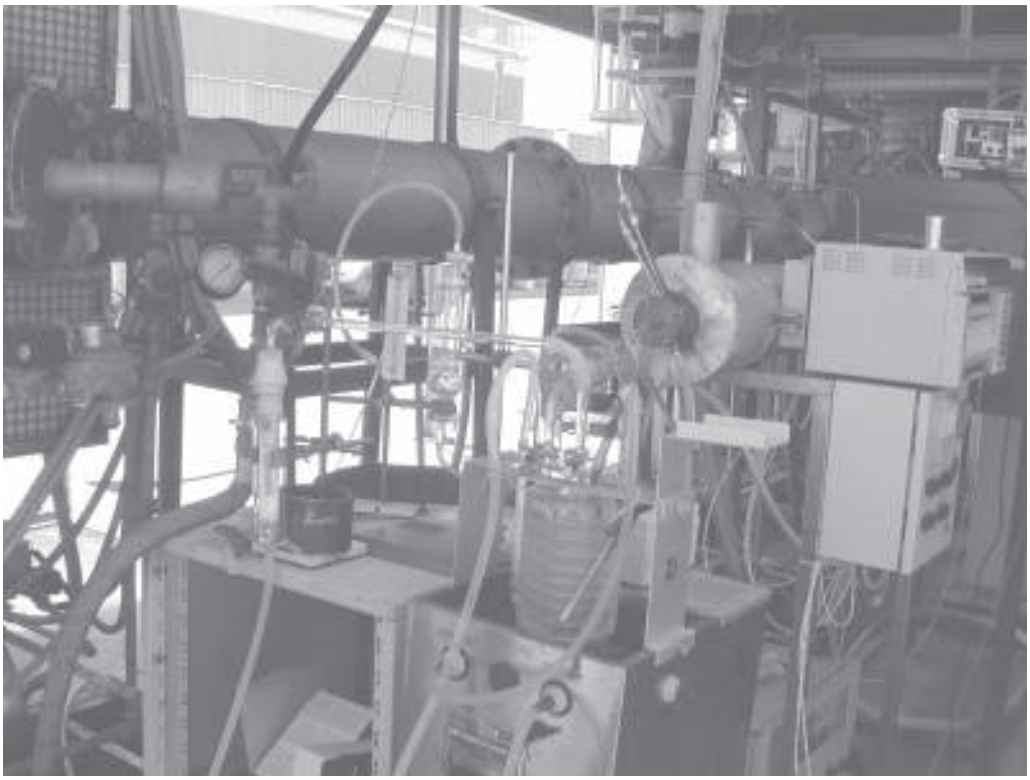

Fig. A2.5: HEART system for sampling fume for PCDD/F analysis

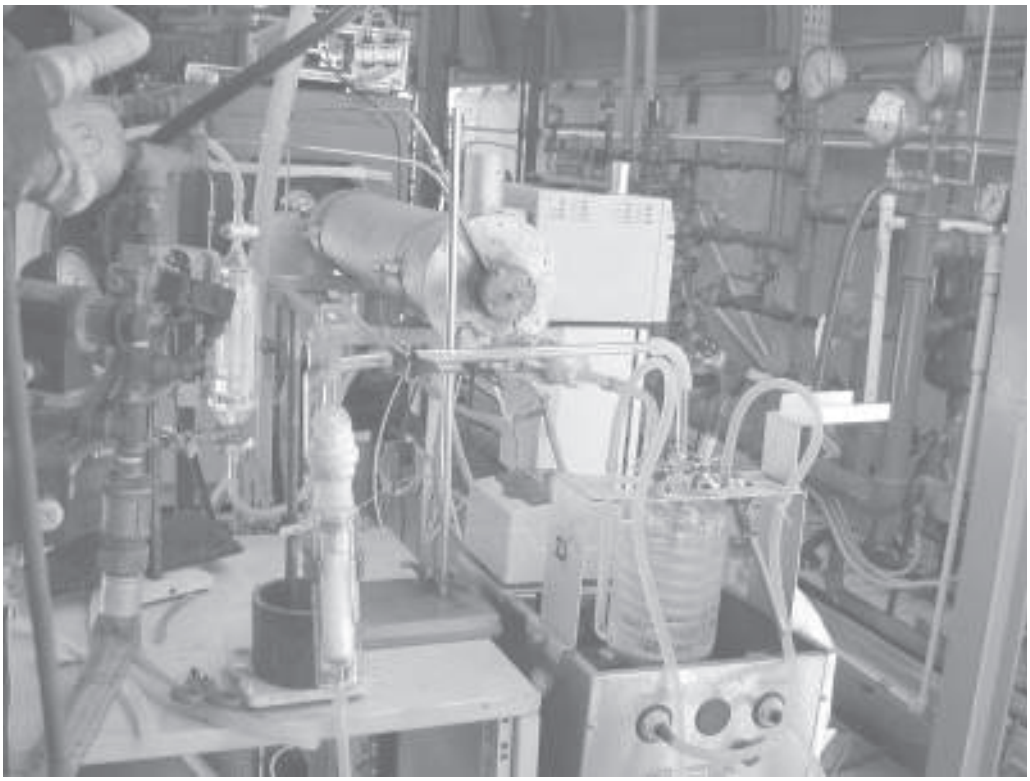

Fig. A2.6: Details of the system to sample fumes produced by HEART for PCDD/F analysis

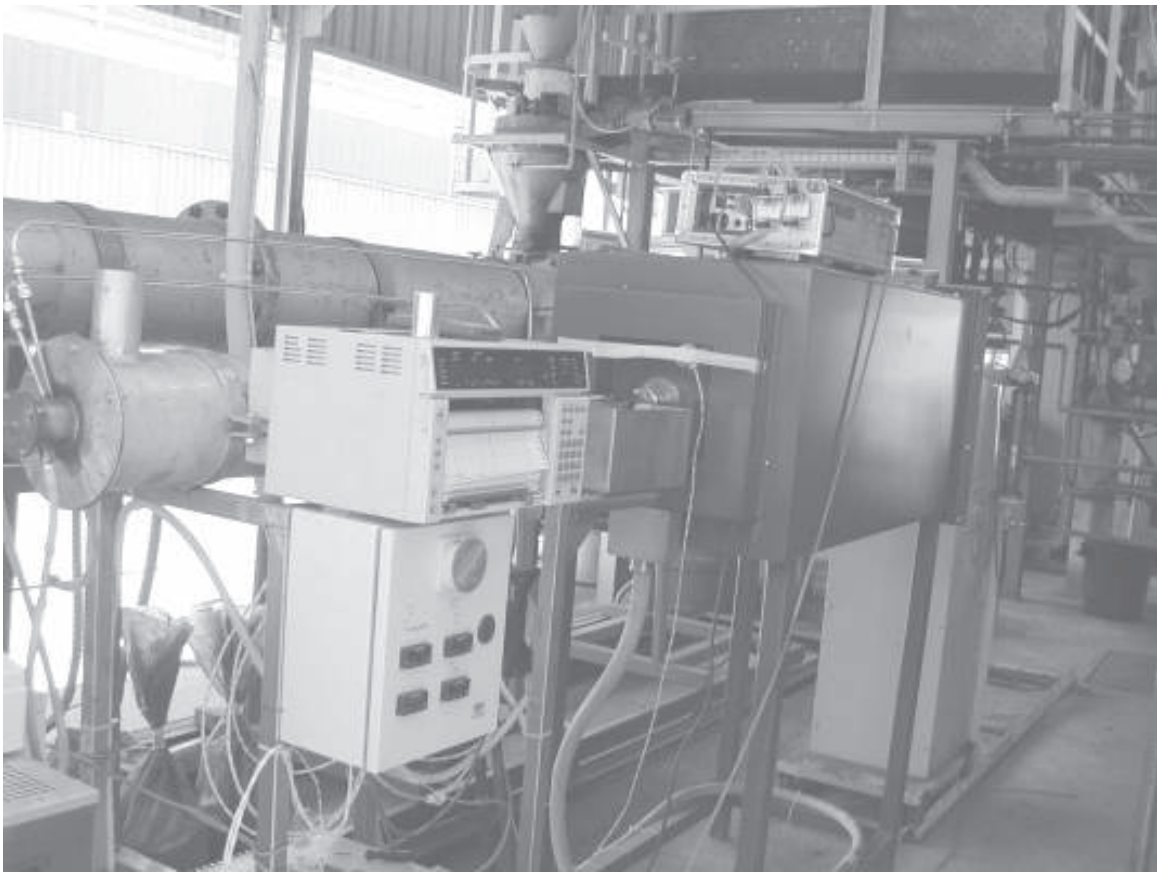

Fig. A2.7: HEART details: System for controlling and to recording temperatures and instrumenting for gas analysis

Appendix 3

Kinetic model

In order to define the kinetic model, the following mechanism has been defined, according to literature:

$$n\ (\tfrac{1}{2}\ O_2 + C_S) \quad \rightarrow P_P \quad \rightarrow \quad D \qquad \ldots \text{(A3.1)}$$

precursors dioxins

where C_S is the concentration of active sites involved in the precursor formation.

This mechanism (1) is described by the general scheme of the 'serial reactions':

$$A \quad \rightarrow \quad B \quad \rightarrow \quad C \qquad \ldots \text{(A3.2)}$$

Assuming that every precursor undergoes a configuration change and PCDD/F molecules are generated, the scheme (2) is described by the following differential equations system:

$$\begin{aligned} -\frac{dC_A}{d\tau} &= k_1 C_A \\ \frac{dC_B}{d\tau} &= k_1 C_A - k_2 C_B \\ \frac{dC_C}{d\tau} &= k_2 C_B \end{aligned} \qquad \ldots \text{(A3.3)}$$

The oxygen variation, caused by precursor formation, is:

$$\left(\frac{dC_{O_2}}{d\tau}\right) = -k_1\, C_{O_2}^{0.5}\, C_S \qquad \ldots \text{(A3.4)}$$

where CO_2, τ and k_1 are respectively oxygen concentration, time and the reaction constant. The active site concentration (C_s) could be determined as follows:

C_s is proportional to the carbon concentration at time t:

$$C_s = n_s\, C_t \qquad \ldots \text{(A3.5)}$$

where n_s is the number of active sites.

If C_o is the carbon concentration at time 0, the residual quantity (C_t) at τ time is:

$$C_t = C_o - k_{sp}\tau \qquad \ldots \text{(A3.6)}$$

where k_{sp} is related to the oxygen concentration.

As a consequence, the oxygen variation is:

$$\left(\frac{dC_{O_2}}{d\tau}\right) = -k_a C_{O_2}^{0.5}\left(C_o - k_{ps}\tau\right) \quad \ldots \text{(A3.7)}$$

where $k_{a=}$ (k_1*n_s), i.e. the product between the kinetic constant and active sites number.

The precursor concentrations vary with time as follow:

$$\left(\frac{dC_p}{d\tau}\right) = k_a C_{O_2}^{0.5}\left(C_O - k_{ps}\tau\right) - k_2 C_p \quad \ldots \text{(A3.8)}$$

in the case where one precursor molecule forms one PCDD/F molecule.

The PCDD/F production is described by:

$$\frac{dC_D}{d\tau} = k_2 C_P \quad \ldots \text{(A3.9)}$$

In the case where two precursor molecules form one PCDD/F molecule, the kinetic equations are:

$$\left(\frac{dC_p}{d\tau}\right) = k_a C_{O_2}^{0.5}\left(C_0 - k_{ps}\tau\right) - k_2 C_p^{\,2} \quad \ldots \text{(A3.10)}$$

and

$$\frac{dC_D}{d\tau} = k_2 C_P^2 \quad \ldots \text{(A3.11)}$$

The relative integration could be effected by numerical method (Runge Kutta and trapezium methods), when experimental values of dioxins with time are obtained.

The curve that fits the points describes the evolution development with time of the reaction.

The slope gives an indication on the kinetic constant.

Appendix 4

Identification or organic compounds present in EAF materials

A4.1 Introduction

In this section are reported in detail the analyses carried out on EAF materials. In particular the identification of long chain fatty acids (LCFA) presents on scrap inlet to PE EAF and of IPA present in the powder picked up after pre-heater are reported.

A4.2 Determination of organic compounds present on the scrap

The scrap was treated with alkaline water (pH ~14) and then the organic compounds of the solution were extracted with CH_2Cl_2.

An initial qualitative gas chromatography analysis was carried out, results of which are shown in Table A4.1 and Fig. A4.1

The presence of the long chain fatty acids (LCFA) present in lubricant used in the rolling mill processes is evident.

Table A4.1: Gas-chromatographic analysis of the scrap extracted

Saturated LCFA	Insatured LCFA
C6-C14 Acid	Oleic Acid
Palmitic Acid	Linoleic Acid
Miristic Acid	
Stearic Acid	

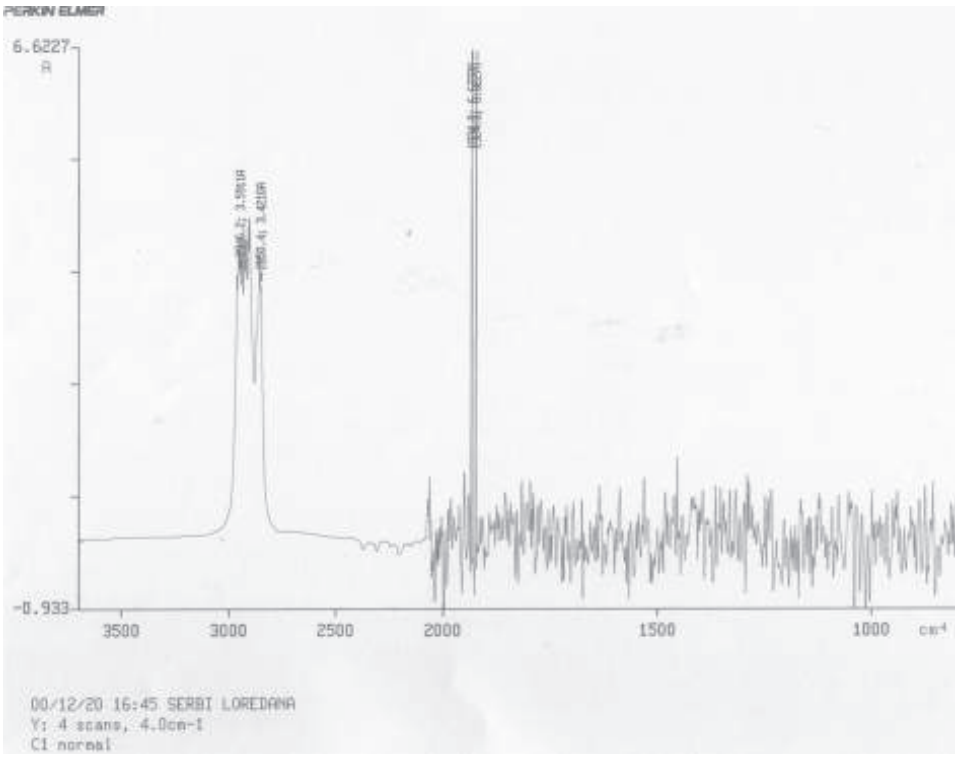

Fig. A4.1: Gas-chromatographic spectrum of the scrap extract

Then a GC-MS analysis of the organic extract was carried out, the result of which are shown in Table A4.2.

Table A4.2: Gas-chromatographic results of the scrap extracted

Ottanoic Acid (C8)	3.5 ppm
Nonanoic Acid (C9)	7.3 ppm
Decanoic Acid (C10)	4.5 ppm
Undecanoic Acid (C11)	2.4 ppm
Tridecanoic Acid (C13)	3.6 ppm
Tetradecanoic Acid (C14)	41.8 ppm
Palmitic Acid (C16)	192.5 ppm
Stearic Acid (C18)	5.9 ppm
Oleic Acid (18:1;9)	482.7 ppm
Linoleic Acid (18:9,12)	141.0 ppm
Anionic surfactants (MBAS*)	3.1 ppm

*MBAS: Mmethylene blue active substance

Detection of IPA PCB/PCT present in the powder picked up after pre-heater, and in the residue is derived from the partial combustion of the long chain fatty acids (LCFA) present on the scrap.

Samples of powder collected after the pre-heater, and of the residue derived from the partial combustion of the long chain fatty acids (LCFA) were extracted with diethyl ether, dried and redissolved in isoctane. These solutions were injected into a GC-MS equipped with a specific column for IPA and for PCB/PCT. Owing to the small amounts of PCB/PCT detected in both the samples, in the results (Tables A4.3 and A4.4) the are reported total concentrations.

Table A4.3: GC-MS results of the fly ashes extracted

Compound	ng/g
Benzo(a)anthracene	467.14
Dibenzo(a,h)anthracene	344.64
Σ IPA	811.64

Table A4.4: GC-MS results of the EAF dust extracted

Compound	ng/g
Benzo(a)anthracene	285.14*
Benzo(b+j)fluoranthene	159.52*
Benzo(k)fluoranthene	155.3*
Benzo(a)pyrene	17.02
Indeno(123,cd)pyrene	22.96
Dibenzo(a,h)anthracene	103.64*
Dibenzo(a,l)pyrene	13.96
Dibenzo(a,e)pyrene	4.46
Dibenzo(a,i)pyrene	3.16
Dibenzo(a,h)pyrene	1.76
Σ IPA	786.92

* Compounds chosen for Synthetic dust preparation

Table A4.5: Composition of organic matter of the synthetic dust type 2

Compound	ng/g
Oleic Acid (18:1;9)	500
Benzo(a)anthracene	500
Dibenzo(a,h)anthracene	350
Benzo(k)fluoranthene	200
Dibenzo(a,h)anthracene	150
Total	1700

Appendix 5

Example of calculation of the kinetics of 'De Novo Synthesis'

The following exemplifies the kinetic model calculations using an Excel spreadsheet.

carica g	**5000**		
% C in carica	**10**		
portata gas Nm^3/ora	**2**		
frazione % oss.ingresso	**0,03**	**g/Nm^3 =**	**42,83037387**

$K_{sperimentale}$	**2,141**

K_1=	7,9092E-07

	calcolo della concentrazione dell'ossigeno					
τ (ore)	kuno	kdue	ktre	kquattro	C_O (g/Nm3)	C_O (fraz.%)
0					42,83037387	0,0300000000
0,01	-1,03523E-08	-1,03537E-08	-1,03537E-08	-1,03537E-08	42,83037386	0,0300000000
0,02	-1,03523E-08	-1,03536E-08	-1,03536E-08	-1,03536E-08	42,83037385	0,0300000000
0,03	-1,03523E-08	-1,03536E-08	-1,03536E-08	-1,03536E-08	42,83037384	0,0300000000
0,04	-1,03523E-08	-1,03536E-08	-1,03536E-08	-1,03536E-08	42,83037383	0,0300000000
0,05	-1,03523E-08	-1,03536E-08	-1,03536E-08	-1,03536E-08	42,83037382	0,0300000000
0,06	-1,03523E-08	-1,03536E-08	-1,03536E-08	-1,03536E-08	42,83037381	0,0300000000
0,07	-1,03523E-08	-1,03536E-08	-1,03536E-08	-1,03536E-08	42,8303738	0,0299999999
0,08	-1,03523E-08	-1,03536E-08	-1,03536E-08	-1,03536E-08	42,83037379	0,0299999999
0,09	-1,03523E-08	-1,03536E-08	-1,03536E-08	-1,03535E-08	42,83037378	0,0299999999
0,1	-1,03523E-08	-1,03535E-08	-1,03535E-08	-1,03535E-08	42,83037377	0,0299999999
0,11	-1,03523E-08	-1,03535E-08	-1,03535E-08	-1,03535E-08	42,83037376	0,0299999999
0,12	-1,03523E-08	-1,03535E-08	-1,03535E-08	-1,03535E-08	42,83037375	0,0299999999
0,13	-1,03523E-08	-1,03535E-08	-1,03535E-08	-1,03535E-08	42,83037374	0,0299999999
0,14	-1,03523E-08	-1,03535E-08	-1,03535E-08	-1,03535E-08	42,83037373	0,0299999999
0,15	-1,03523E-08	-1,03535E-08	-1,03535E-08	-1,03535E-08	42,83037372	0,0299999999
0,16	-1,03523E-08	-1,03535E-08	-1,03535E-08	-1,03535E-08	42,83037371	0,0299999999
0,17	-1,03523E-08	-1,03534E-08	-1,03534E-08	-1,03534E-08	42,8303737	0,0299999999
0,18	-1,03523E-08	-1,03534E-08	-1,03534E-08	-1,03534E-08	42,83037369	0,0299999999
0,19	-1,03523E-08	-1,03534E-08	-1,03534E-08	-1,03534E-08	42,83037368	0,0299999999
0,2	-1,03523E-08	-1,03534E-08	-1,03534E-08	-1,03534E-08	42,83037367	0,0299999999
0,21	-1,03523E-08	-1,03534E-08	-1,03534E-08	-1,03534E-08	42,83037366	0,0299999998
0,22	-1,03523E-08	-1,03534E-08	-1,03534E-08	-1,03534E-08	42,83037365	0,0299999998
0,23	-1,03523E-08	-1,03534E-08	-1,03534E-08	-1,03534E-08	42,83037364	0,0299999998
0,24	-1,03523E-08	-1,03534E-08	-1,03534E-08	-1,03533E-08	42,83037362	0,0299999998
0,25	-1,03523E-08	-1,03533E-08	-1,03533E-08	-1,03533E-08	42,83037361	0,0299999998
0,26	-1,03523E-08	-1,03533E-08	-1,03533E-08	-1,03533E-08	42,8303736	0,0299999998
0,27	-1,03523E-08	-1,03533E-08	-1,03533E-08	-1,03533E-08	42,83037359	0,0299999998
0,28	-1,03523E-08	-1,03533E-08	-1,03533E-08	-1,03533E-08	42,83037358	0,0299999998
0,29	-1,03523E-08	-1,03533E-08	-1,03533E-08	-1,03533E-08	42,83037357	0,0299999998
0,3	-1,03523E-08	-1,03533E-08	-1,03533E-08	-1,03533E-08	42,83037356	0,0299999998

sub 9 e 8

	nuova	vecchia
modello a tre costanti e con precursori al quadrato — somma degli scarti al quadrato =	1,302142E-16	3,25331E-18

costante stechiometrica x = 1 k' = 7,9092E-07

K_2 = 0,868251

K_1	7,90920E-07
K_2	0,868251

calcolo della concentrazione dei precursori					diossine
k1	k2	k3	k4	C_P	D modello (g/Nm^3)
				0	0
1,03523E-08	1,03074E-08	1,03076E-08	1,02628E-08	1,03E-10	4,475E-13
1,02628E-08	1,02183E-08	1,02185E-08	1,01741E-08	2,05E-10	1,786E-12
1,01741E-08	1,013E-08	1,01301E-08	1,00862E-08	3,07E-10	4,008E-12
1,00862E-08	1,00424E-08	1,00426E-08	9,99897E-09	4,07E-10	7,106E-12
9,99897E-09	9,95557E-09	9,95575E-09	9,91253E-09	5,07E-10	1,107E-11
9,91253E-09	9,8695E-09	9,86969E-09	9,82684E-09	6,05E-10	1,590E-11
9,82684E-09	9,78418E-09	9,78436E-09	9,74189E-09	7,03E-10	2,158E-11
9,74189E-09	9,6996E-09	9,69978E-09	9,65767E-09	8,00E-10	2,810E-11
9,65767E-09	9,61574E-09	9,61593E-09	9,57418E-09	8,96E-10	3,547E-11
9,57418E-09	9,53262E-09	9,5328E-09	9,49141E-09	9,92E-10	4,366E-11
9,49141E-09	9,45021E-09	9,45039E-09	9,40936E-09	1,09E-09	5,268E-11

Dati sperimentali

D (g/Nm3)	Tempo (ore)
0,0E+00	0
0,0E+00	0,5
2,0E-08	3
3,0E-08	4
4,0E-08	5

Statistica

1,80E-08	= media yi
1,28E-15	=yi-media
1,30E-16	=ystimato-yi
0,947771	= r
26,49	= F

ΔO_2	integrale di C_p con r. dei trapezi
0,00E+00	
7,25E-12	5,154E-13
1,45E-11	2,057E-12
2,18E-11	4,61615E-12
2,90E-11	8,18388E-12
3,63E-11	1,27515E-11
4,35E-11	1,83104E-11
5,08E-11	2,4852E-11
5,80E-11	3,23678E-11
6,53E-11	4,08494E-11
7,25E-11	5,02884E-11
7,98E-11	6,06766E-11
8,70E-11	7,20057E-11
9,43E-11	8,42676E-11
1,02E-10	9,74543E-11
1,09E-10	1,11558E-10
1,16E-10	1,2657E-10
1,23E-10	1,42483E-10

	integrale Cp		
tempo	+ teorico	+ sperimentale	ΔO_2
1	7,38709E-09	7,38709E-09	7,25E-10
2	2,34142E-08	2,34142E-08	1,45E-09
3	4,30673E-08	2,30673E-08	2,18E-09
4	6,42423E-08	3,42423E-08	2,90E-09
5	8,6056E-08	4,60560E-08	3,63E-09

Rapporto +sperimentale e $\Delta O2$	
1,01869E+01	
16,14511414	
10,60453763	
11,80706071	
12,7050921	
media	varianza
1,22897E+01	5,632803023

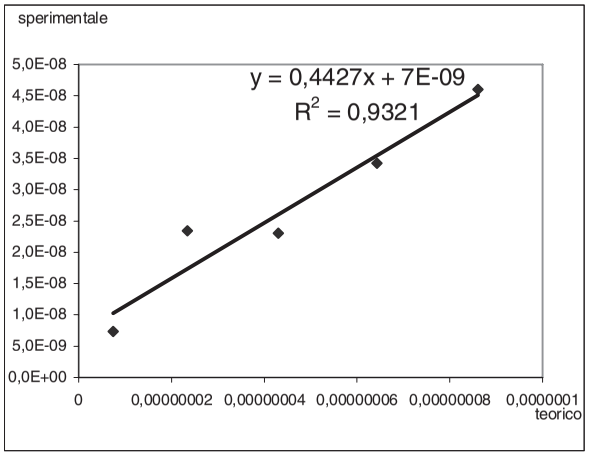

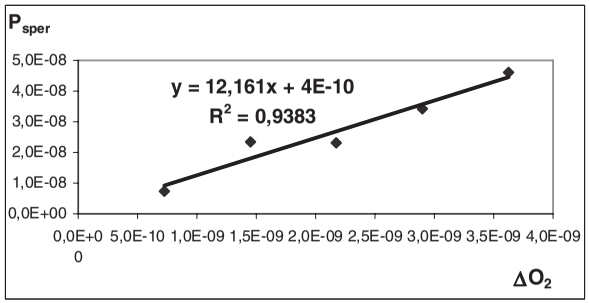

valore istantaneo

τ (ore)	C_O (g/Nm3)	C_P	C_D
0	42,83037	0	0
0,01	42,83037	1,03075E-10	4,47E-11
0,02	42,83037	2,05259E-10	1,34E-10
0,03	42,83037	3,0656E-10	2,22E-10
0,04	42,83037	4,06985E-10	3,10E-10
0,05	42,83037	5,06542E-10	3,97E-10
0,06	42,83037	6,05238E-10	4,83E-10
0,07	42,83037	7,03082E-10	5,68E-10
0,08	42,83037	8,00079E-10	6,53E-10
0,09	42,83037	8,96237E-10	7,36E-10
0,1	42,83037	9,91565E-10	8,20E-10
0,11	42,83037	1,08607E-09	9,02E-10
0,12	42,83037	1,17975E-09	9,84E-10
0,13	42,83037	1,27263E-09	1,06E-09
0,14	42,83037	1,3647E-09	1,14E-09
0,15	42,83037	1,45598E-09	1,22E-09
0,16	42,83037	1,54647E-09	1,30E-09
0,17	42,83037	1,63618E-09	1,38E-09
0,18	42,83037	1,72511E-09	1,46E-09
0,19	42,83037	1,81327E-09	1,54E-09
0,2	42,83037	1,90067E-09	1,61E-09
0,21	42,83037	1,98731E-09	1,69E-09
0,22	42,83037	2,07321E-09	1,76E-09
0,23	42,83037	2,15836E-09	1,84E-09
0,24	42,83037	2,24278E-09	1,91E-09
0,25	42,83037	2,32646E-09	1,98E-09
0,26	42,83037	2,40943E-09	2,06E-09
0,27	42,83037	2,49167E-09	2,13E-09
0,28	42,83037	2,57321E-09	2,20E-09
0,29	42,83037	2,65404E-09	2,27E-09
0,3	42,83037	2,73417E-09	2,34E-09
0,31	42,83037	2,81361E-09	2,41E-09

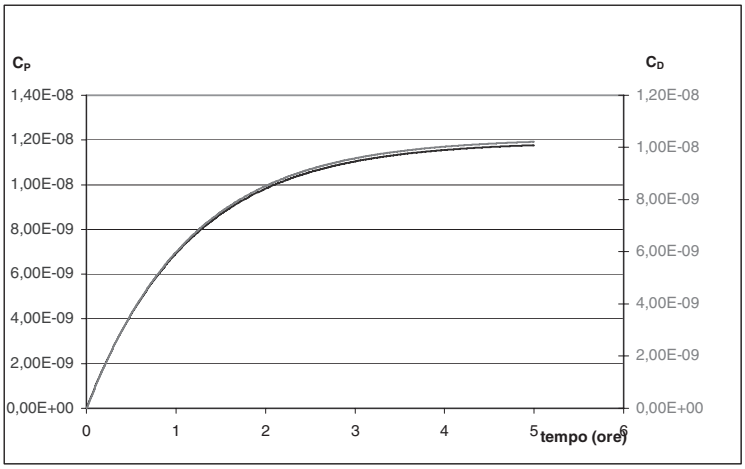

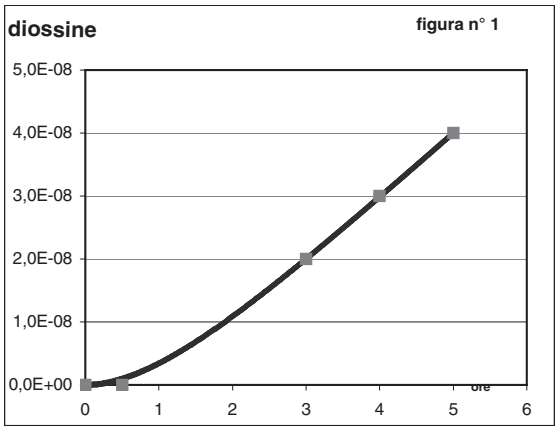

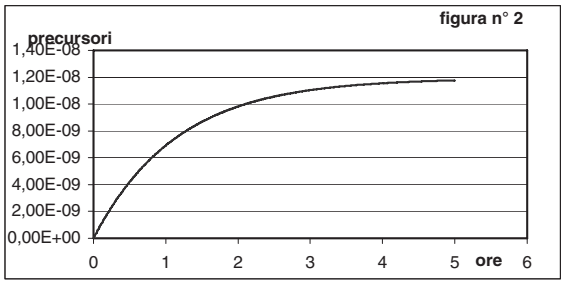

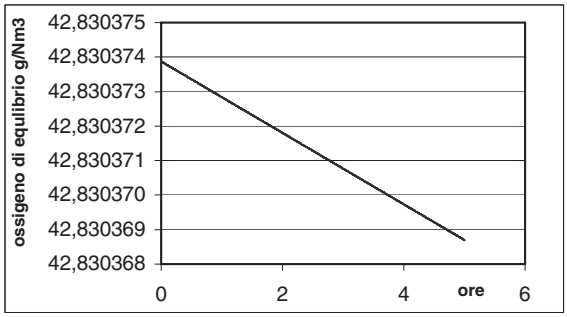

ΔO_2	integrale di C_p con r. dei trapezi
0,00E+00	
7,25E-12	5,154E-13
1,45E-11	2,057E-12
2,18E-11	4,61615E-12
2,90E-11	8,18388E-12
3,63E-11	1,27515E-11
4,35E-11	1,83104E-11
5,08E-11	2,4852E-11
5,80E-11	3,23678E-11
6,53E-11	4,08494E-11
7,25E-11	5,02884E-11
7,98E-11	6,06766E-11
8,70E-11	7,20057E-11
9,43E-11	8,42676E-11
1,02E-10	9,74543E-11
1,09E-10	1,11558E-10
1,16E-10	1,2657E-10
1,23E-10	1,42483E-10
1,31E-10	1,5929E-10
1,38E-10	1,76981E-10
1,45E-10	1,95551E-10
1,52E-10	2,14991E-10
1,60E-10	2,35294E-10
1,67E-10	2,56452E-10
1,74E-10	2,78457E-10

Appendix 6

De Novo trials results

Results of the de novo synthesis trials are reported in Table A6.1. These data are obtained by differences between trials with chloride salts and trials without chlorine salts.

Table A6.1: De Novo formation results

Trial	T (°C) II reactor	O_2 (%)	Oxidation time (h)	PCDD/Fs ITEQ (pg/g) De Novo
	350	5	0.0	0
1b	350	5	2.0	3
2b	350	5	1.5	3
3a	350	5	1.0	1
4b	350	5	0.5	1
	300	10	0.0	0
5b	300	10	2.0	44
6b	300	10	1.5	30
7a	300	10	1.0	18
	300	20	0.0	0
8b	300	20	2.0	53
9b	300	20	1.0	43
	350	20	0.0	0
10b	350	20	2	80
11b	350	20	1	68
12b	350	20	0.5	22
	400	5	0	0
13b	400	5	1.5	5
14b	400	5	1.0	4
15b	400	5	0.5	2
	400	10	0.0	0
16b	400	10	2.0	10
18b	400	10	1.0	18
	400	20	0.0	0
18b	400	20	2.0	5
19b	400	20	1.0	6
	350	10	0.0	0
Ib	350	10	0.5	1
Lb	350	10	0.8	3
Mb	350	10	1.0	5
Nb	350	10	1.5	10
Ob	350	10	2.0	13

Mathematical model computation give a cubic equation according to the mechanism in which the precursor concentration (see Appendix 3) varies with time as follows:

$$\left(\frac{dC_p}{d\tau}\right) = k_a C_{O_2}^{0.5}\left(C_0 - k_{ps}\tau\right) - k_2 C_p \qquad \ldots \text{(A6.1)}$$

In the case where one precursor molecule forms one PCDD/F molecule,

the PCDD/F production is described by:

$$\frac{dC_D}{d\tau} = k_2 C_P \qquad \ldots \text{(A6.2)}$$

If precursor concentrations depend only on formation, the term $-k_2C_p$ in Equation (A6.1) may be ignored. So:

$C_p = C_p^o + a\,t - b\,t^2$

where $a = k_a CO_2^{0.5} C_0$ and $b = ½ * k_a\, k_{ps}\, CO_2^{0.5}$

and the expression of PCDD/F concentration varying time becomes a cubic polynomial.

$C_D = C_{D0} + m\,t + nt^2 + ot^3$

where $m = k_2 C_p^o$, $n = 1/2 * k_a\, k_2 CO_2^{0.5} C_0$ and $o = -1/6 * k_a\, k_2\, k_{ps}\, CO_2^{0.5}$

In Table A6.2 the value of these coefficients, obtained by trial result computations are shown.

Table A6.2: De Novo coefficients

T	O_2 (%)	m	n	o
300	15	14	4	0
350	5	0.16	2	-0.66
350	10	-2.62	10.98	-3.2
350	20	-5.3	124	-50
400	5	3.33	2	-1.33

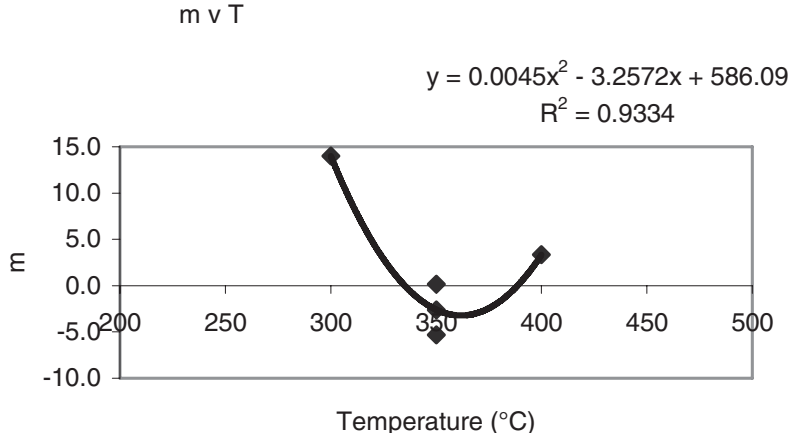

Fig. A6.1: Diagram and expression of De Novo 'm' coefficient as a function of T

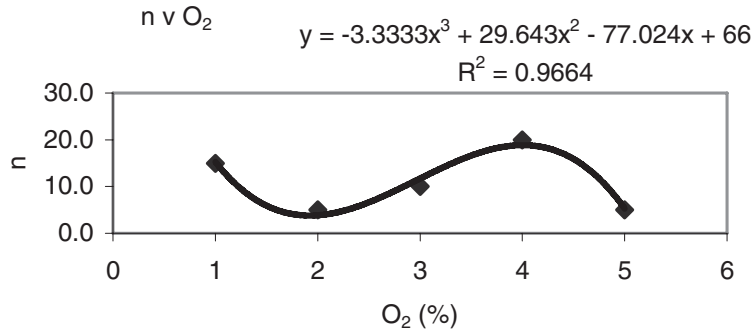

Fig. A6.2: Diagram and expression of De Novo 'n' coefficient as a function of Oxygen

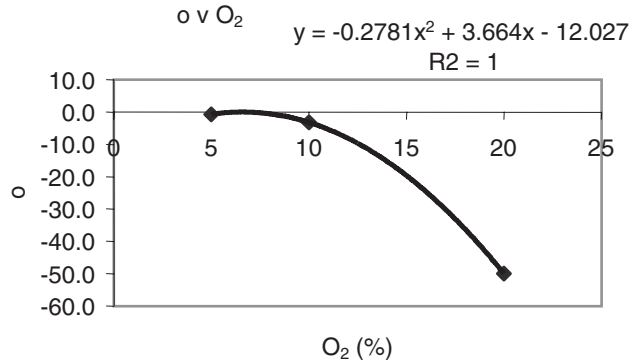

Fig. A6.3: Diagram and expression of De Novo 'o' coefficient as a function of Oxygen

From the data analyses it is possible to derive a simplified expression, that, in first approximation, yields the hourly production of PCDD'Fs owing to de novo systems, taking into account that:

the hourly formation of PCDD/F is clearly influenced by oxygen (Table A6.3),

the hourly production of PCDD/F (see Table A6.4) is effectively constant with temperature variation, in the 300-400°C range (the variation is similar to measurement error).

So, the hourly production of PCDD/F could be expressed as a function of oxygen %.

Hourly production, of PCDD/F at different oxygen concentrations, is shown in Table A6.3 and the function PCDD/F v oxygen (%) is represented in Fig A6.4.

Table A6.3: PCDD/F hourly production at different Oxygen concentration

T	O_2	PCDD/F (pg/g)/h
350	5	1
350	10	5
350	20	68

Table A6.4: PCDD/F hourly production at different temperature

O_2	T	PCDD/F (pg/g)/h
10	200	0
10	300	3
10	350	5

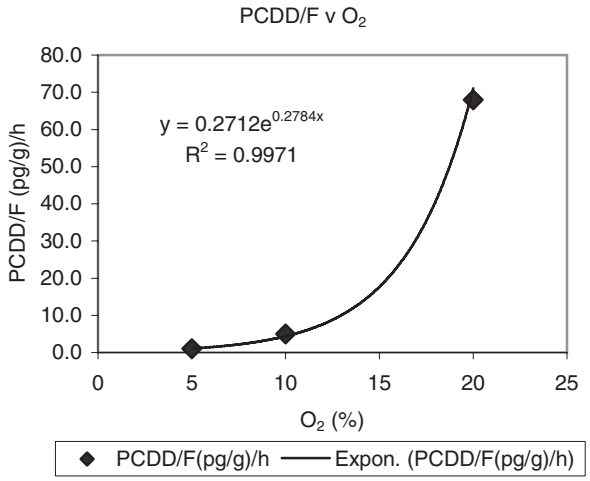

The PCDD/F hourly formation could be, qualified as follows:
$PCDD/F\ (pg/gh) = 0.271 * e^{0.278 * O_2}$

Fig. A6.4: PCDD/F in function of O_2%

European Commission

EUR 21432 — Steelmaking processes
Effects of operational factors on the formation of toxic organic micropollutants in EAF steelmaking

R. Fisher, A. M. W. Briggs, S. S. Baker, M. I. Pistelli, G. Harp, J. Pereira Gomes

Luxembourg: Office for Official Publications of the European Communities

2005 — 154 pp. — 21 x 29.7 cm

Technical steel research series

ISBN 92-79-00083-7

Price (excluding VAT) in Luxembourg: EUR 25